

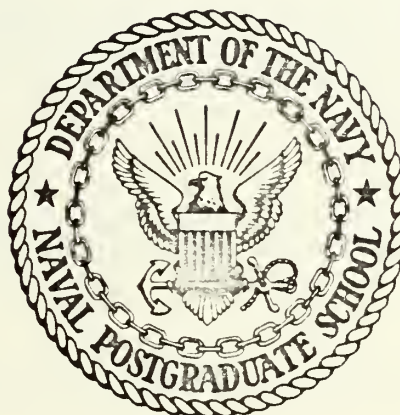
A NUMERICAL MODEL DEPICTING A WIND-DRIVEN
CIRCULATION IN AN OCEAN BASIN
CONTAINING AN ISLAND

James Vincent Sullivan

LIBRARY
NAVAL POSTGRADUATE SCHOOL
MONTEREY, CALIF. 93940

NAVAL POSTGRADUATE SCHOOL

Monterey, California



THESIS

A Numerical Model Depicting a Wind-Driven
Circulation in an
Ocean Basin Containing an Island

by

James Vincent Sullivan, Jr.

Thesis Advisor:

R. L. Haney

September 1972

Approved for public release; distribution unlimited.

T149349

A Numerical Model Depicting a Wind-Driven
Circulation in an Ocean Basin Containing an Island

by

James Vincent Sullivan, Jr.
Lieutenant, United States Navy
B.S., United States Naval Academy, 1966

Submitted in partial fulfillment of the
requirements for the degree of

MASTER OF SCIENCE IN METEOROLOGY

from the
NAVAL POSTGRADUATE SCHOOL
September 1972

ABSTRACT

A numerical model was developed depicting the wind-driven circulation in an ocean basin containing an island. This linear, barotropic, filtered model was utilized to test and evaluate the "Hole Relaxation" technique (Allen 1954) in preparation for future comparative studies with a free surface model and later incorporation in a multi-level world-ocean model with islands. Eight different data cases were studied to evaluate the model's ability to properly treat a variety of island sizes and locations. It was found that as the relative size of the island was increased at a specific location in the western half of the basin, the volume transport per unit depth between the mainland and the island, as well as the total kinetic energy at the end of a 210 day integration decreased; if the island size was decreased, the parameters' magnitudes were noted to be larger.

TABLE OF CONTENTS

I.	INTRODUCTION -----	8
II.	THE MATHEMATICAL STATEMENT OF THE PROBLEM----	11
	A. VORTICITY EQUATION DERIVATION -----	11
	B. BASIN COASTLINE AND ISLAND BOUNDARY CONDITIONS -----	14
	C. PHYSICAL CHARACTERISTICS OF THE NUMERICAL MODEL -----	14
	D. EXPERIMENTS CONDUCTED -----	15
III.	FINITE DIFFERENCE EQUATIONS -----	18
	A. THE BETA TERM -----	18
	B. CURL OF WIND STRESS TERM -----	19
	C. CURL OF FRICTION FORCE TERM -----	20
	D. OTHER TERMS -----	24
	E. RELAXATION DESCRIPTION -----	25
	1. Open Ocean Area -----	25
	2. Island Areas -----	26
IV.	RESULTS -----	31
	A. A RESTATEMENT OF THE PURPOSE OF THE MODEL	31
	B. GENERAL DESCRIPTION OF ISLAND DATA CASE STUDIES -----	31
	C. EQUILIBRIUM CONSIDERATIONS AND FINDINGS--	32
V.	CONCLUSIONS -----	71
	APPENDIX A COMPUTER PROGRAM -----	72
	LIST OF REFERENCES -----	85
	INITIAL DISTRIBUTION LIST -----	86
	FORM DD 1473 -----	89

LIST OF FIGURES

1.	Illustration of ocean basin and island including a portion of the finite difference grid -----	16
2.	Illustration of the computational grid in the area of the island perimeter -----	23
3.	Total kinetic energy for Case 2 island sizes compared to Case 1, the islandless case -----	39
4.	Same as Figure 3, except for Case 3 -----	40
5.	Same as Figure 3, except for Case 4 -----	41
6.	Same as Figure 3, except for Case 5 -----	42
7.	Same as Figure 3, except for Case 6 -----	43
8.	Same as Figure 3, except for Case 7 -----	44
9.	Same as Figure 3, except for Case 8 -----	45
10.	Streamfunction map for Case 1. Isolines are drawn for every $0.2 \times 10^8 \text{ cm}^2 \text{ sec}^{-1}$ -----	46
11.	Same as Figure 10 except for Case 2a -----	47
12.	Same as Figure 10 except for Case 2b -----	48
13.	Same as Figure 10 except for Case 2c -----	49
14.	Same as Figure 10 except for Case 3a -----	50
15.	Same as Figure 10 except for Case 3b -----	51
16.	Same as Figure 10 except for Case 3c -----	52
17.	Same as Figure 10 except for Case 4a -----	53
18.	Same as Figure 10 except for Case 4b -----	54
19.	Same as Figure 10 except for Case 4c -----	55
20.	Same as Figure 10 except for Case 4d -----	56
21.	Same as Figure 10 except for Case 5a -----	57
22.	Same as Figure 10 except for Case 5b -----	58
23.	Same as Figure 10 except for Case 5c -----	59

24.	Same as Figure 10 except for Case 6a -----	60
25.	Same as Figure 10 except for Case 6b -----	61
26.	Same as Figure 10 except for Case 6c -----	62
27.	Same as Figure 10 except for Case 7a -----	63
28.	Same as Figure 10 except for Case 7b -----	64
29.	Same as Figure 10 except for Case 7c -----	65
30.	Same as Figure 10 except for Case 8a -----	66
31.	Same as Figure 10 except for Case 8b -----	67
32.	Same as Figure 10 except for Case 8c -----	68
33.	Same as Figure 10 except for Case 8d -----	69
34.	Same as Figure 10 except for Case 8e -----	70

LIST OF TABLES

I. Data case studies used and results obtained over a 210 day integration -----	38
--	----

ACKNOWLEDGEMENTS

The author wishes to express his gratitude to Dr. Robert L. Haney, whose endless volumes of patience and encouragement, and constant availability contributed immensely to the successful completion of this thesis project. Further thanks are extended to Dr. Jerry A. Galt, for his conscientious review of the original material. Computer time for the numerical calculations was provided by the W. R. Church Computer Center at the Naval Postgraduate School.

Finally, enough thanks cannot be given to my family, especially to my wife Margie for her unfailing support not only in this thesis project but also throughout my tour of duty at the Naval Postgraduate School.

I. INTRODUCTION

For decades, men driven by the reality of the world's oceans and their geometric configurations have strived to model the physical boundary characteristics and the processes which govern the ocean-atmosphere realm. These men have recognized the future needs of the world's forecasting media by developing models which have answered some old queries and have further related new theories to make present-day phenomena more easily understood. Most studies were considerably enhanced by the advent and sophistication of numerical techniques.

In 1947, Sverdrup showed for the first time the major role of the curl of the wind stress in determining the general mid-ocean distribution of the meridional current. Later, Stommel (1948) demonstrated the decisive role of the latitudinal change in the coriolis parameter in the formation of intensive boundary currents along the eastern shores of continents. Stommel also used the linearized vorticity equation with linear bottom friction. In 1950, Munk, utilizing lateral frictional dissipation, directed his studies at more detailed features of linear viscous boundary currents, all the while restricting these studies to simple domains of integration (i.e., rectangle and triangle) and by zonal wind fields. All of these models used a vorticity equation considered on a Beta plane.

Further studies, now advanced by numerical techniques, were undertaken. Gates in 1968 showed the development of the large-scale wind-driven circulation using the primitive equations of motions for a homogeneous ocean model characterized by a free upper surface. This time-dependent model permitted not only easy observation of the individual transients' role in the circulation development, but also extensive examination of the role of divergence in the large-scale circulation by the use of the free surface upper boundary condition. Bryan in 1968 and later in 1969 with Manabe, by means of a joint atmosphere-ocean numerical model with a rigid upper boundary in the ocean, investigated the role of the ocean circulation in producing realistic features of the climate of the atmosphere.

Also in 1969, Takano studied the barotropic ocean circulation in a doubly connected world ocean using the vorticity equation (non-stationary) and the numerical method of "hole relaxation." Kamenkovich et al. (1969), in an independent effort, further displayed successful simulation of actual shoreline profiles by numerical methods in a complete circulation of the world ocean (stationary). In 1971, Alexander extended Gates' work to a baroclinic free surface model depicting a doubly connected domain, with islands in the western boundary region.

The primary purpose of the following study is to test a numerical technique for calculating the large-scale wind-driven circulation in an ocean basin which contains an island.

It is not the purpose of this model to physically depict any particular ocean or seasonal wind pattern; rather, the goal is to simplify the circulation problem in order to study and evaluate the numerical technique at the sacrifice of precise world simulation.

The numerical solution of a barotropic ocean with an island has been achieved in both linear and non-linear models. The present work is totally a linear effort utilizing the vorticity equation which filters the external high frequency gravity waves. This permits the use of a longer time step (=14 hours) than in the free surface (non-filtered) models. The application of the "Hole Relaxation" technique (Allen 1954) with respect to the island boundaries (interior boundaries to the ocean model) is employed with a major goal to test and evaluate the techniques on this simple model for future development. Furthermore, the results of this evaluation will be used in calculating the barotropic mode in more sophisticated world ocean models which can ill-afford the luxury of short time steps as required in the free surface models.

The present study did not attempt to argue in favor of a filtered model rather than a free surface model for the calculation of the barotropic mean currents. Its goal is to simply test a technique whereby the merits of the two numerical approaches (free surface vs. rigid surface) may be compared.

II. THE MATHEMATICAL STATEMENT OF THE PROBLEM

A. VORTICITY EQUATION DERIVATION

The problem is to obtain a solution to the wind driven ocean circulation in a rectangular ocean basin of uniform depth containing an island.

The linearized equations of horizontal motion (1) and (2) together with the continuity equation (3) for a homogeneous fluid are as follows:

$$\frac{\partial u}{\partial t} - fv + \frac{1}{\rho_0} \frac{\partial p}{\partial x} = A \nabla^2 u + \frac{1}{\rho_0} \frac{\partial \tau_x}{\partial z} \quad (1)$$

$$\frac{\partial v}{\partial t} + fu + \frac{1}{\rho_0} \frac{\partial p}{\partial y} = A \nabla^2 v + \frac{1}{\rho_0} \frac{\partial \tau_y}{\partial z} \quad (2)$$

$$\frac{\partial u}{\partial x} + \frac{\partial v}{\partial y} + \frac{\partial w}{\partial z} = 0 \quad (3)$$

Friction forces are crudely represented by a lateral eddy diffusion of momentum ($A \nabla^2 u, A \nabla^2 v$) and a vertical eddy stress (τ_x, τ_y). All other symbols have their usual meaning. Cross differentiation of (1) and (2) to eliminate pressure results in the following vorticity equation:

$$\begin{aligned} \frac{\partial}{\partial t} \left(\frac{\partial v}{\partial x} - \frac{\partial u}{\partial y} \right) + v\beta + f \left(\frac{\partial u}{\partial x} + \frac{\partial v}{\partial y} \right) = \\ A \left(\frac{\partial}{\partial x} \nabla^2 v - \frac{\partial}{\partial y} \nabla^2 u \right) + \frac{1}{\rho_0} \frac{\partial}{\partial z} \left(\frac{\partial \tau_y}{\partial x} - \frac{\partial \tau_x}{\partial y} \right), \quad (4) \end{aligned}$$

$$\text{where } \beta = \frac{\partial f}{\partial y} = \text{constant}$$

By vertically integrating the continuity equation (3) from the bottom of the ocean ($z = -D$) to the mean sea level ($z=0$), we have

$$\frac{\partial \bar{u}}{\partial x} + \frac{\partial \bar{v}}{\partial y} + \frac{w(0) - w(-D)}{D} = 0 \quad (5)$$

where (\bar{u}, \bar{v}) is the vertically integrated velocity defined by

$$\bar{u} = \frac{1}{D} \int_{-D}^0 u \, dz \quad ,$$

and

$$\bar{v} = \frac{1}{D} \int_{-D}^0 v \, dz \quad . \quad (6)$$

The boundary conditions on $w(-D)$ and $w(0)$ are

$$\begin{aligned} w(-D) &= 0 \\ w(0) &= 0 \quad . \end{aligned} \quad (7)$$

The first boundary condition in (7) is kinematic and applies at the flat ocean floor. The second condition is the approximation which removes external gravity waves from the model and thereby allows longer time steps to be utilized. The inaccuracy of the solution due to the balance approximation of requiring the vertical velocity to be zero at the sea surface can be examined by comparison of the results of this present calculation with similar calculations using a barotropic primitive equation model with a free surface as used for example by Gates in 1967. As a result of (7), (5) becomes

$$\frac{\partial \bar{u}}{\partial x} + \frac{\partial \bar{v}}{\partial y} = 0 \quad ; \quad (8)$$

Consequently, a streamfunction $\psi(x, y)$ is defined for the vertically integrated velocity as follows:

$$\begin{aligned} \bar{u} &= - \frac{\partial \psi}{\partial y} \\ \bar{v} &= \frac{\partial \psi}{\partial x} \quad . \end{aligned} \quad (9)$$

The vertical integration of the vorticity equation (4) and the use of (8) and (9) results in

$$\frac{\partial}{\partial t} \nabla^2 \psi + \beta \frac{\partial \psi}{\partial x} = A \nabla^2 (\nabla^2 \psi) + \frac{1}{\rho_0 D} \left[\left(\frac{\partial \tau_y}{\partial x} - \frac{\partial \tau_x}{\partial y} \right)_{z=0} - \left(\frac{\partial \tau_y}{\partial x} - \frac{\partial \tau_x}{\partial y} \right)_{z=-D} \right] . \quad (10)$$

The boundary conditions on the stress at the ocean floor ($z = -D$) and at the sea surface ($z = 0$) are as follows:

At $z = -D$

$$\tau_x = \tau_y = 0 \quad (11)$$

while at $z = 0$

$$\begin{aligned} \tau_x &= -F \cos \left(\frac{\pi y}{b} \right) \\ \tau_y &= 0 , \end{aligned} \quad (12)$$

where F is the amplitude of the zonal components of the wind stress and b is the north-south extent of the ocean basin. This model in the islandless case was a time dependent representation of Munk's model (1950). Therefore, the results can easily be compared with Munk's analytic solution as a check on the accuracy of the numerical solution.

Thus, there is no bottom stress, and the surface stress corresponds to a pattern of westerly winds in the northern half of the basin, and to easterly winds in the southern half of the basin. In addition, it is important to have a stress that has a non-zero curl since only the curl of the wind stress actually does the forcing in the vorticity equation. Using (11) and (12), the vorticity equation takes the final form,

$$\nabla^2 \frac{\partial \psi}{\partial t} = -\beta \frac{\partial \psi}{\partial x} - \frac{\pi F}{\rho_0 D b} \sin \left(\frac{\pi y}{b} \right) + A \nabla^2 (\nabla^2 \psi) . \quad (13)$$

B. BASIN COASTLINE AND ISLAND BOUNDARY CONDITIONS

The boundary conditions along the island and basin coastlines (mainland) extremities used in the solution of (13) are those of zero normal flow and of zero slip.

The condition of no normal flow ($v_n = 0$) was implemented by requiring that the streamfunction be equal to zero on the ocean periphery and that the same function be a constant function of time on the island's perimeter. These conditions are written as:

$$\begin{aligned}\psi &= 0 \text{ (mainland boundary)} \\ \psi &= c(t) \text{ (island boundary)}\end{aligned}\quad (14)$$

The value of the constant $c(t)$ determines the net flow (volume transport) between the mainland and the island and is calculated by the "hole relaxation" procedure (Allen 1954) as a part of the solution.

The conditions of zero slip and no normal flow are implemented in the calculation of the lateral friction force term on the right hand side of (13). These conditions are written as:

$$\bar{u}, \bar{v} = 0 \text{ (all island and mainland boundaries).} \quad (15)$$

Details of the formulation of these boundary conditions are contained in section three where the finite difference equations are given.

C. PHYSICAL CHARACTERISTICS OF THE NUMERICAL MODEL

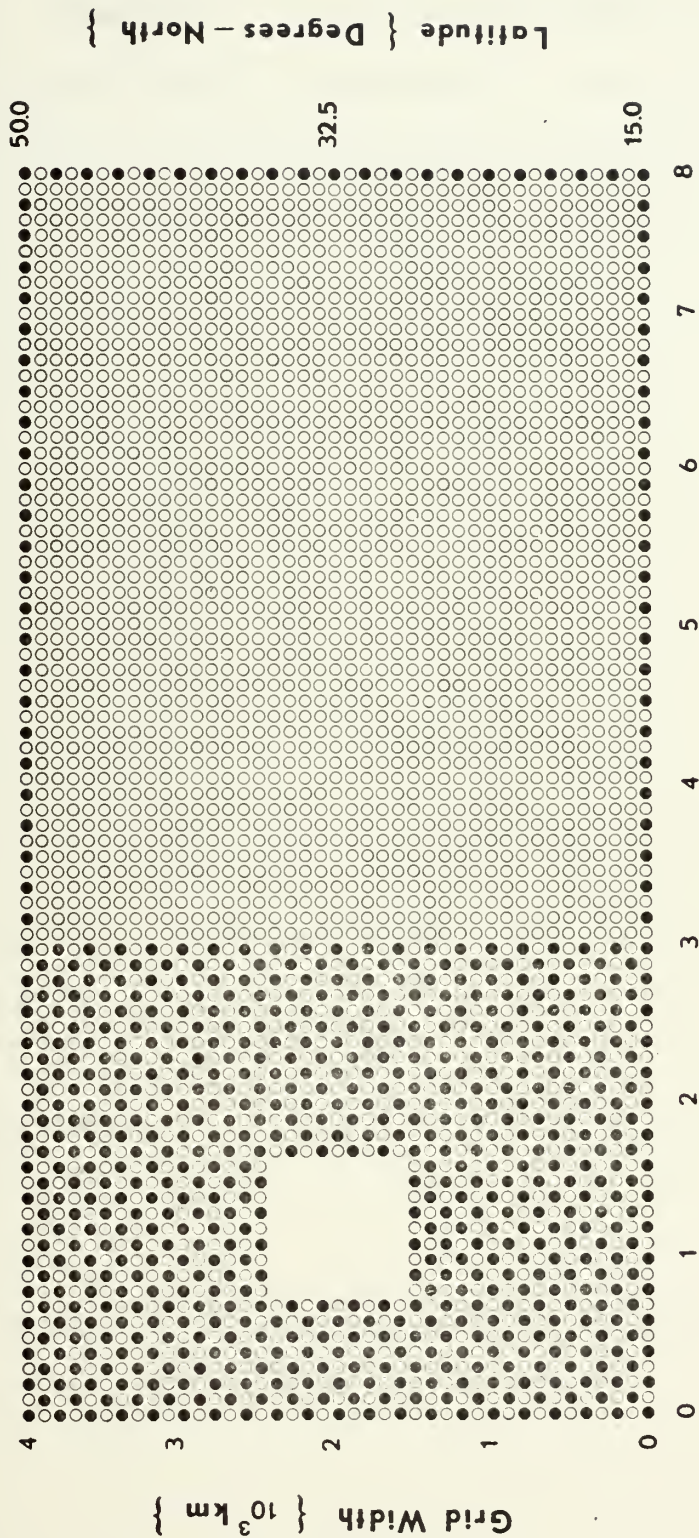
The model presented here is a rectangular basin of length, $L = 8000$ km; of breadth, $b = 4000$ km; and of constant

depth, Depth = 2 km. (See Figure 1.) The total grid size is 41 x 21 in the horizontal while the computational grid size is 40 x 20. The distance between adjacent grid points is 200 km in both x and y. The value chosen for Beta makes the grid centered at 32.5°N. Figure (1) also displays a portion of the 861 nodal points and shows how an arbitrary island may appear. The arbitrarily sized, rectangularly shaped island may be placed at any selected location throughout the grid. The model is not strictly designed to simulate any particular ocean or ocean currents system, but rather is utilized to evaluate the solution techniques to be tested and secondarily to evaluate the evolution of the physical flow patterns around the island with respect to time.

D. EXPERIMENTS CONDUCTED

Initially, an islandless ocean model was studied. This model utilized the same equation (13) as its basis of solution. Again, this model was analogous to the solution of Munk's model (1950) when the numerical solution achieved steady-state conditions. All characteristics were as described above with the exception of an island. A duration of 210 days was selected as the run time for this phase in order to be able to compare all possible "island" integrations with this islandless case.

Next, an island-ocean basin phase was introduced by adapting the boundary conditions and restrictions of the hole relaxation technique to be tested (Allen 1954). A



Grid Length { 10³ km }

Figure 1: Illustration of ocean basin and island including the finite difference grids, where darkened circles denote the location of the streamfunction against an unshaded circle background. The distance between adjacent grid points is 200 km and the grid is centered at 32.5°N. The portion of the full 861 grid points shown illustrates the density of the points in contrast with an island example which is centered in the western half of the basin. The island size shown is 800 km on a side. This is the island used in Case 2b. (See Table 1.)

time plot of the total kinetic energy showed that 210 days was adequate to reach a statistical steady state, and to give an accurate comparison to the steady-state characteristics of the islandless phase results.

III. FINITE DIFFERENCE EQUATIONS

Individual terms on the right hand side of (13) are expressed in finite difference form in the following paragraphs. The grid points in the annulus are discussed first in each case, then follows a discussion of the grid points on the island perimeter. Island corner points and the points on the perimeter adjacent to the corners are not discussed. Readers are referred to the documented computer program in Appendix A for further details. It should also be clarified that all terms on the right hand side of (13) were calculated after multiplying the entire equation by the area represented by a grid point, namely $(\Delta x)^2$. The reason for this action was that the time rate of change of vorticity multiplied by the area represents the time rate of change of the circulation. This time rate of change of the circulation was the variable "F1" as seen in Appendix A.

It should be pointed out that a forcing function of $F1=0$ was assumed (Allen 1954) in the interior nodes of the island. Finally, since it was assumed that $\Delta x = \Delta y$ throughout the grid, the term " Δx " was utilized throughout the subsequent discussion and all sections of this thesis.

A. THE BETA TERM

In the annular locations while maintaining boundary condition (14), the beta term was expressed as

$$-\beta \frac{\partial \psi}{\partial x} \Delta x^2 \Rightarrow -\beta \left(\frac{\psi_{I+1} - \psi_{I-1}}{2} \right) \Delta x \quad (16)$$

If the beta terms on the north and south perimeters were considered to be zero due to boundary condition (14), namely, zero normal flow, then the boundary conditions of constant values of ψ on the perimeter of the island and zero values of ψ on the mainland, inherent in (14), had to be maintained on the east and west island perimeter nodal points. The constraint that the integrated sum of all beta terms along any latitudinal plane or axis was to be zero, guided the formulation of the finite difference form of the beta term on the east-west perimeters. This integral constraint which was a property of the differential expression for $\beta \frac{\partial \psi}{\partial x}$, also had to hold true in the finite difference analogues, as long as the meridional velocity component on the island perimeter was evaluated by means of an uncentered difference approximation. Therefore, when the beta term was calculated on the island perimeter as described above, the uncentered finite difference forms used were:

$$-\beta \frac{\partial \psi}{\partial x} \Delta x^2 \Rightarrow -\beta (\psi_I - \psi_{I-1}) \Delta x , \quad (17)$$

for the western perimeter, and

$$-\beta \frac{\partial \psi}{\partial x} \Delta x^2 \Rightarrow -\beta (\psi_{I+1} - \psi_I) \Delta x , \quad (18)$$

for the eastern perimeter.

B. CURL OF WIND STRESS TERM

In both the case of the annular location and that of the island perimeter locations, the wind stress term was defined in the same manner, namely:

$$-\frac{\pi F}{\rho_o D b} \Delta x^2 \sin\left(\frac{\pi y}{b}\right) \Rightarrow -\frac{\pi F}{\rho_o D b} \Delta x^2 \sin(Y), \quad (19)$$

$$\text{where} \quad Y = \frac{\pi(J-1)\Delta x}{b}. \quad (20)$$

C. CURL OF FRICTION FORCE TERM

Boundary conditions utilizing zero slip and zero normal flow (14) were again selected to enable dissipation to occur at the boundaries through the linear curl of the friction force term in the model.

The friction force term was expressed as follows:

$$[A\nabla^2(\nabla^2\psi)]_{I,J} = [A\nabla^2\zeta]_{I,J} = [A(\frac{\partial}{\partial x}\nabla^2 v - \frac{\partial}{\partial y}\nabla^2 u)]_{I,J}. \quad (21)$$

The finite difference form in the open oceanic areas away from the boundaries was based on (21) as

$$[(A\nabla^2\zeta)_{I,J}\Delta x^2] \Rightarrow A\Delta x \left[\left(\frac{\nabla^2 v_{I,J} + \nabla^2 v_{I,J-1}}{2} \right) - \left(\frac{\nabla^2 v_{I-1,J} + \nabla^2 v_{I-1,J-1}}{2} \right) \right. \\ \left. - \left(\frac{\nabla^2 u_{I,J} + \nabla^2 u_{I-1,J}}{2} \right) + \left(\frac{\nabla^2 u_{I,J-1} + \nabla^2 u_{I-1,J-1}}{2} \right) \right], \quad (22)$$

where

$$\nabla^2 v_{I,J} = \left(\frac{v_{I+1,J+2} + v_{I+1,J} + v_{I+2,J+1} + v_{I,J+1} - 4v_{I+1,J+1}}{\Delta x^2} \right), \quad (22a)$$

with a similar expression for $\nabla^2 u_{I,J}$, and where $u_{I,J}$ and $v_{I,J}$ are defined in terms of $\psi_{I,J}$ as,

$$u_{I,J} = \frac{1}{\Delta x} \left[\left(\frac{\psi_{I-1,J-1} + \psi_{I,J-1}}{2} \right) - \left(\frac{\psi_{I-1,J} + \psi_{I,J}}{2} \right) \right], \quad (22b)$$

and

$$v_{I,J} = \frac{1}{\Delta x} \left[\left(\frac{\psi_{I,J} + \psi_{I,J-1}}{2} \right) - \left(\frac{\psi_{I-1,J} + \psi_{I-1,J-1}}{2} \right) \right]. \quad (22c)$$

On the island perimeter, the same basic finite difference form (21) applied except that the following alterations existed:

i) on the northern and southern perimeters,

$$\frac{\partial}{\partial x} \nabla^2 v = 0 , \quad (23)$$

and ii) on the eastern and western perimeters,

$$\frac{\partial}{\partial y} \nabla^2 u = 0 . \quad (24)$$

These conditions preserved boundary condition (14) with respect to no normal flow.

Having made use of (23) and (24) along with the zero slip condition, the following finite difference forms resulted for use in (22) on the island perimeter:

i) southern perimeter of the island

$$(22) \Rightarrow \frac{A}{\Delta x} [-4u_{I,J} - 4u_{I+1,J} + u_{I-1,J} + u_{I,J-1} + u_{I+1,J-1} + u_{I+2,J}]; \quad (25)$$

ii) northern perimeter of the island

$$(22) \Rightarrow \frac{A}{\Delta x} [4u_{I,J+1} + 4u_{I+1,J+1} - u_{I-1,J+1} - u_{I+2,J+1} - u_{I,J+2} - u_{I+1,J+2}]; \quad (26)$$

iii) western perimeter of the island

$$(22) \Rightarrow \frac{A}{\Delta x} [4v_{I,J} + 4v_{I,J+1} - v_{I,J+2} - v_{I-1,J+1} - v_{I-1,J} - v_{I,J-1}]; \quad (27)$$

and iv) eastern perimeter of the island

$$(22) \Rightarrow \frac{A}{\Delta x} [-4v_{I+1,J+1} - 4v_{I+1,J} + v_{I+1,J+2} + v_{I+2,J+1} + v_{I+2,J} + v_{I+1,J-1}]. \quad (28)$$

This complex perimeter calculation has been clearly illustrated in Figure 2.

Suppose the point (I,J) in Figure 2 was assumed to be located on the western perimeter of the island. The relationship, for example,

$$\left(\frac{\partial}{\partial x}\nabla^2 v\right)_{I,J} = \left(\frac{\nabla^2 v_3 + \nabla^2 v_4}{2}\right) - \left(\frac{\nabla^2 v_2 + \nabla^2 v_1}{2}\right), \quad (29)$$

demonstrated how the staggered grid points, numbered one through 12, were used to compute $\left(\frac{\partial}{\partial x}\nabla^2 v\right)_{I,J}$.

The right hand side of (29) was written as the sum $\sum_{i,j} w_{I+i,J+j} v_{I+i,J+j}$ where $w_{I+i,J+j}$ was the net weighting factor assigned to v at the nodal point $(I + i, J + j)$ in the computation of $\frac{\partial}{\partial x}\nabla^2 v$ at the nodal point (I,J) in the island perimeter. Having rewritten the right hand side of (29), and having used the zero slip condition, $v_{I+i,J+j} = -v_{I-i,J+j}$, it was found that:

$$(29) \Rightarrow 4v_{I,J} + 4v_{I,J+1} - v_{I,J+2} - v_{I-1,J+1} - v_{I-1,J} - v_{I,J-1}. \quad (30)$$

Readers should note that in the staggered grid depicted, $v_{I,J}$ was located at point number one, $v_{I,J+1}$ was located at point number two, etc., and that the terms of (30) were signed as a result of (29), i.e., points one and two had $w = +4$, while points nine through 12 had $w = -1$.

The above served to demonstrate the derivation of (27). Equations (25), (26), and (28) were derived in a similar fashion.



Island Perimeter

Key:

- = Grid Nodal Points
- o = Staggered Nodal Points
- = ψ
- o = $u, v, \nabla^2 u, \nabla^2 v$

Figure 2: Illustration represents a portion of the computational grid, which includes the island perimeter. The side of the grid which represents ocean or island depends on the case to be evaluated, i.e., on the right for the Equation (29) cited. The shifting and/or re-orientation of the island portion of the figure will permit north, south, east or west perimeter calculations.

D. OTHER TERMS

In addition to the three terms on the right hand side of (13), the finite difference forms for the residual calculation in the relaxation phase of the model's solution were to have been expressed. Yet prior to that discussion, a brief description of the time differencing procedures was formulated.

For accuracy, a centered time difference scheme was used. This was the so-called "leapfrog" scheme which was characterized by the desirable property of being neutral and the undesirable property of producing a computational mode in time for the system solution. This resulting mode, caused by the presence and utilization of three time levels in the description of $\frac{\partial \psi}{\partial t}$, was removed by the periodic employment of a Euler-Backward (Matsuno) time scheme. The Euler-Backward scheme was used initially at the first time step and again at every 50 time steps thereafter to prevent separation of the solution in time. This scheme removed the computational mode by utilization of only two time levels for the calculation of $\frac{\partial \psi}{\partial t}$.

The relaxation phase of the model solution had an equation that was to be solved which was expressed as,

$$\nabla^2 \left(\frac{\partial \psi}{\partial t} \right) - F1 = 0 \quad (31)$$

where F1 was expressed by the right hand side of (13) multiplied by Δx^2 . If it is assumed that the symbol ψ' was the first derivative of ψ with respect to time, then the relaxation residual, RESID, was expressed as

$$(\text{RESID})_{I,J} = [\psi'_{I+1,J} + \psi'_{I-1,J} + \psi'_{I,J+1} + \psi'_{I,J-1} - 4\psi'_{I,J}] - [F1]_{I,J} , \quad (32)$$

in both the ocean basin grid points and at the island grid points.

E. RELAXATION DESCRIPTION

1. Open Ocean Area

The Liebmann over-relaxation technique was utilized in all open ocean areas of the computational grid. This technique was found to have the most successful application to the model in which forcing by large scale stress dominated.

Following the standard relaxation technique, if it was found that in the solution of (31) the absolute value of $\text{RESID}_{I,J}$ in (32) was greater than some small allowable error, ϵ , a new $\psi'_{I,J}$ denoted by $\psi'^{*}_{I,J}$ was defined as follows:

$$\psi'^{*}_{I,J} \equiv \psi'_{I,J} + C_{I,J} , \quad (33)$$

where the correction $C_{I,J}$ was determined by the condition that the new residual value $\text{RESID}^*_{I,J}$ calculated using $\psi'^{*}_{I,J}$, must be a negative fraction of $\text{RESID}_{I,J}$, i.e.,

$$\text{RESID}^*_{I,J} \equiv -\alpha \text{RESID}_{I,J} . \quad (34)$$

A value of $\alpha = 0$ therefore corresponds to no over-relaxation. Since

$$\text{RESID}^*_{I,J} = [\psi'_{I+1,J} + \psi'_{I,J+1} + \psi'_{I-1,J} + \psi'_{I,J-1} - 4\psi'^{*}_{I,J}] - F1_{I,J} \quad (35)$$

is true, then it was easily found that the relationship for the correction $C_{I,J}$ was

$$C_{I,J} = \left[\frac{1.0 + \alpha}{4.0} \right] \text{RESID}_{I,J} \quad (36)$$

An optimum value for the over-relaxation coefficient, α , of 0.75 was selected for use in these open oceanic regions. This value was the result of several test evaluation runs and was rather large due to the large scale nature of the forcing and resultant motion. More details as to the application of this technique to the open oceanic areas of the grid can be found in the ample commentary of the computer program located in Appendix A.

2. Island Areas

In the island areas, the "Hole Relaxation" technique was used (Allen 1954). This technique assumed that the same Equation (31) was to be solved with the exception that the island points were cumulatively treated like a block where the residual on the island, RESIDI, was defined as

$$\text{RESIDI} \equiv \sum_{\text{island}} \overline{(\nabla^2 \psi' - F1_{I,J})} \quad , \quad (37)$$

where the '————' symbol represented a four grid point average, and the symbol ' \sum_{island} ' represents the finite difference approximations to an integral over the island of the individual residual values. This total residual value, RESIDI, was made to approach zero in compliance with the hole relaxation technique in order to achieve an accurate solution for (31). As a result of the averaging process used, RESIDI was written as the sum of the individual nodal point residuals, each multiplied by a weighting factor where

the corner perimeter nodal points were assigned a factor of 0.25, while the lateral perimeter points were given a factor of 0.50, and the interior points a factor of 1.0.

If the subscripts 1,2,3,4; E,W,N,S; and INT. were used to denote the contribution to RESIDI from the four corners, the east, west, north and south lateral perimeter points and the interior nodal points respectively, then since $F_1 = 0$ on the island interior, (37) was expanded as:

$$\begin{aligned} \text{RESIDI} = & 0.25 [(\nabla^2 \psi' - F_1)_1 + (\nabla^2 \psi' - F_1)_2 + (\nabla^2 \psi' - F_1)_3 + (\nabla^2 \psi' - F_1)_4] \\ & + 0.50 [\sum_E (\nabla^2 \psi' - F_1) + \sum_W (\nabla^2 \psi' - F_1) + \sum_N (\nabla^2 \psi' - F_1) + \sum_S (\nabla^2 \psi' - F_1)] \\ & + 1.0 [\sum_{\text{INT.}} (\nabla^2 \psi')] \quad . \quad (38) \end{aligned}$$

In accordance with the hole relaxation technique (Allen 1954), and the boundary conditions of no normal flow (14), ψ' had the same value at all points on the island, i.e.,

$$\psi'_{I,J} \equiv \psi' \text{ (on the island) } . \quad (39)$$

The object of the hole relaxation technique was to find the value of ψ' for which the absolute value of RESIDI was less than the error tolerance ϵ . The procedure used to do this was as follows. After completing each relaxation sweep over all interior ocean points, RESIDI was calculated from (38) and its absolute value tested. If it was equal to or less than ϵ , no correction was added to ψ' , and if no correction had been made to any of the interior ocean points on that last sweep, then $\psi'_{I,J}$ and ψ' comprised the solution. If the absolute value of RESIDI was larger than ϵ , a correction, CI, was added to ψ' and a new relaxation sweep over

all grid points was initiated. The correction CI was determined in such a way that the new RESIDI would be a negative fraction of the current RESIDI. The correction CI for the island block was determined similarly to the development of $C_{I,J}$ for the ocean points as follows:

It was first noted that in (38),

a. for each corner grid point,

$$(\nabla^2 \psi')_{n=1,2,3,4} = -2\psi' + \text{non-island } \psi'_{I,J} ; \quad (40)$$

b. for each group of lateral nodes not on a corner, for example the eastern perimeter,

$$\sum_E (\nabla^2 \psi') = \sum_E (-\psi') + \sum_E (\text{non-island } \psi')_{I,J} , \quad (41)$$

or

$$\sum_E (\nabla^2 \psi') = (-\psi') (NO_E) + \sum_E (\text{non-island } \psi')_{I,J} , \quad (42)$$

where NO_E was the number of non-corner nodal points on the island's eastern perimeter. Finally

c. for the nodal points on the interior of the island,

$$(\nabla^2 \psi')_{I,J} = 0 . \quad (43)$$

If the domain of the island was described by designated I,J indices such that the minimum and maximum values of I and J were IMIN and IMAX, JMIN and JMAX respectively, then the number of nodal points on a particular island side were expressed in terms of these indices. The number of non-corner lateral nodal points in the example stated in (42) was,

$$NO_E = JMAX - (JMIN + 1) \quad . \quad (44)$$

Similar expressions for westerly, northerly, and southerly lateral side descriptions were evolved for NO_W , NO_N , and NO_S , respectively.

When Equations (40), (42), (43), and (44) and their associated counterparts for the other perimeters were used to expand (38), the resulting expression for the island residual was,

$$\begin{aligned} RESIDI = & 0.25[-8\psi' + \sum_{n=1,2,3,4} (\text{non-island } \psi'_{I,J})_n - \sum_{n=1,2,3,4} (F1)_n] \\ & + 0.50[-\psi'(2IMAX-2IMIN-2+2JMAX-2JMIN-2) \\ & + \sum_{n=E,W,N,S} (\text{non-island } \psi'_{I,J})_n - \sum_{n=E,W,N,S} (F1)_n] \quad , \end{aligned}$$

which was simplified to

$$RESIDI = -(\text{TERM})(\psi') + \sum (\text{non-island } \psi') \quad , \quad (45)$$

where

$$\text{TERM} = IMAX - IMIN + JMAX - JMIN \quad . \quad (46)$$

The "hole relaxation" stipulated that individually there was no need for restriction on the values of island residuals, provided only that their sum, namely RESIDI, was eventually brought to zero. Therefore, when the absolute value of (45) was greater than the tolerable error ϵ , a new value of the island ψ' , denoted ψ'^* , was defined by

$$\psi'^* \equiv \psi' + CI \quad , \quad (47)$$

where CI was determined by requiring that the new island residual, $RESIDI^*$, be a negative fraction of RESIDI, that is,

$$RESIDI^* \equiv -(\alpha I) RESIDI \quad , \quad (48)$$

where αI was the appropriate over-relaxation coefficient for the chosen island. Since from (45)

$$\text{RESIDI} \equiv (\text{TERM})(\psi'^*) + \Sigma(\text{non-island } \psi') \quad , \quad (49)$$

by substituting (47) into (49) and using (48), the constant CI was obtained to be

$$\text{CI} = \frac{(1.0 + \alpha I)}{\text{TERM}} \text{RESIDI} \quad (50)$$

The optimum value of the over relaxation coefficient, αI , was found to depend upon the size of the island selected for study. When the island sizes were small with respect to the scale of the dominant wind stress, a value of 0.40 was assigned to αI . If the island sizes were comparable to the scale of the stress, a smaller value of 0.20 was assigned. These time-tested selections were based upon the comparative need for more or less over-relaxation respectively as the island size was varied from small to large.

More precisely, greater over-relaxation was necessary when the scale of the island was small in comparison to the scale of the wind stress and less over-relaxation was found necessary when the scale of the island was comparable to the scale of the wind stress. These results were to be expected since the scale of the motion, and hence the scale of the residuals will be determined by the scale of the wind stress forcing.

Further details as to the application of this technique in conjunction with that of the open oceanic areas can be found in Appendix A.

IV. RESULTS

A. A RESTATEMENT OF THE PURPOSE OF THE MODEL

The main purpose of this model was to fully test and evaluate the boundary and relaxation techniques utilized. The accuracy of these results with the filtered model will be evaluated in later comparative studies with a free surface model. If the comparison is favorable, eventual incorporation will be made in a multi-level world-ocean model with islands.

The reader is reminded that the requirements of the model's solution are already required in more complicated multi-level baroclinic models.

In the programming of the model, no special efforts were made to minimize computer time other than by selecting a value of the over-relaxation coefficient which was believed to be near the optimum value. With this in mind, the model required 28 minutes of C.P.U. time on the IBM 360/65 to integrate 364 time steps. Thus, with a time step of approximately 14 hours, each of the 210 day integrations shown in the following section used less than one-half of one hour (.47 hours) of computer time.

B. GENERAL DESCRIPTION OF ISLAND DATA CASE STUDIES

Altogether, there were eight studies considered. Of these studies, there were seven different island positions examined, six of which were in the vicinity of the western

boundary; while the other island position was in the eastern boundary vicinity. The remaining study showed the island-less case. Because of the linearized form of the equations and the barotropic assumptions, the primary motivation for these eight studies was to specifically test and evaluate the model techniques and arrive at some quantitative idea as to what to expect in a more general, non-linear, multi-level future application of this model without excessive computer cost.

Each island case study contained a variation of three or more island sizes centered about a specifically chosen grid location. For example, in the second data study, a specific grid position of "WESTERN GRID HALF-CENTERED" was chosen. The three distinct island sizes comprising this particular set were 400 kilometers square, 800 kilometers square, and 1200 kilometers square. All three islands in this set were centered in the western portion of the grid so that symmetrical streamfunction patterns would appear to the north and south of the island. Each of the other island case studies was similarly structured and can be referred to in Table I.

C. EQUILIBRIUM CONSIDERATIONS AND FINDINGS

A most important aspect of the numerical solution was to determine if the model had achieved a steady-state condition in each case study. The existence of an equilibrium condition was accurately evaluated by means of a total kinetic energy (T.K.E.) calculation (Appendix A). At the end of each time step, this mathematical indicator projected an integral

picture of the steady-state characteristics of the evaluated island case. Specific illustrative comparisons between the steady-state characteristics of the islandless case and those of the island cases are shown in Figures 3 through 9. From an examination of these figures, it was clear that a statistical equilibrium was achieved in all cases by 210 days of integration. The streamline maps for the 210th day for each case is shown in Figures 10 through 34, while some of the data on each case is summarized in Table I.

As shown in Table I, the following trends were noted:

a) When the island was located in a region of strong currents (Cases 2,3,4,6,7,8), the larger the size of the island, the lower the final value of the total kinetic energy. (Case 8-d was an unexplained exception to this rule.) When the island was located in a region of weak currents (Case 5), the streamlines were easily bent around the island (Figure 23) producing a stronger flow in the central open ocean. Because the kinetic energy depends on the square of the current speed, this streamline bending by the island increased the total kinetic energy. b) Except for Case 8-d, the closer the island was positioned to the mainland in the westerly located studies, the smaller the final value of the total kinetic energy. c) In Case 6 and in Case 7, the placement of a larger island in the path of a strong current reduced the final total kinetic energy value. d) The comparative examination of Case 3 and Case 4 pointed out that the same final T.K.E. values were achieved by the symmetric placement

of equivalently sized islands south and north of the central latitude. In Case 4-b, an asymmetrically placed island showed a different T.K.E. value which still conformed, however, to those conditions stipulated above in (a) and (c). e) Finally, as might be anticipated, all island cases of comparatively small size had final T.K.E. values similar to that achieved in Case 1, the islandless case.

As an additional guide in the above interpretation, the average kinetic energy was calculated from the T.K.E. by dividing by the number of non-island values which entered into the total. The results were unchanged; namely, that the larger the island, the smaller the average kinetic energy in all cases except the Eastern Island Case 5 and Case 8-b, where a large average kinetic energy appeared with the larger island.

The contents of Table I display among other things the value of the streamfunction on the island (ψ_{island}) and maximum streamfunction value in the ocean basin ($\psi_{\text{max.}}$). These values were significant in that they presented two quantitative measures of the current's volume transport per unit depth. Because of the zero normal flow boundary condition (14), ψ_{island} displayed the actual value of the volume transport per unit depth between the island and the mainland. The reader is especially cautioned to note (in Case 8) that because of recirculation between the westerly boundary and the island, this value of ψ_{island} should be interpreted only

as a measure of the net transport between an island and any mainland.

The $\psi_{\max.}$ value accurately pointed out the maximum volume transport per unit depth to be found in the ocean basin. This value always was found in the area immediately adjacent to the western boundary of the mainland.

As shown in Table I, in each data case study: a) The values of ψ_{island} were smaller in magnitude than those of $\psi_{\max.}$. b) When the size of the island was relatively larger, the magnitudes of ψ_{island} and $\psi_{\max.}$ were both smaller (Cases 2, 3 and 4). c) When the island was positioned closer to the southern mainland boundary in the westerly located studies, the values of ψ_{island} and those of $\psi_{\max.}$ were both smaller. In the easterly located studies (Case 5), the ψ_{island} values were nearly all the same, but the $\psi_{\max.}$ values, found near the western boundary of the ocean basin, consistently increased with the size of the island. This $\psi_{\max.}$ increase seemed to be related to the increased gradient of the streamfunction near the central latitudinal axis of the basin; however, a further, more satisfactory explanation has not yet been found. d) In both Cases 3 and 4, the corresponding values of ψ_{island} and $\psi_{\max.}$ were identical, again demonstrating the symmetrical characteristics of the linear solution. e) Finally, in Cases 6 and 7, smaller transports were recorded around the islands which were fully extended in the paths of strong currents, while the $\psi_{\max.}$ values found near the western ocean basin boundary were seen to be

significantly smaller only in the case where the island was fully extended north to south.

Many features of the different solutions can only be seen in the streamfunction isoline maps which are displayed in Figures 10 through 34.

Figure 10 showed the islandless case in which the numerical solution compared favorably with the analytic solution of Munk. Figures 11 to 13 showed that when an island was placed in the center of an ocean gyre, the solution was not changed appreciably until the island size was about the same size or larger than the gyre itself.

One of the interesting features found in Cases 3, 4 and 5 (Figures 14 through 23) was that in this linear model, when an island was placed in the southern (northern) part of the basin, the latitude of maximum meridional transport shifted northward (southward). This shift was imperceptible in Case 8 (Figures 30 through 34) in which the island had only a small north-south extent. There was some form of western intensification evident on the eastern shore of the island in every case study. Yet the maximum streamfunction values found on the eastern side of the island were always smaller in magnitude than the ψ_{\max} values depicted in Table I, which were always found adjacent to the western boundary of the basin. The island's eastern shore intensification was most evident in Case 6 (Figures 24 through 26) in which there was an anticyclonic gyre in the center of the basin,

and two western intensified cyclonic gyres near the northern and southern ends of the fully extended island.

DATA CASE:	GRID POSITION:	SIZE: (km ²)	DISTANCE TO MAINLAND: (km)	I.K.E.: (cm ² sec ⁻²)	ψ ISLAND (x10 ⁸ cm ² sec ⁻¹)	ψ MAX. (x10 ⁸ cm ² sec ⁻¹)
1	ISLAND—LESS	—	—	800.6	—	2.23
2a	WEST—CNTRD	400 x 400	1000	800.9	1.44	2.18
2b	↓	800 x 800	800	774.3	1.38	2.06
2c	↓	1200 x 1200	600	698.4	1.23	1.85
3a	WEST—SOUTH	400 x 400	1000	804.2	1.17	2.23
3b	↓	800 x 800	800	777.9	1.07	2.20
3c	↓	1200 x 1200	600	726.2	0.98	2.13
4a	WEST—NORTH	400 x 400	1000	802.0	1.15	2.23
4b	↓	800 x 1200	800	765.4	1.18	2.07
4c	↓	800 x 800	800	777.9	1.07	2.20
4d	↓	1200 x 1200	600	726.2	0.98	2.13
5a	EAST—CNTRD	400 x 400	1000	727.8	0.21	2.12
5b	↓	800 x 800	800	771.6	0.22	2.18
5c	↓	1200 x 1200	600	802.1	0.19	2.22
6a	WEST—N-S EXT	800 x 3600	200	624.5	0.80	1.30
6b	↓	800 x 3200	400	701.7	0.96	1.51
6c	↓	800 x 2800	600	719.8	1.04	1.63
7a	WEST—S EXT	800 x 1600	200	716.8	0.79	2.14
7b	↓	800 x 1400	400	755.0	0.96	2.13
7c	↓	800 x 1200	600	768.2	1.06	2.13
8a	WEST—W EXT	400 x 400	1000	806.0	1.17	2.23
8b	↓	600 x 400	800	798.3	1.18	2.21
8c	↓	800 x 400	600	786.9	1.14	2.20
8d	↓	1000 x 400	400	807.5	1.17	2.21
8e	↓	1200 x 400	200	746.6	1.34	2.22

TABLE I: Data Case Studies used and results obtained over a 210 day integration

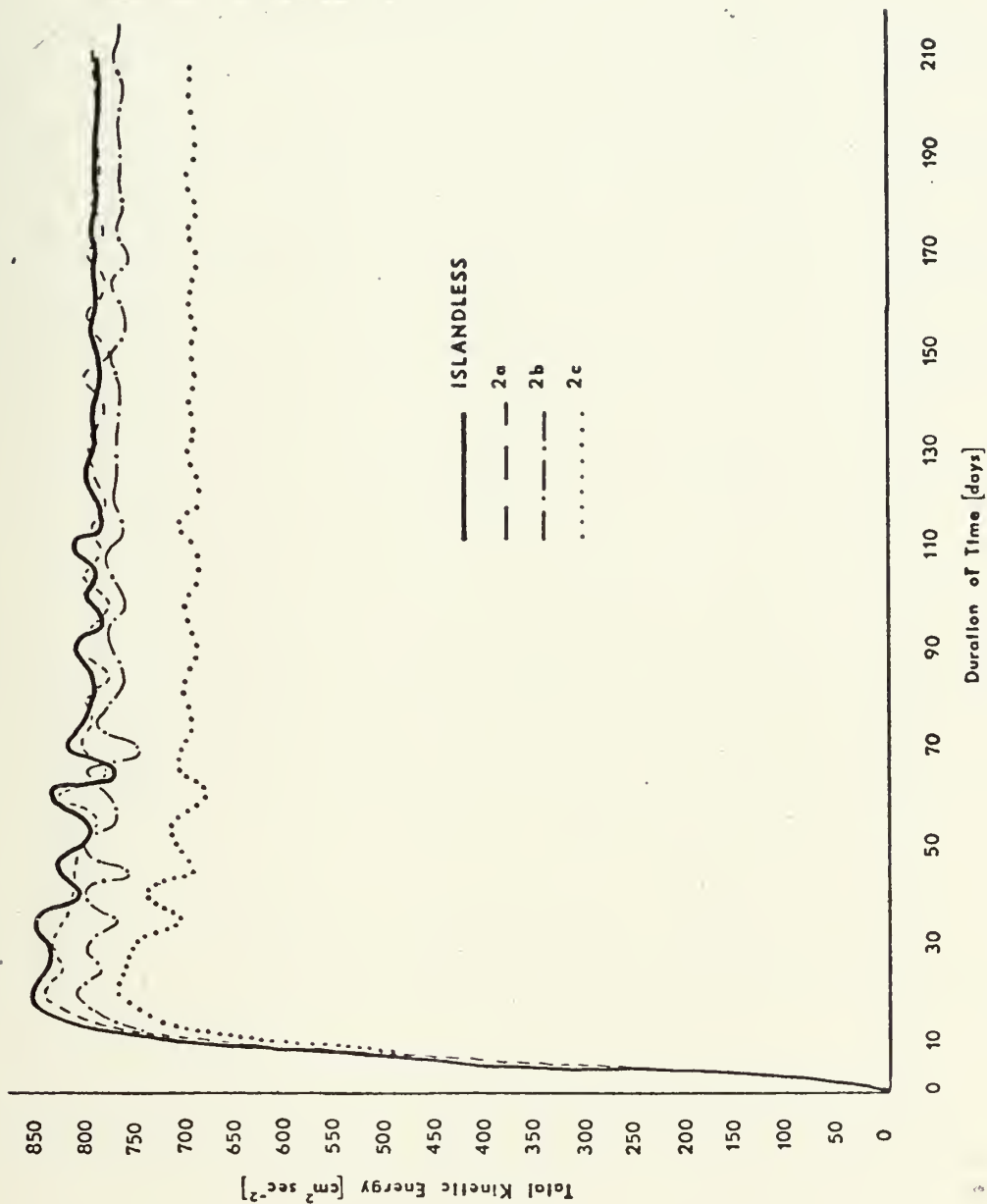


Figure 3: Total Kinetic Energy for Case 2 for island sizes -
a) 400 km on a side; b) 800 km on a side; and
c) 1200 km on a side, compared to Case 1, the
islandless case

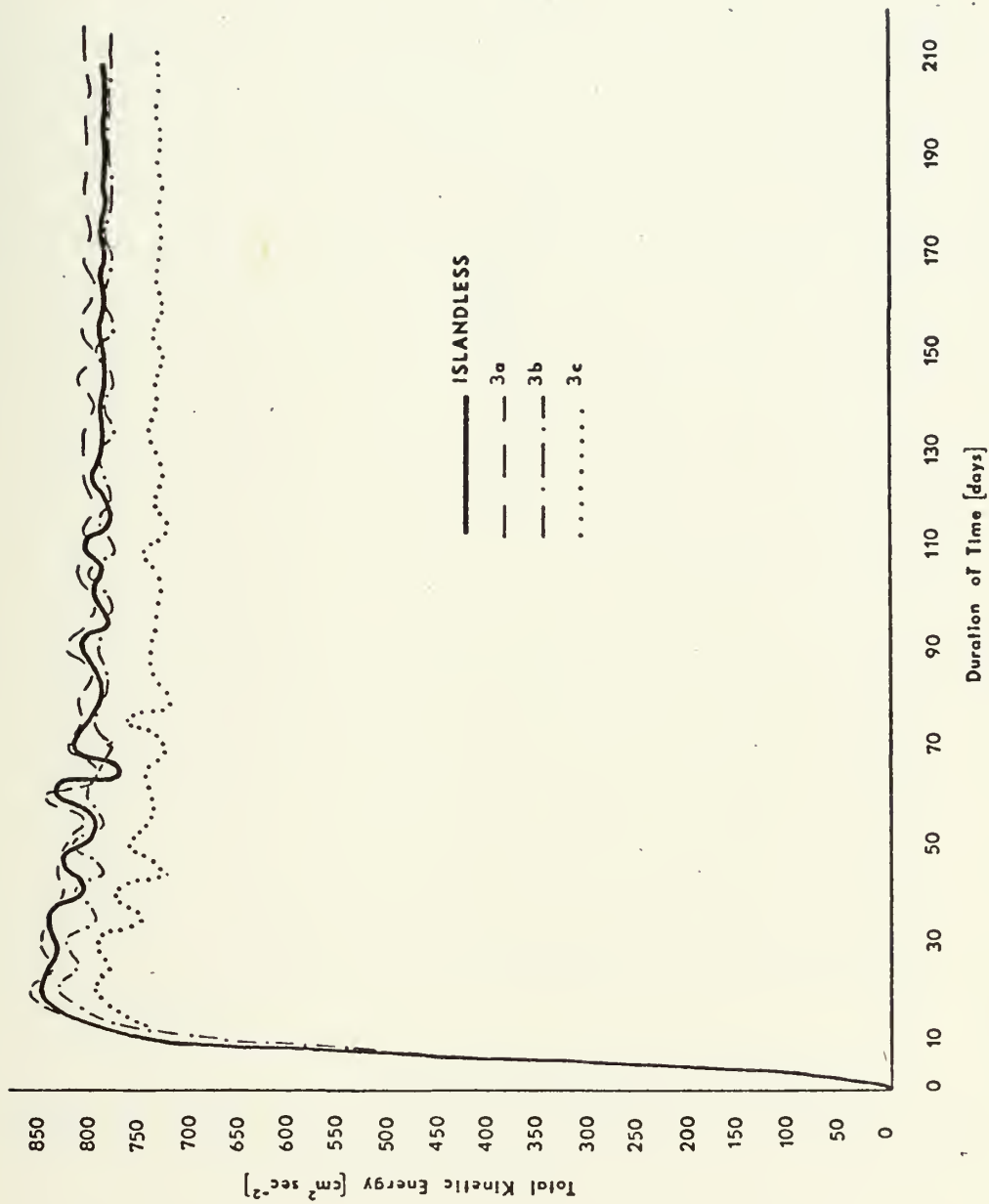


Figure 4: Same as Figure 3 except for Case 3

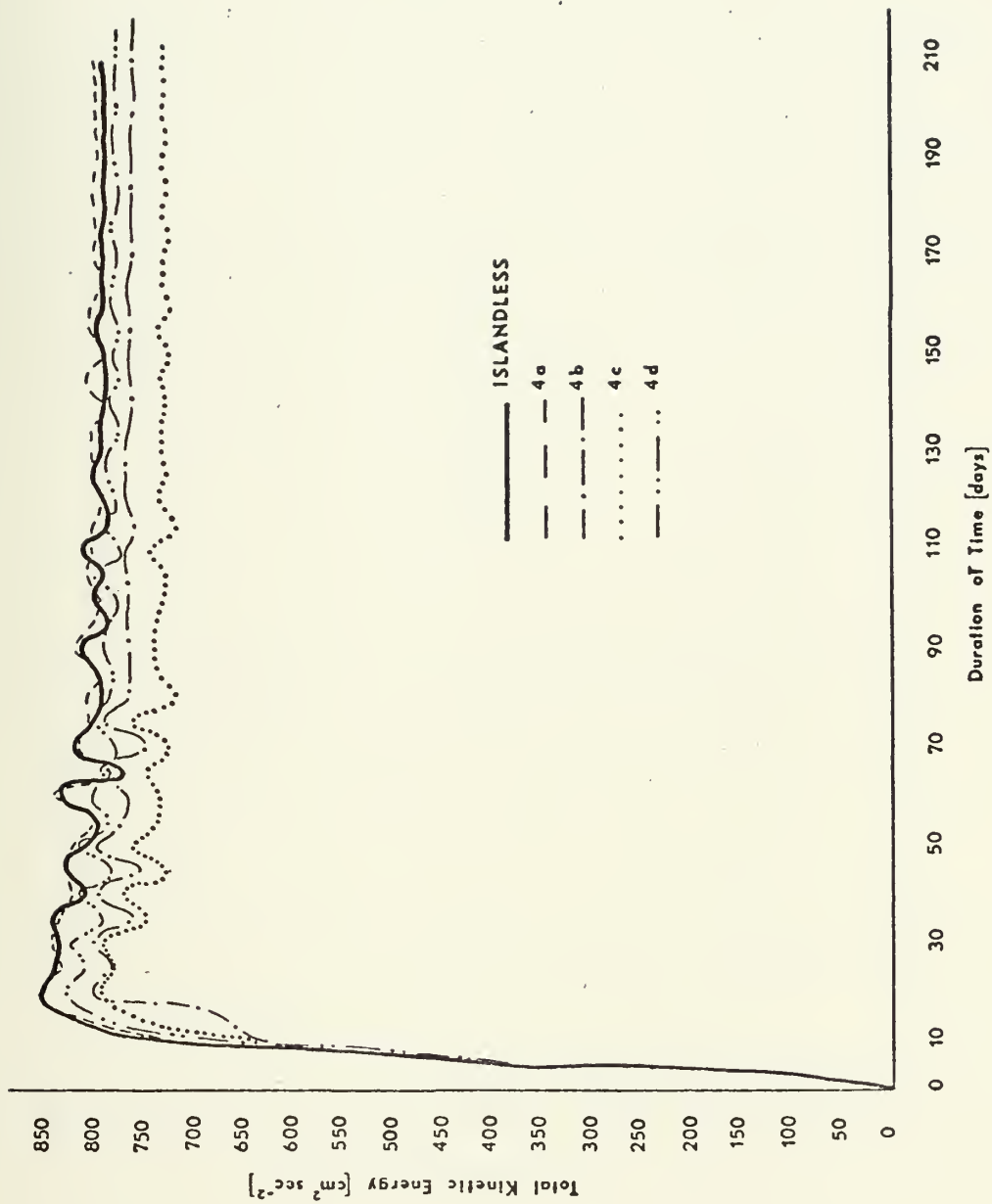


Figure 5: Same as Figure 3 except for Case 4, island sizes -
a) 400 km on a side; b) 800 x 1200 km²;
c) 800 km on a side; d) 1200 km on a side

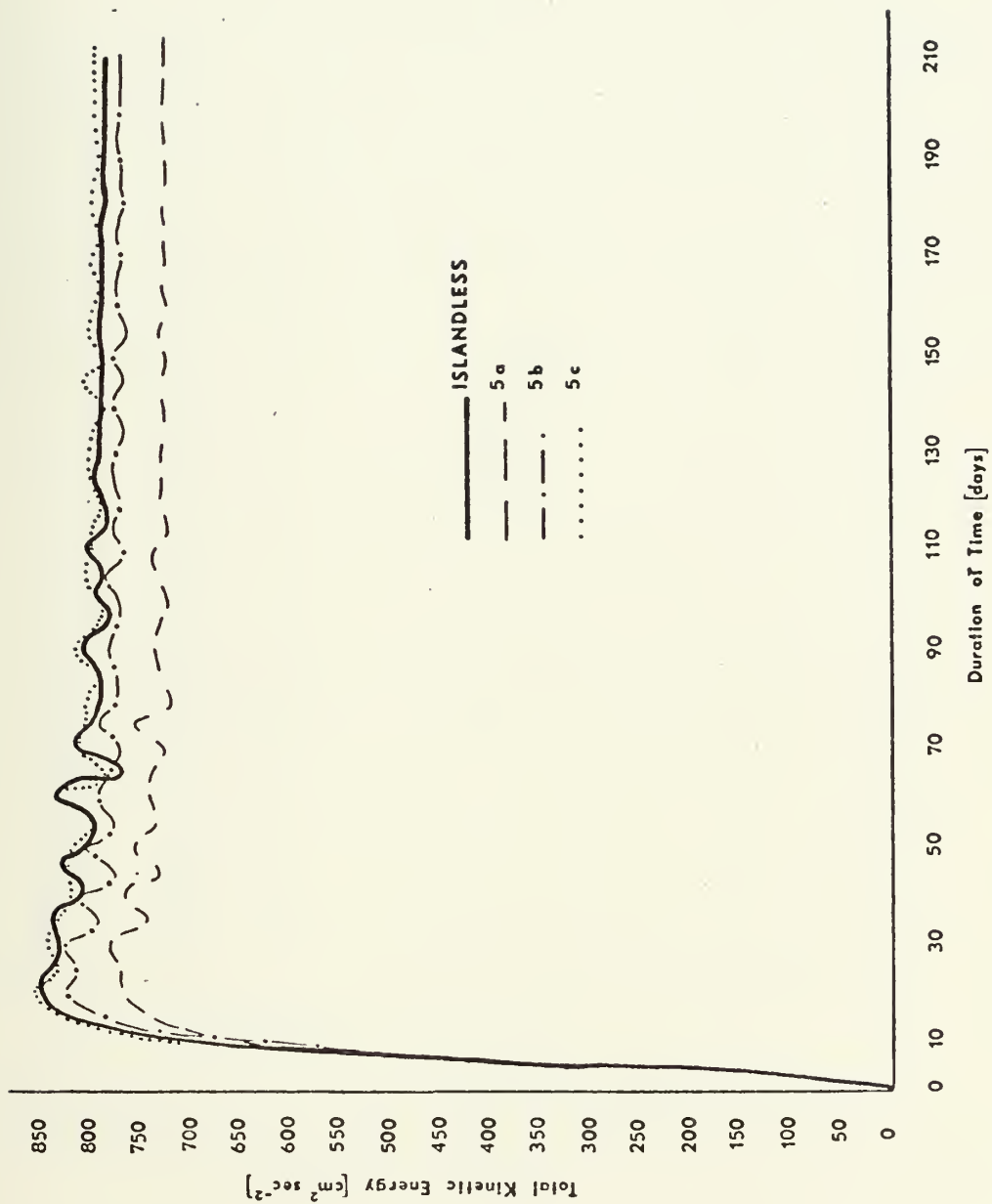


Figure 6: Same as Figure 3 except for Case 5

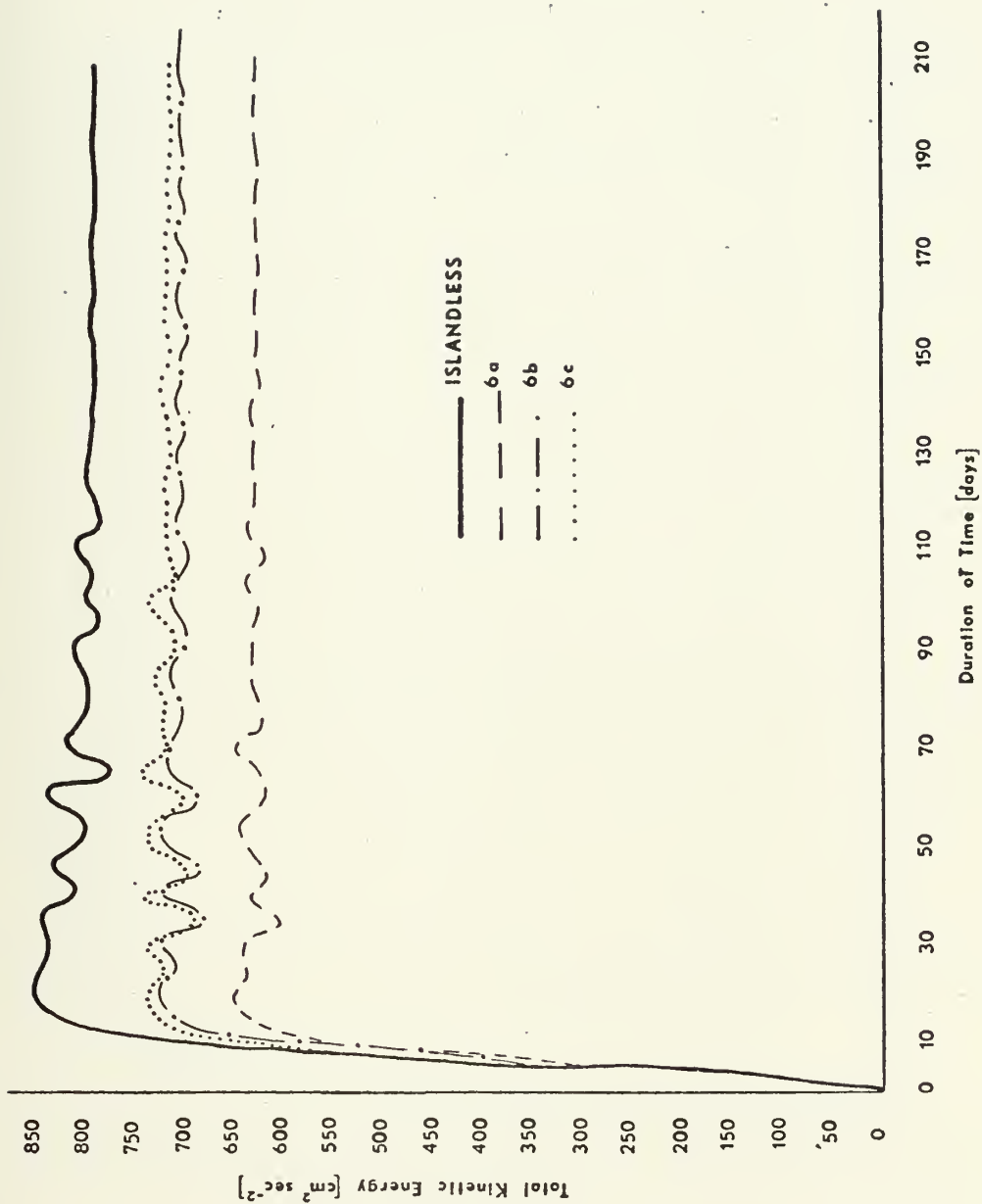


Figure 7: Same as Figure 3 except for Case 6, island sizes -
a) $800 \times 3600 \text{ km}^2$; b) $800 \times 3200 \text{ km}^2$; and
c) $800 \times 2800 \text{ km}^2$

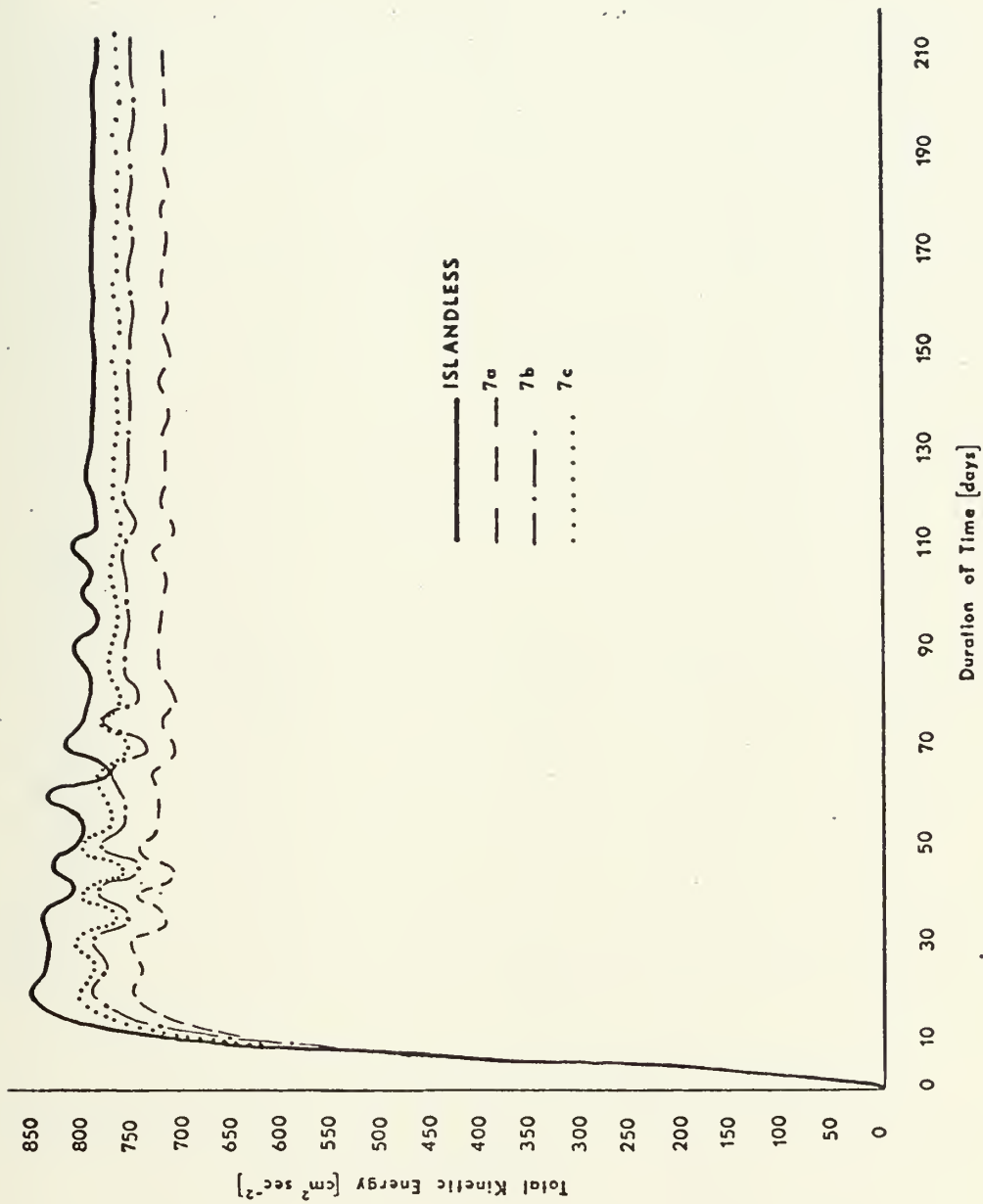


Figure 8: Same as Figure 3 except for Case 7, island sizes -
 a) $800 \times 1600 \text{ km}^2$; b) $800 \times 1400 \text{ km}^2$; and
 c) $800 \times 1200 \text{ km}^2$

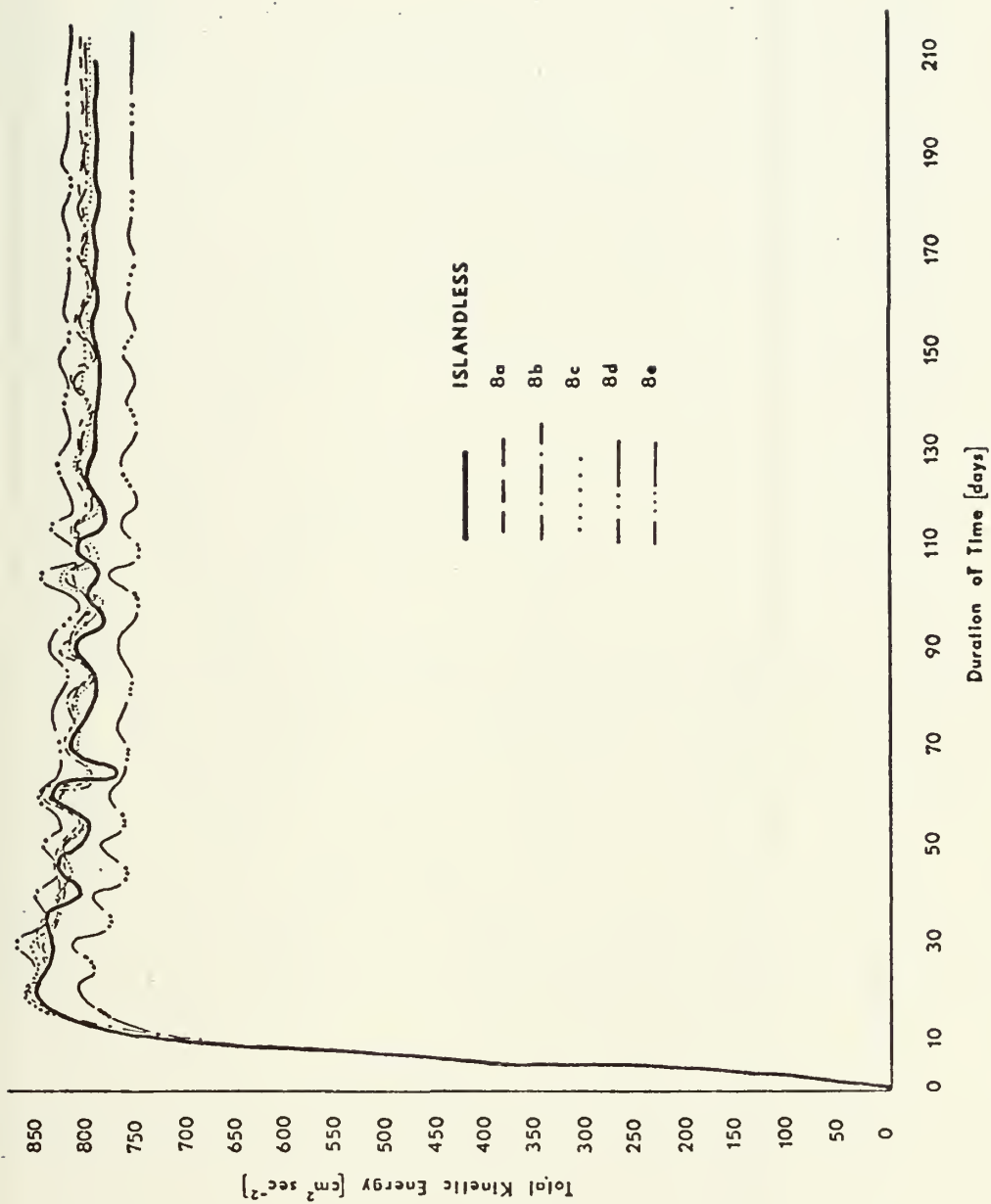


Figure 9: Same as Figure 3 except for Case 8, island sizes -
 a) 400 km on a side; b) 600 x 400 km²; c) 800 x 400 km²;
 d) 1000 x 400 km²; and e) 1200 x 400 km²

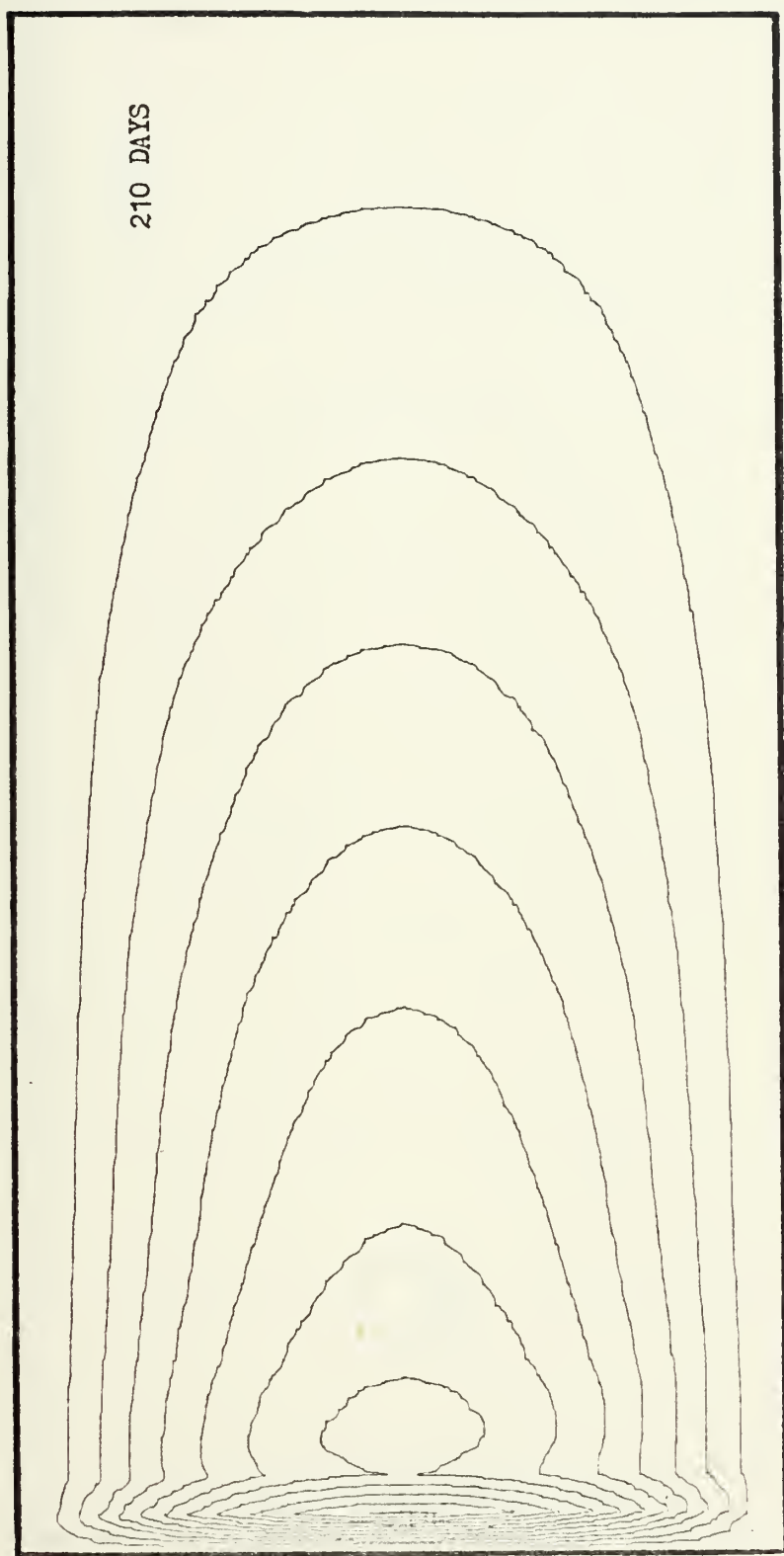


Figure 10: Streamfunction map for Case 1. Isolines are drawn for every $0.2 \times 10^8 \text{ cm}^2 \text{ sec}^{-1}$

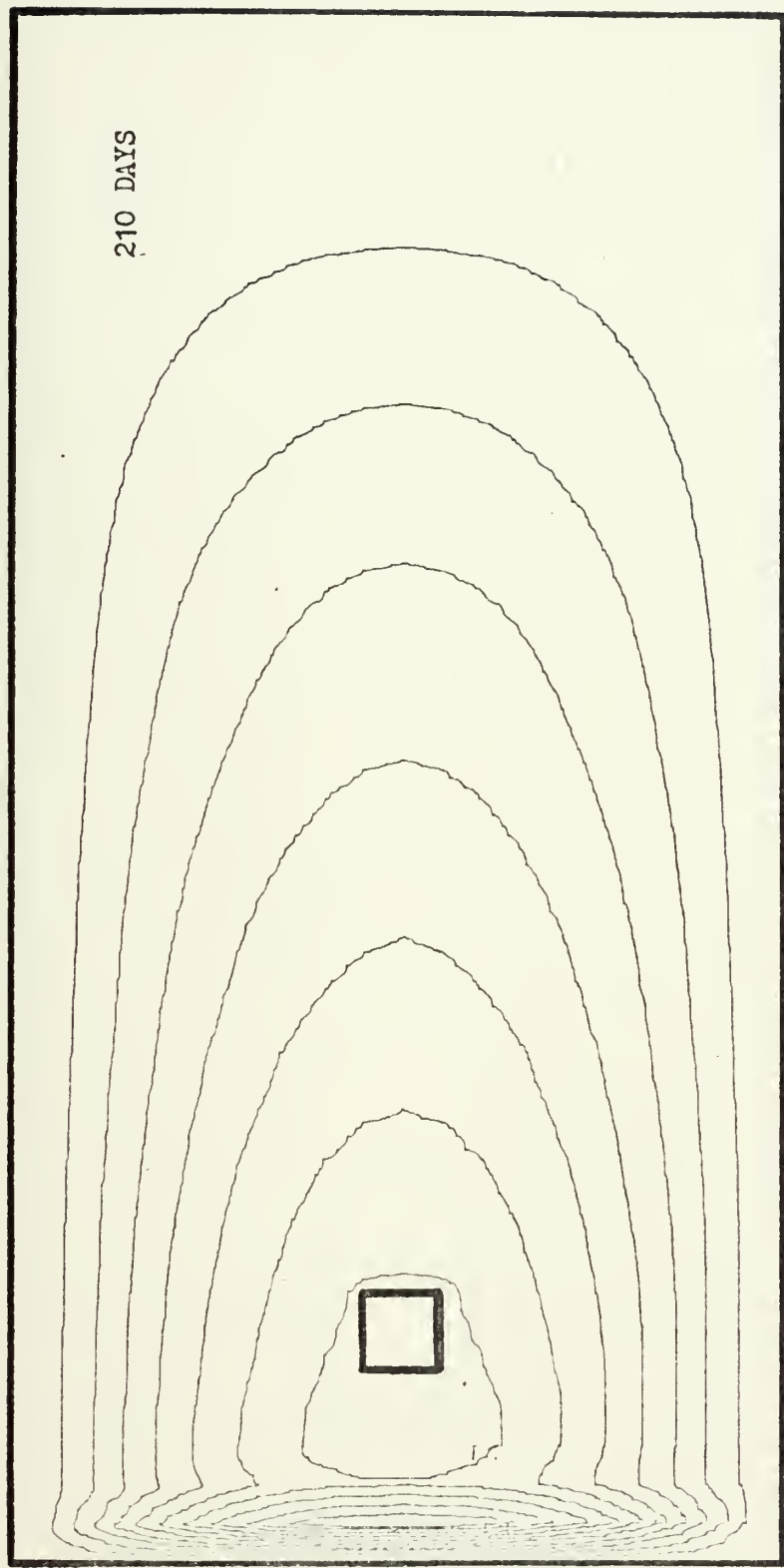


Figure 11: Same as Figure 10 except for Case 2a

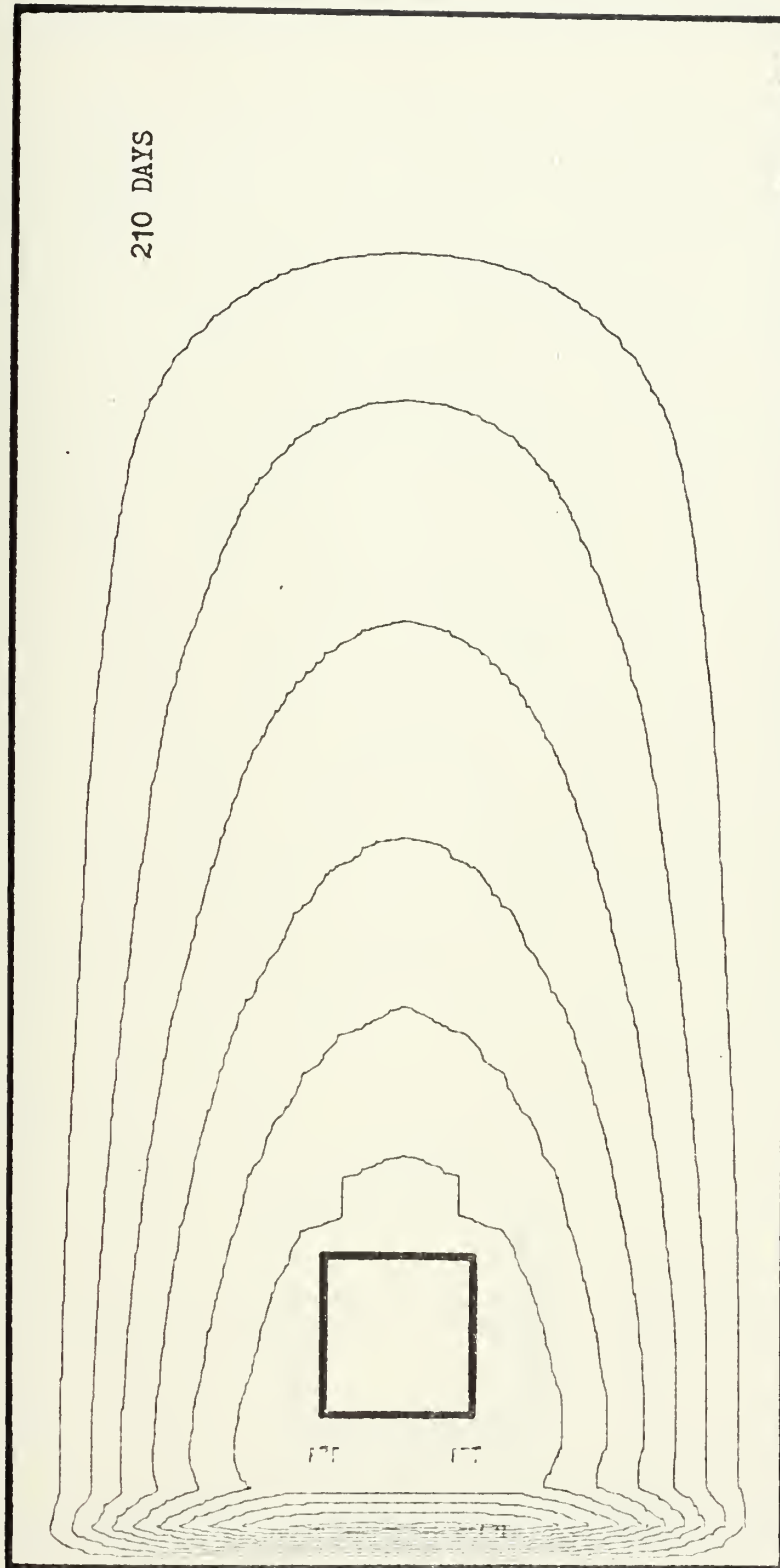


Figure 12: Same as Figure 10 except for Case 2b

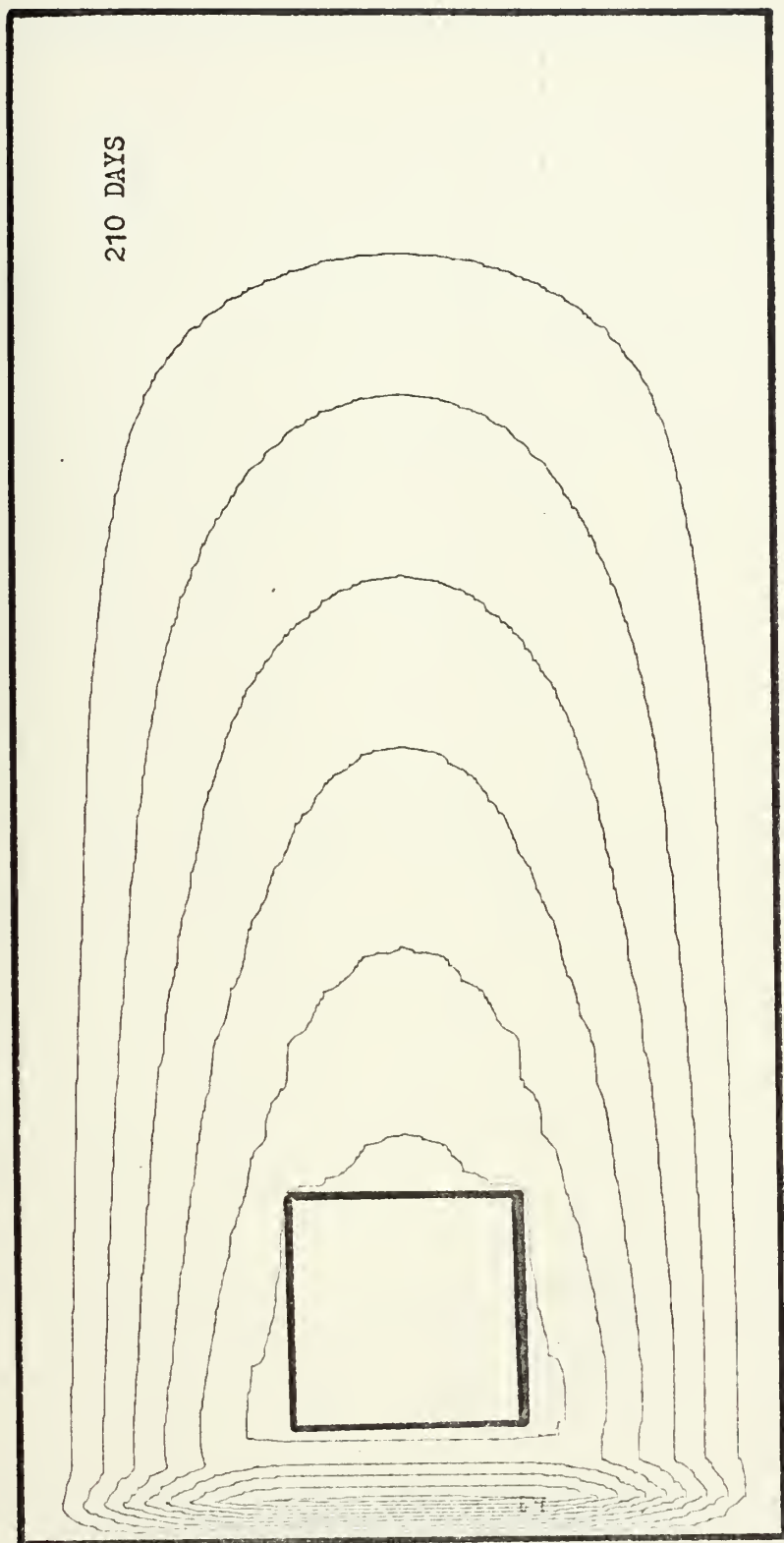


Figure 13: Same as Figure 10 except for Case 2c

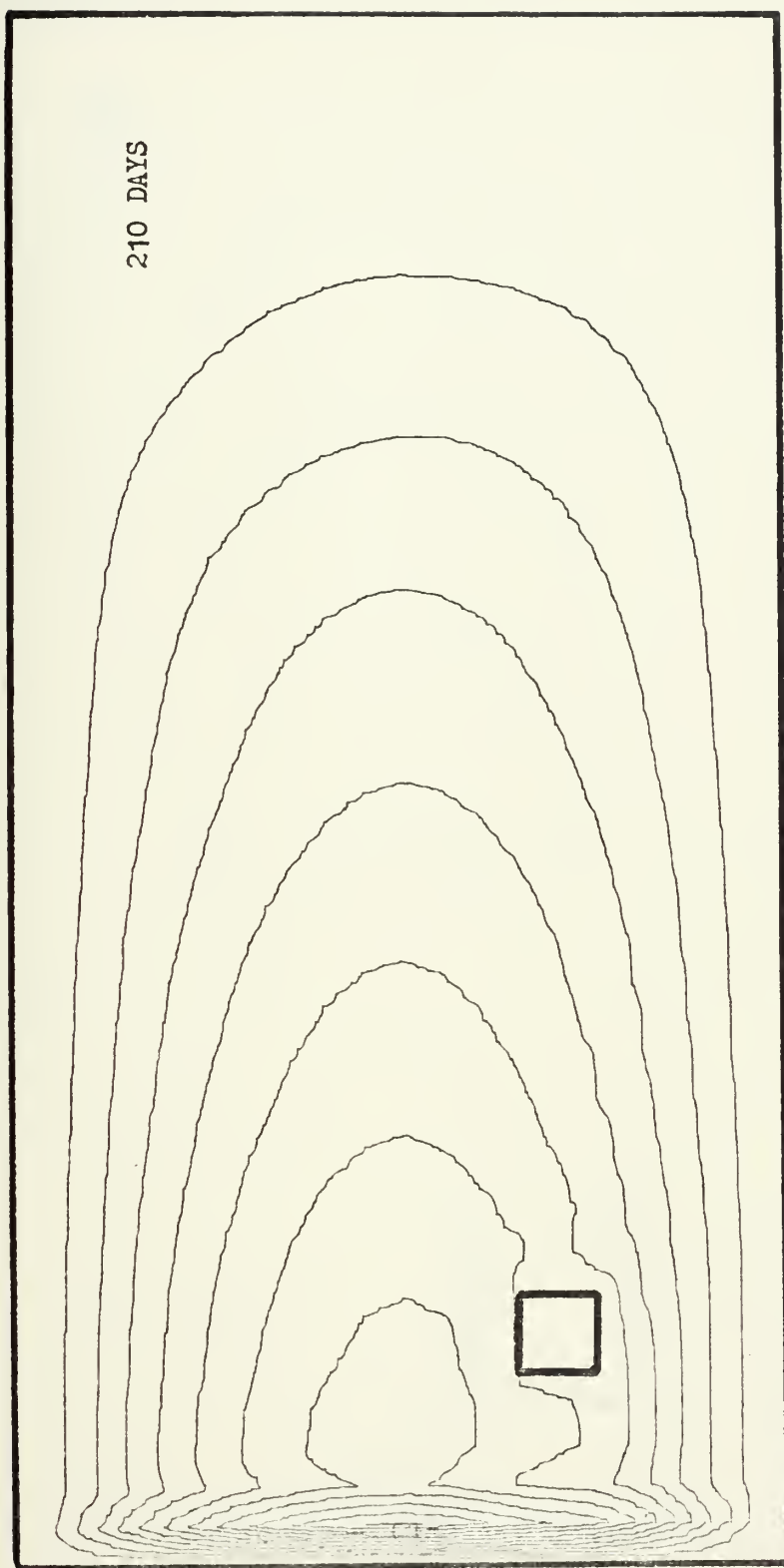


Figure 14: Same as Figure 10 except for Case 3a



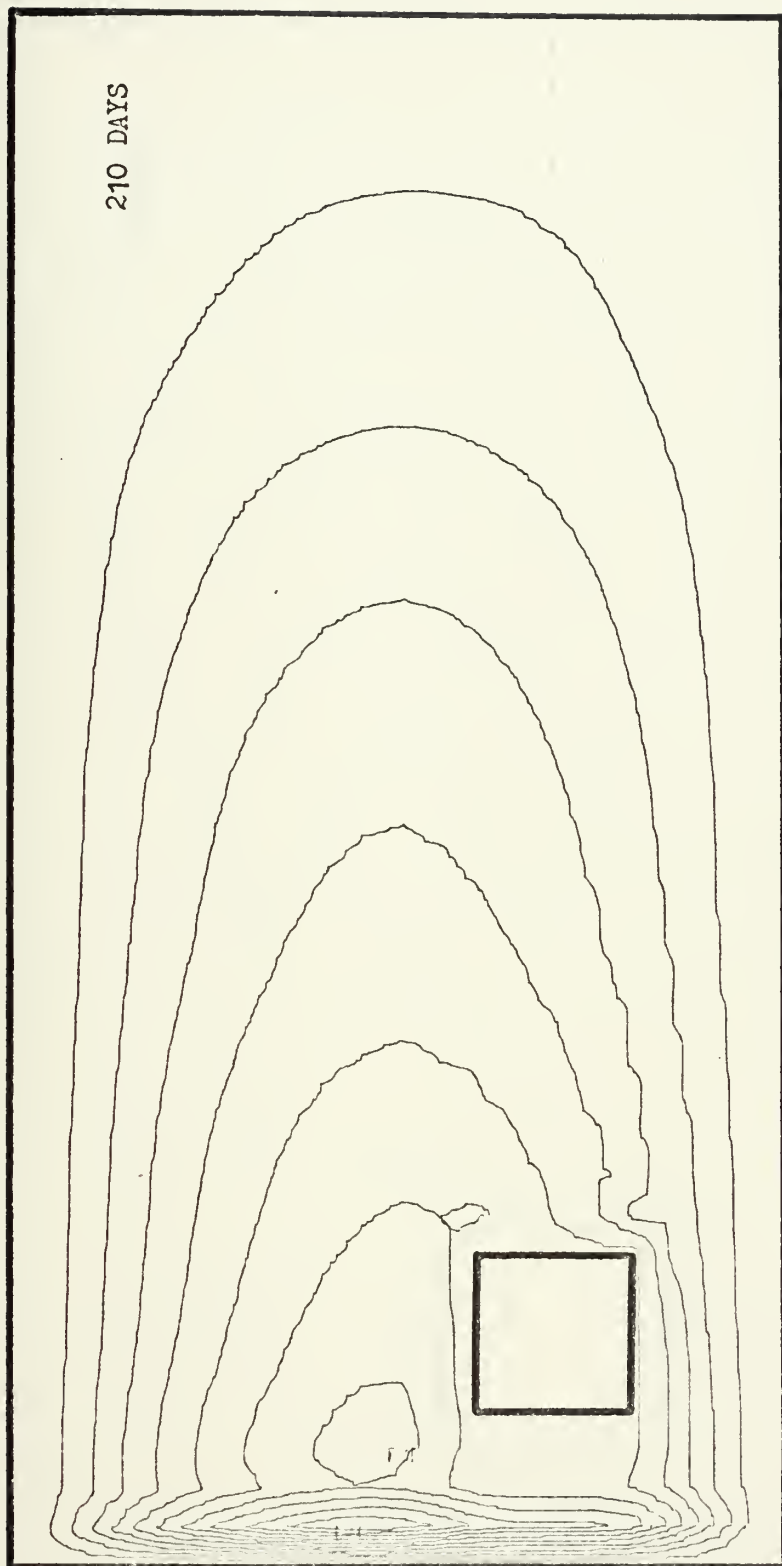


Figure 15: Same as Figure 10 except for Case 3b

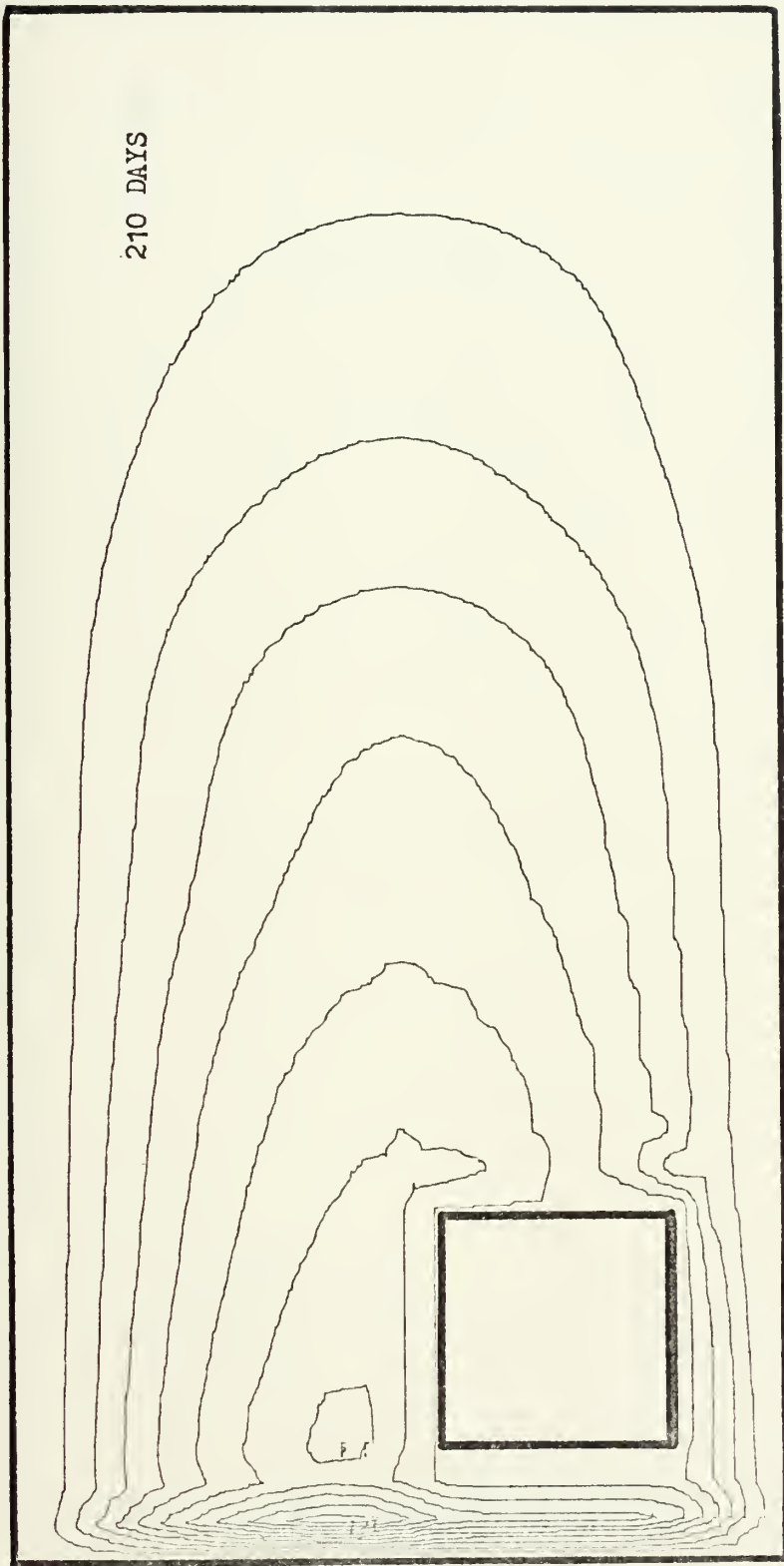


Figure 16: Same as Figure 10 except for Case 3c

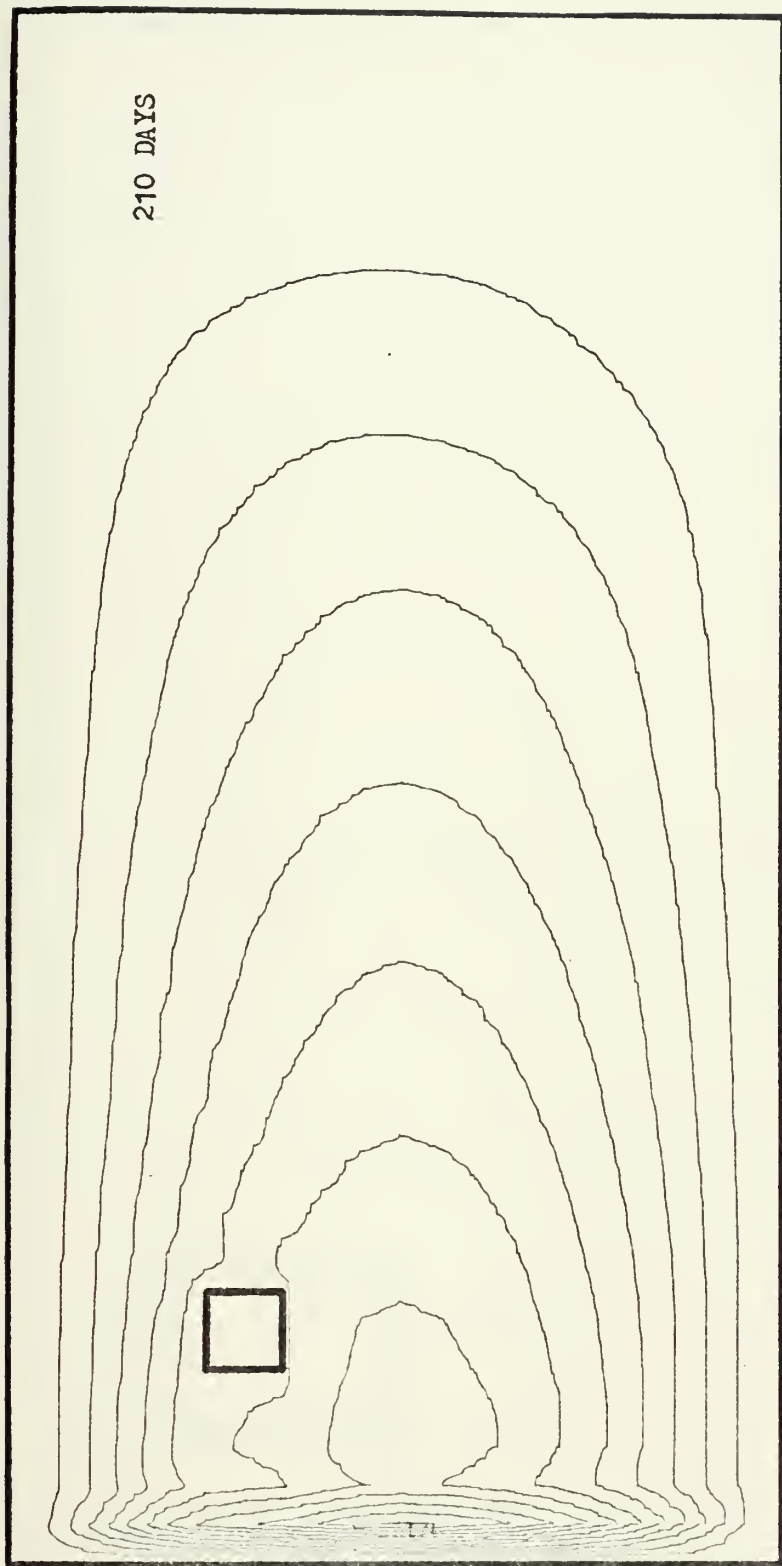


Figure 17: Same as Figure 10 except for Case 4a

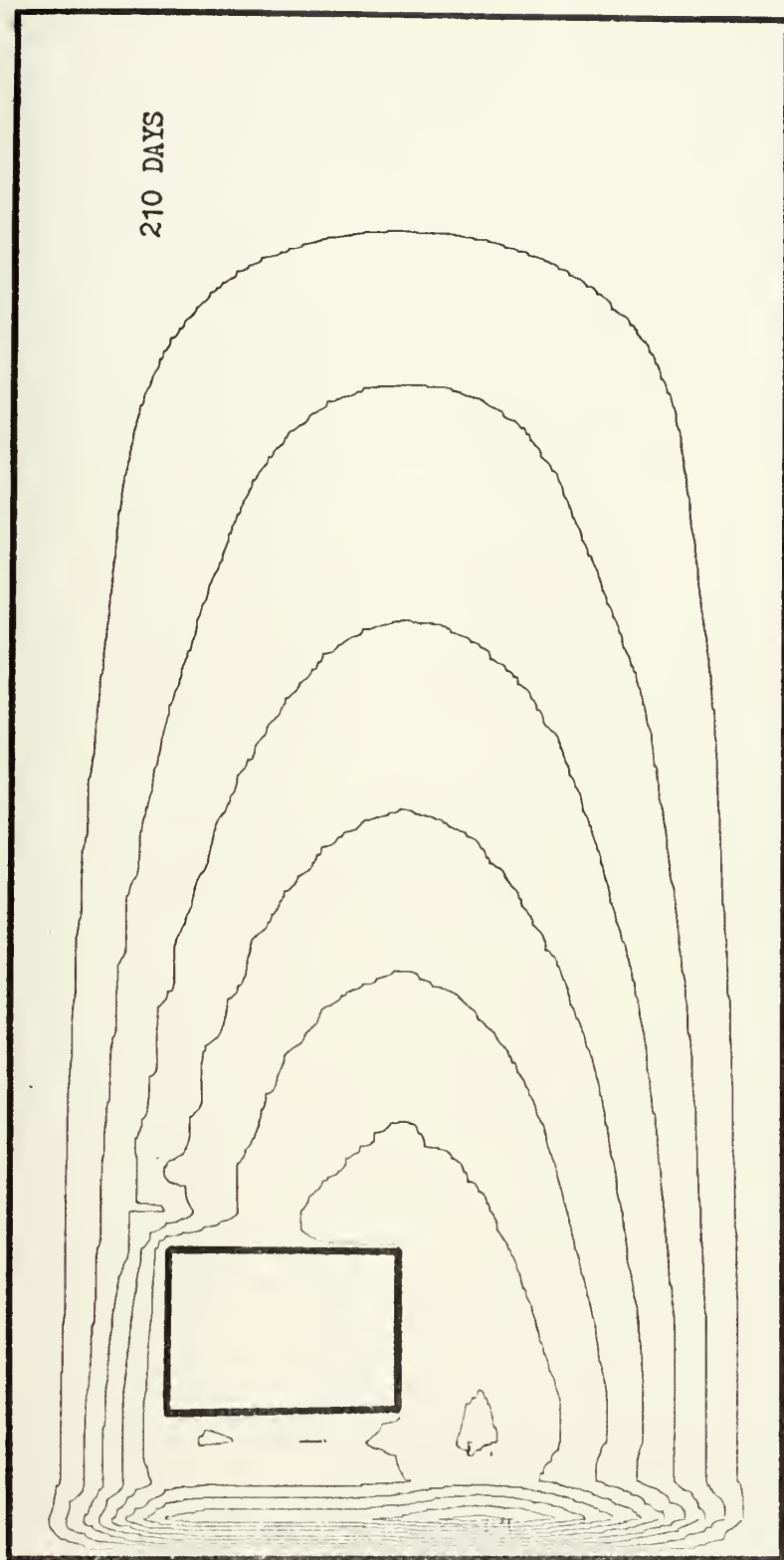


Figure 18: Same as Figure 10 except for Case 4b

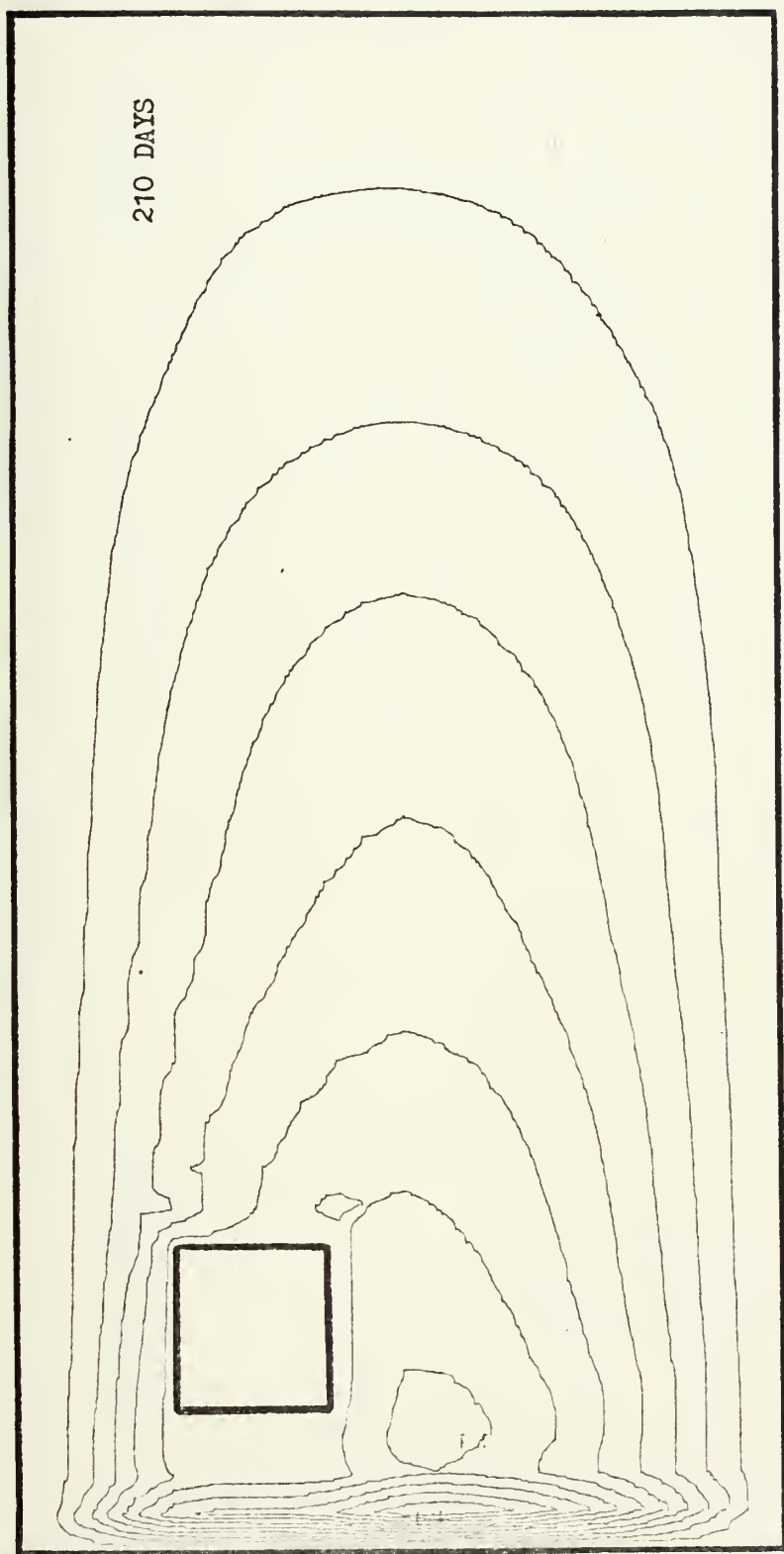


Figure 19: Same as Figure 10 except for Case 4c

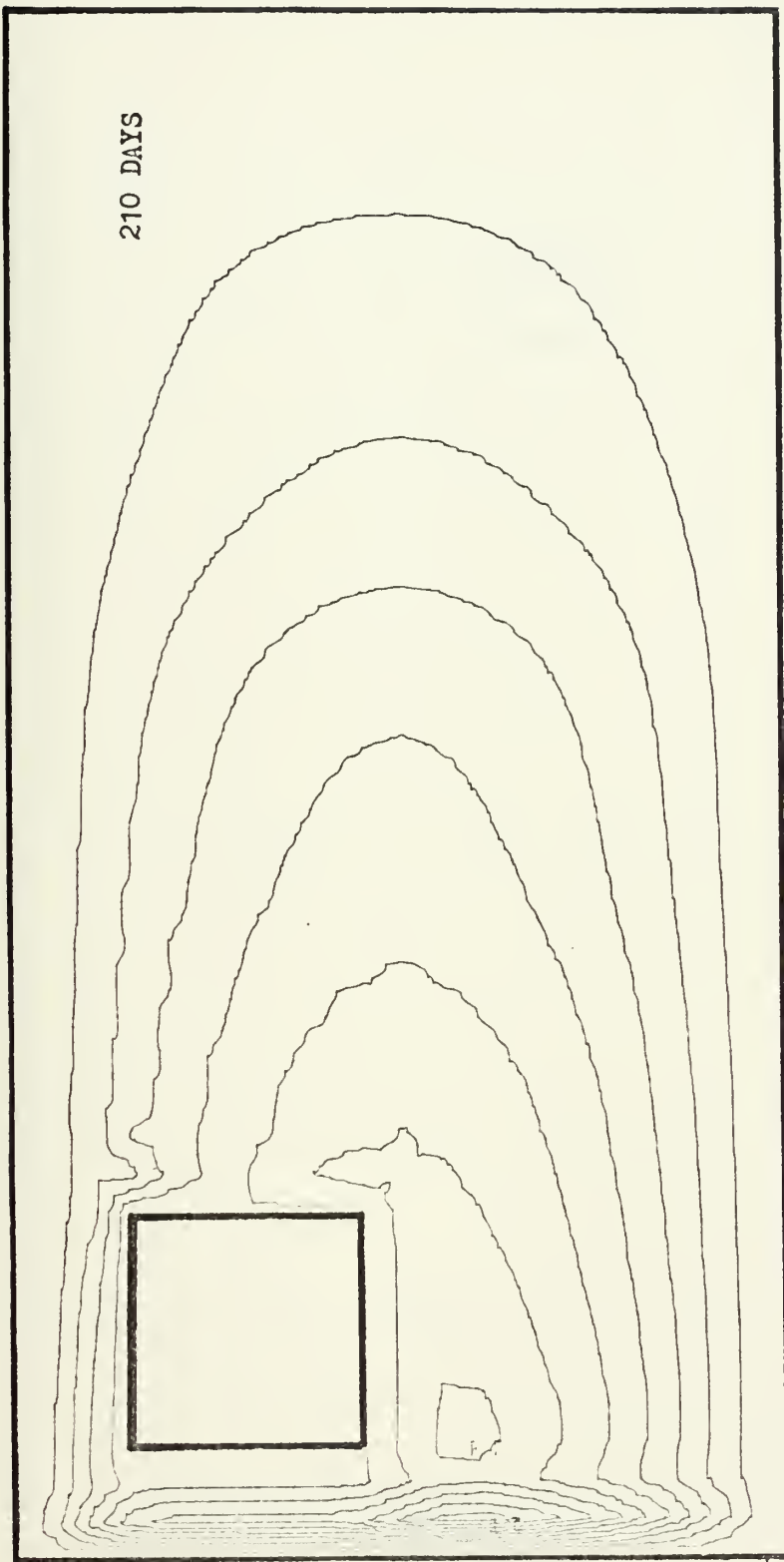


Figure 20: Same as Figure 10 except for Case 4d

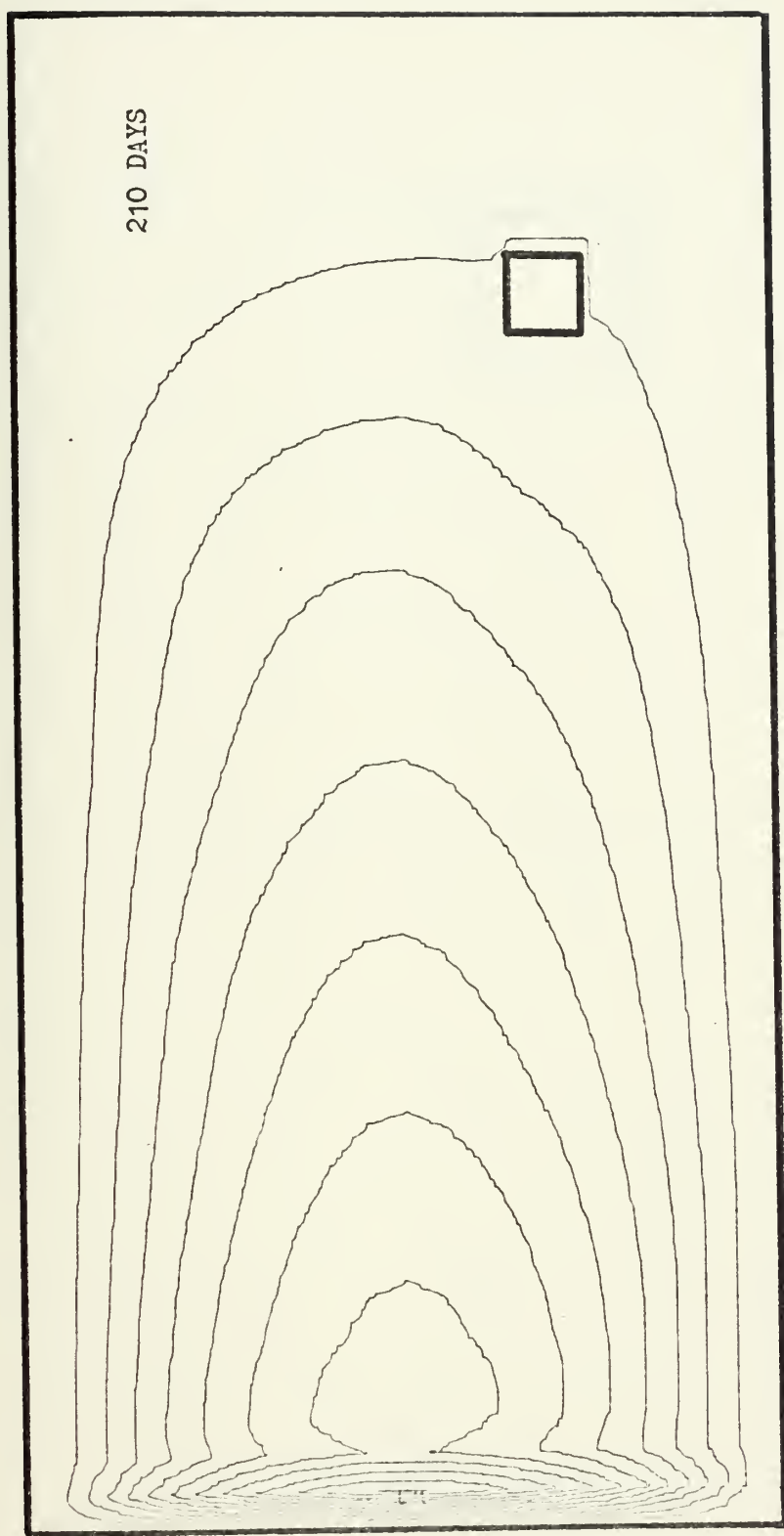


Figure 21: Same as Figure 10 except for Case 5a

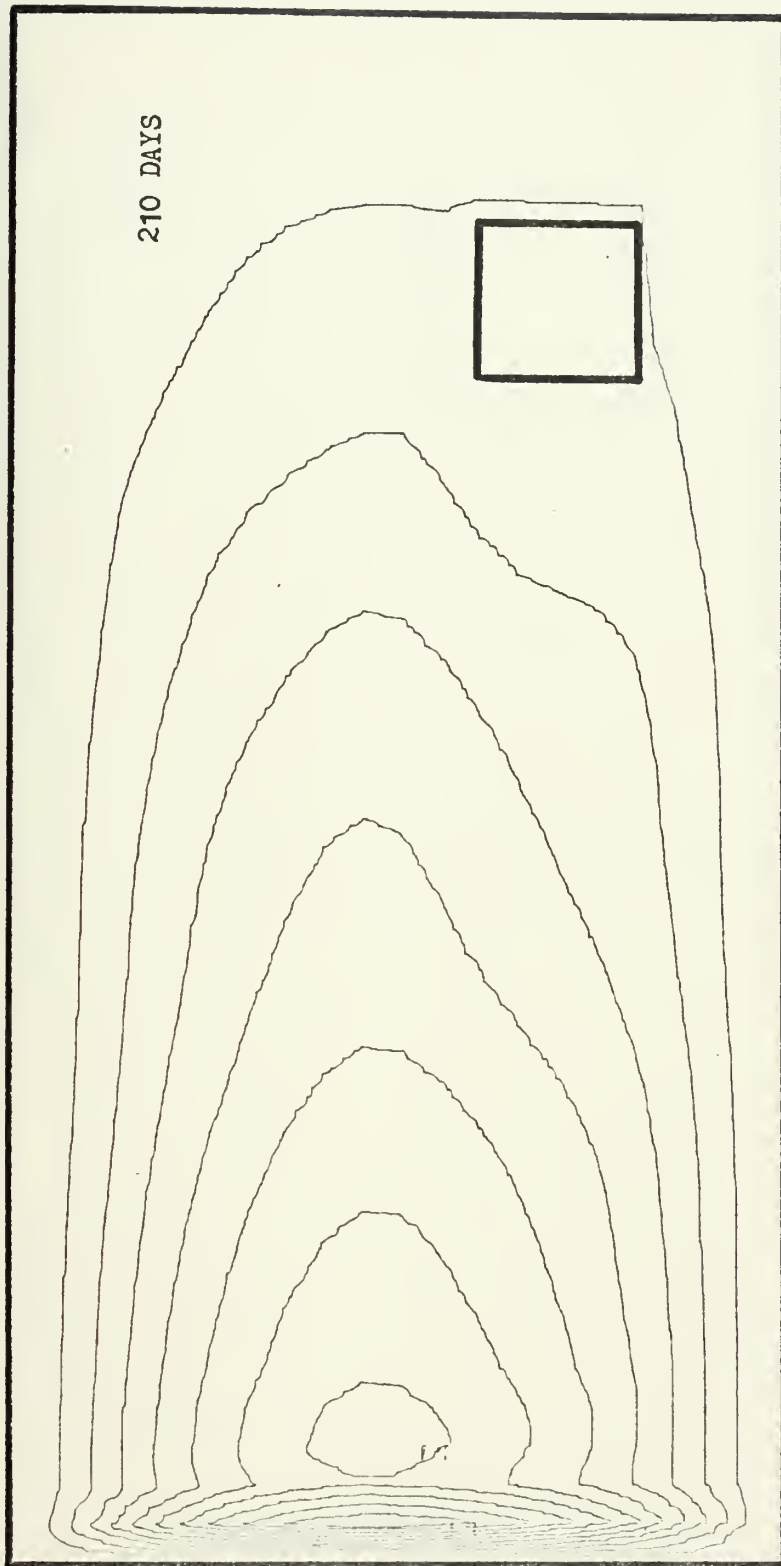


Figure 22: Same as Figure 10 except for Case 5b

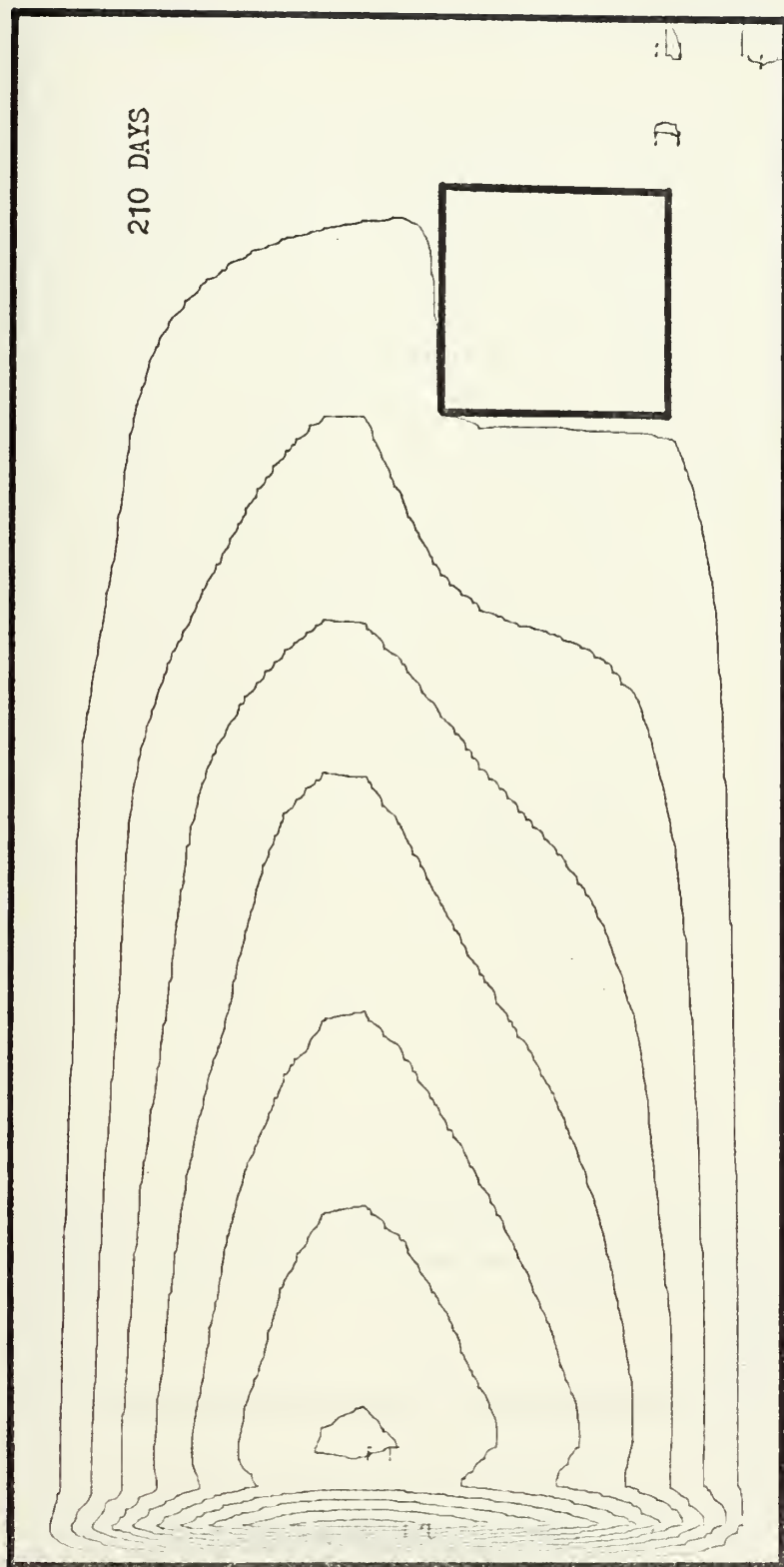


Figure 23: Same as Figure 10 except for Case 5c

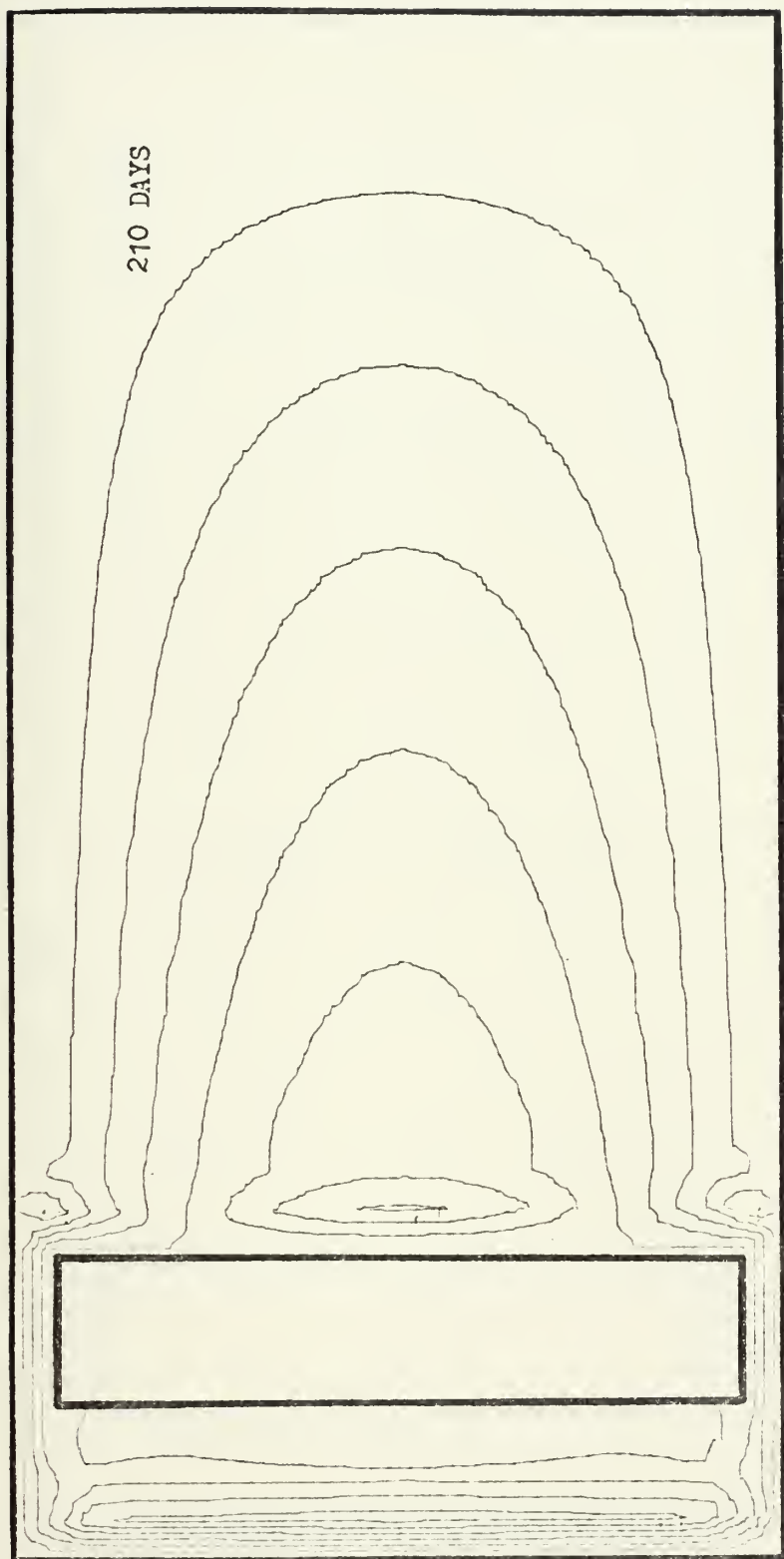


Figure 24: Same as Figure 10 except for Case 6a

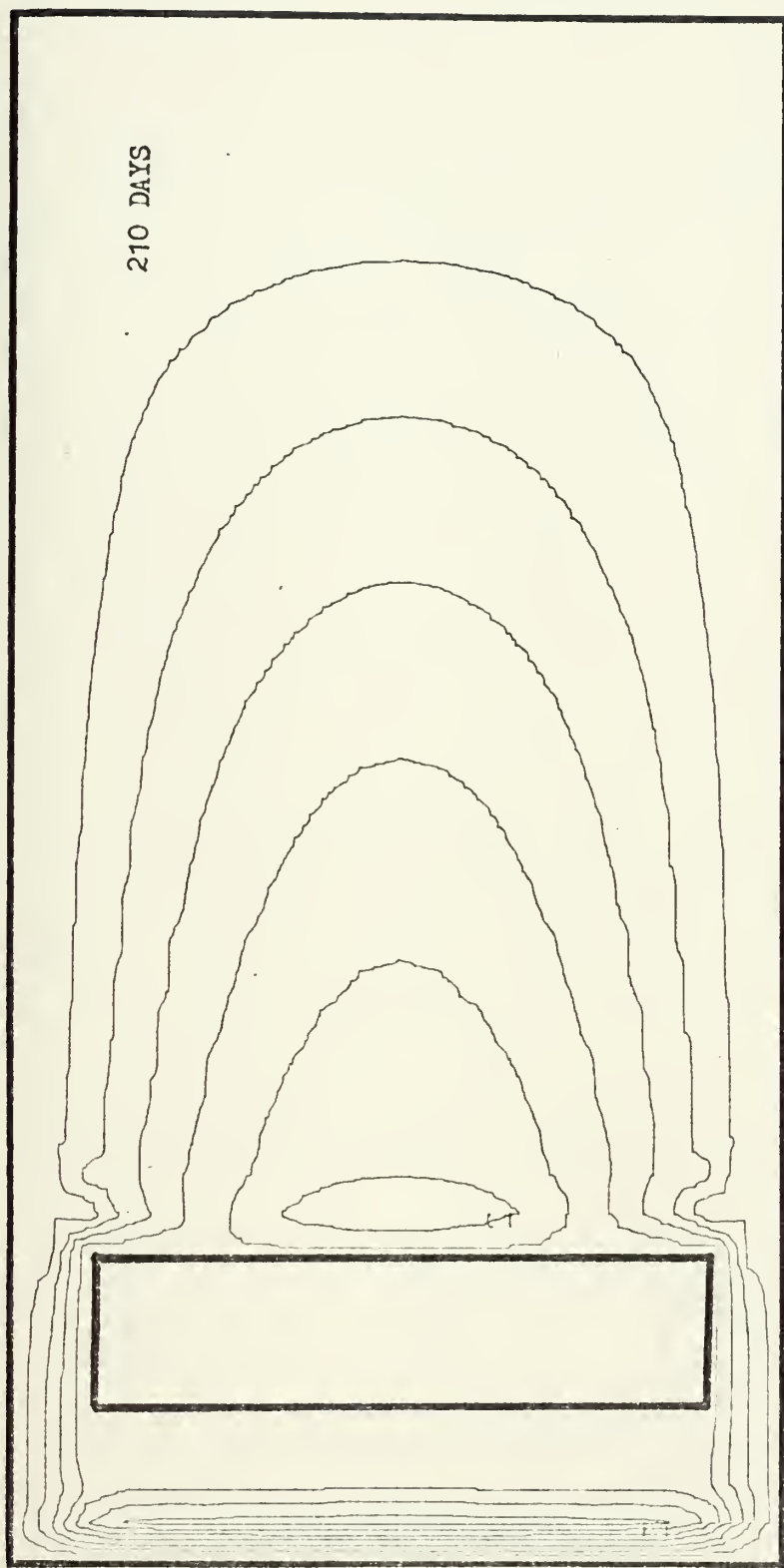


Figure 25: Same as Figure 10 except for Case 6b

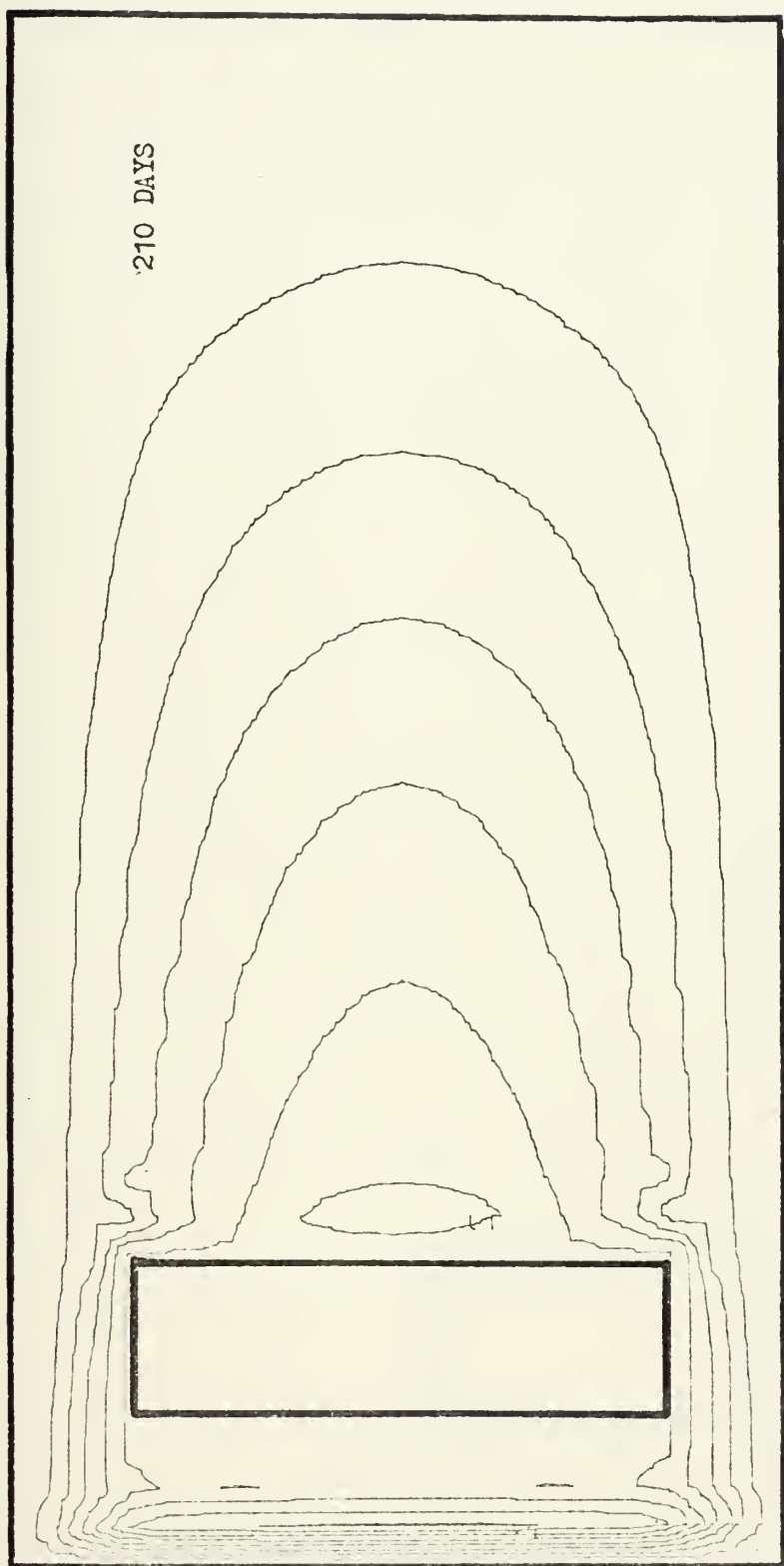


Figure 26: Same as Figure 10 except for Case 6c

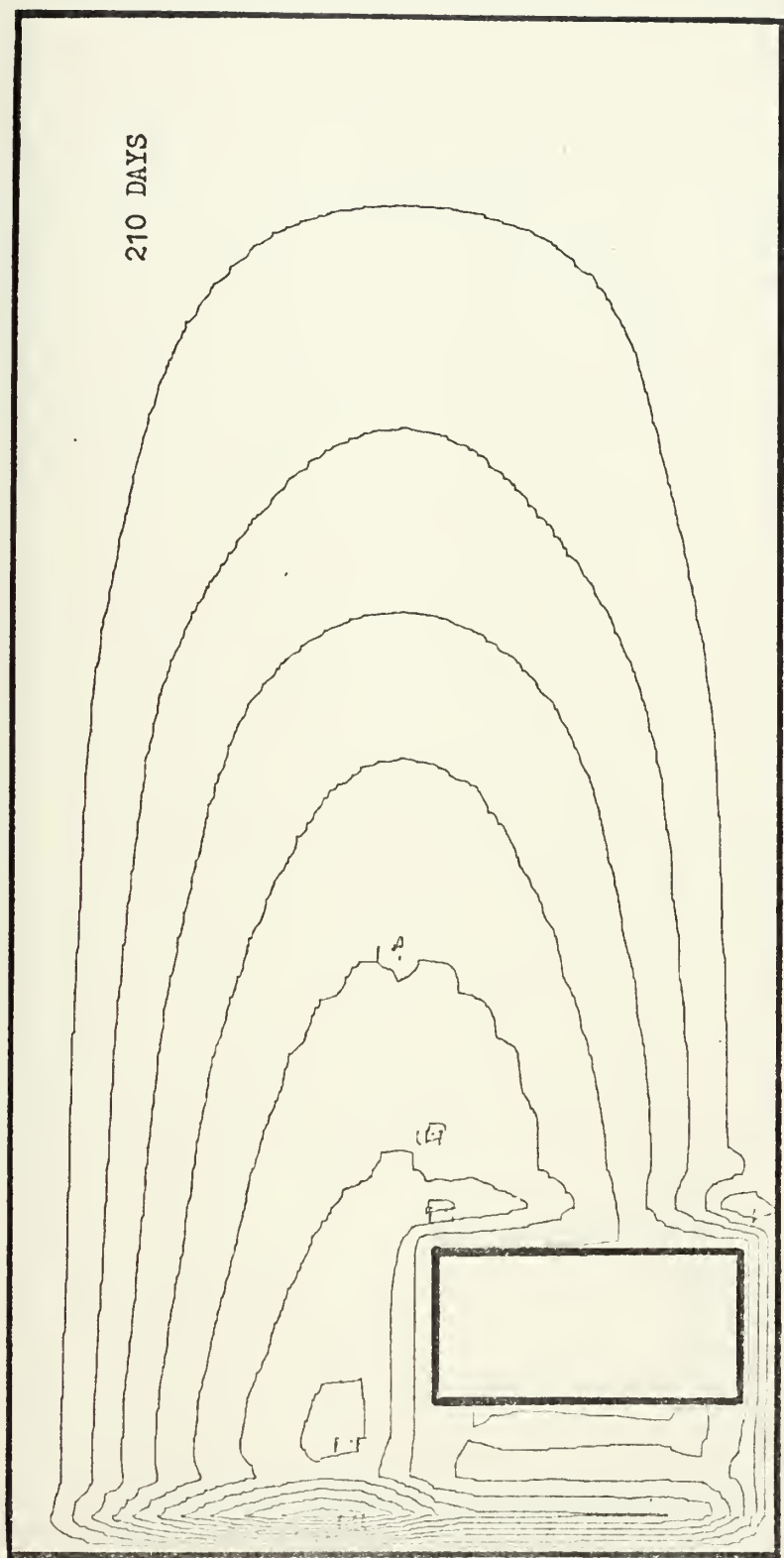


Figure 27: Same as Figure 10 except for Case 7a

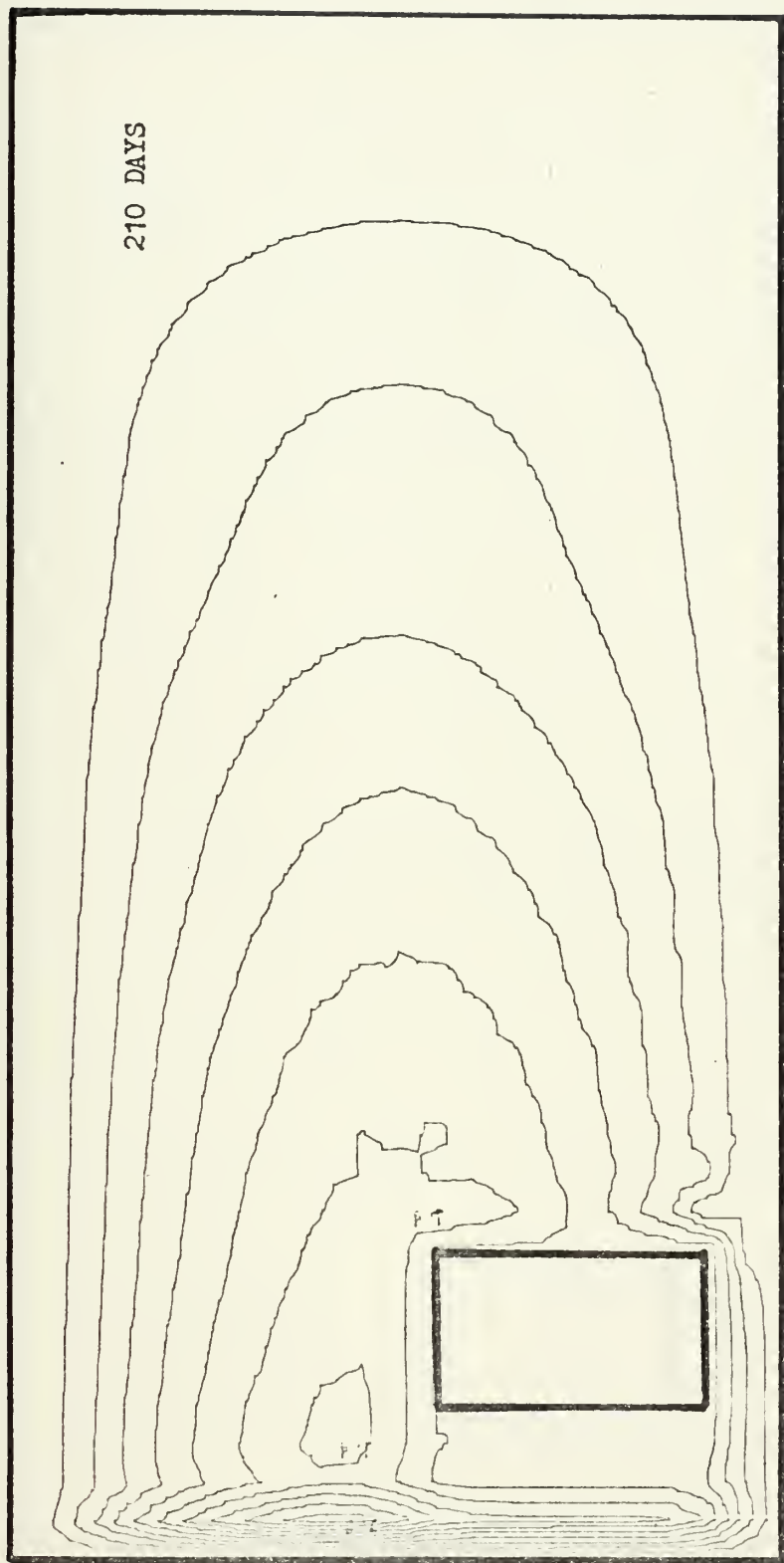


Figure 28: Same as Figure 10 except for Case 7b

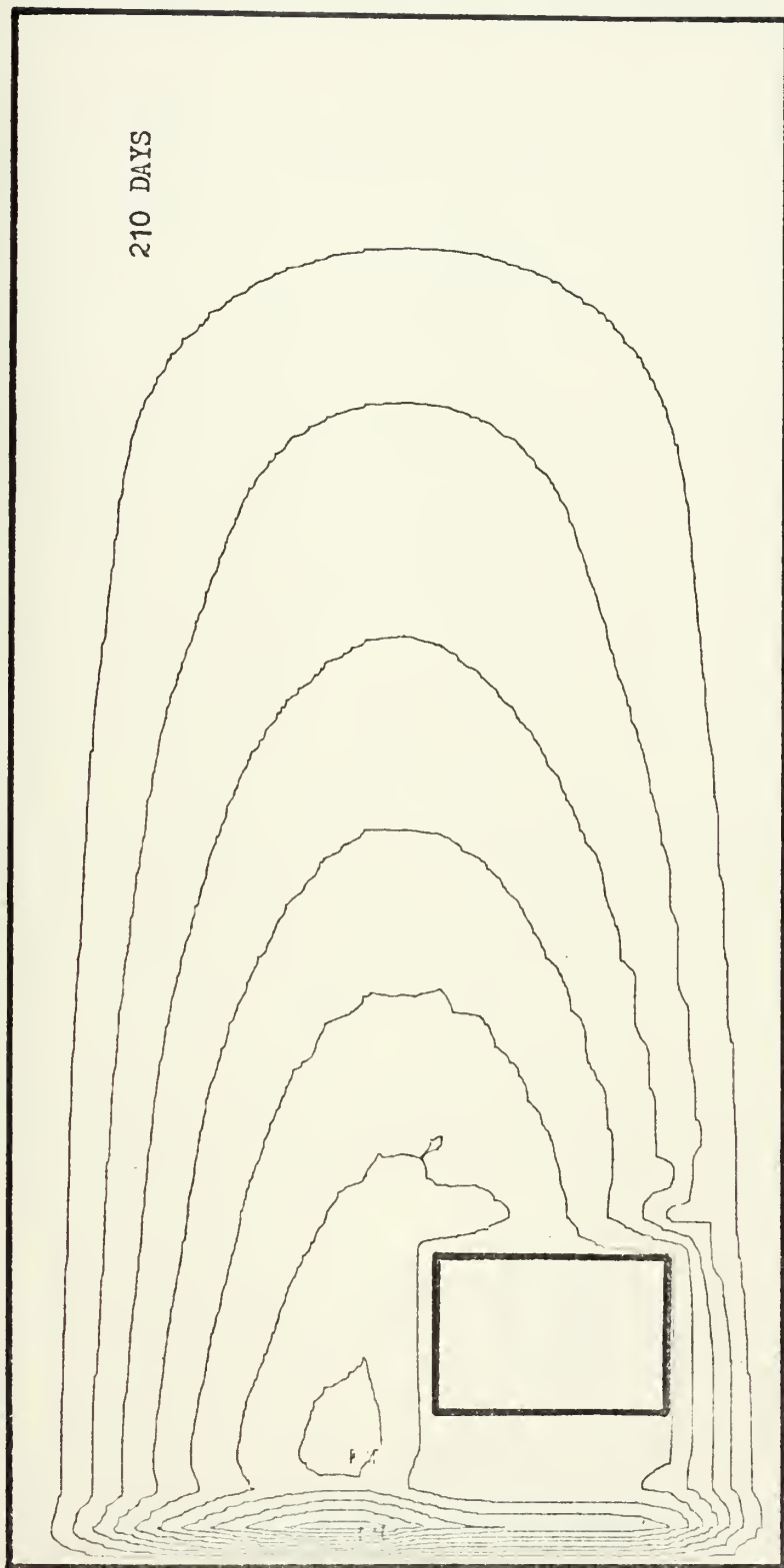


Figure 29: Same as Figure 10 except for Case 7c

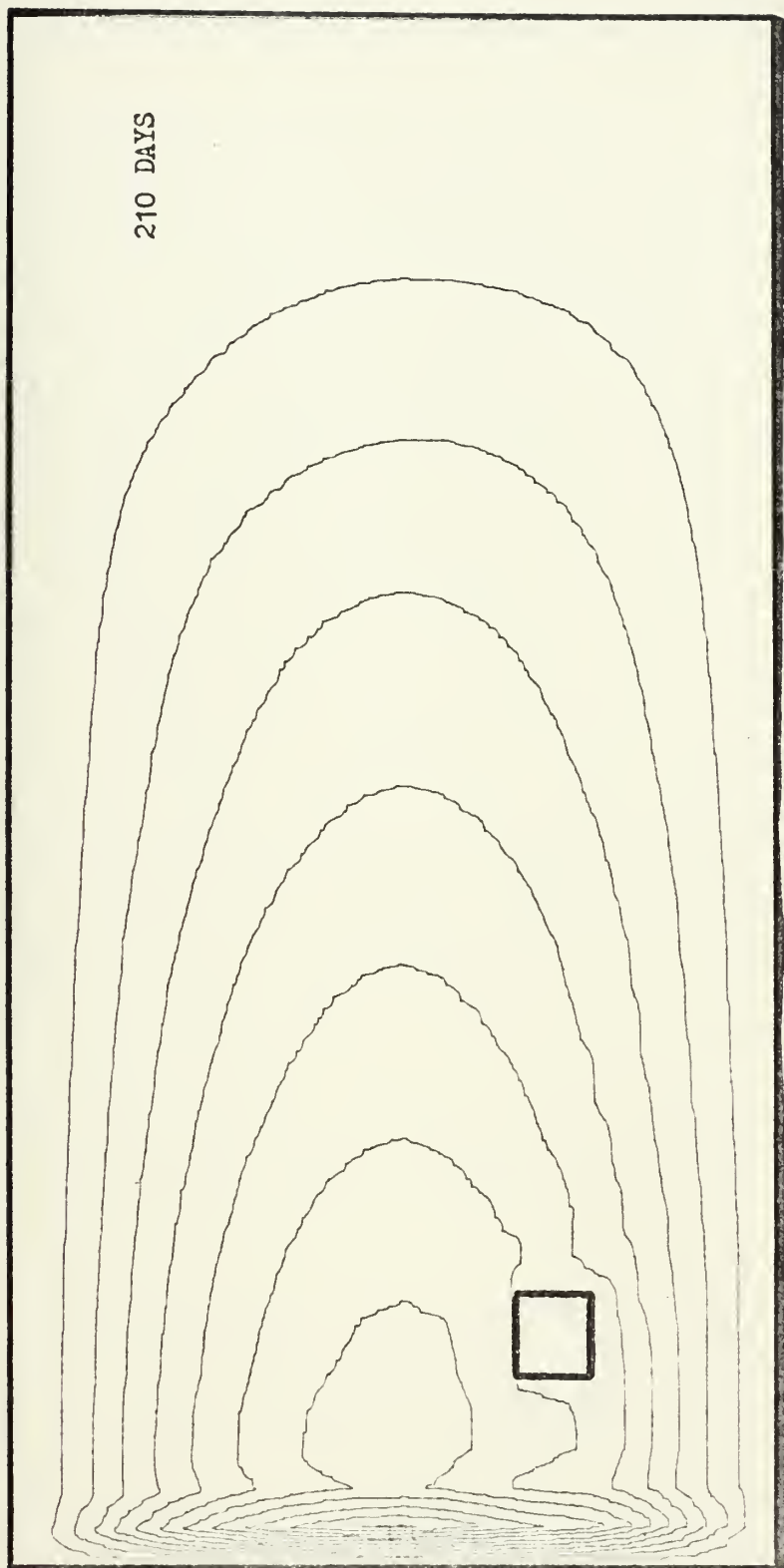


Figure 30: Same as Figure 10 except for Case 8a

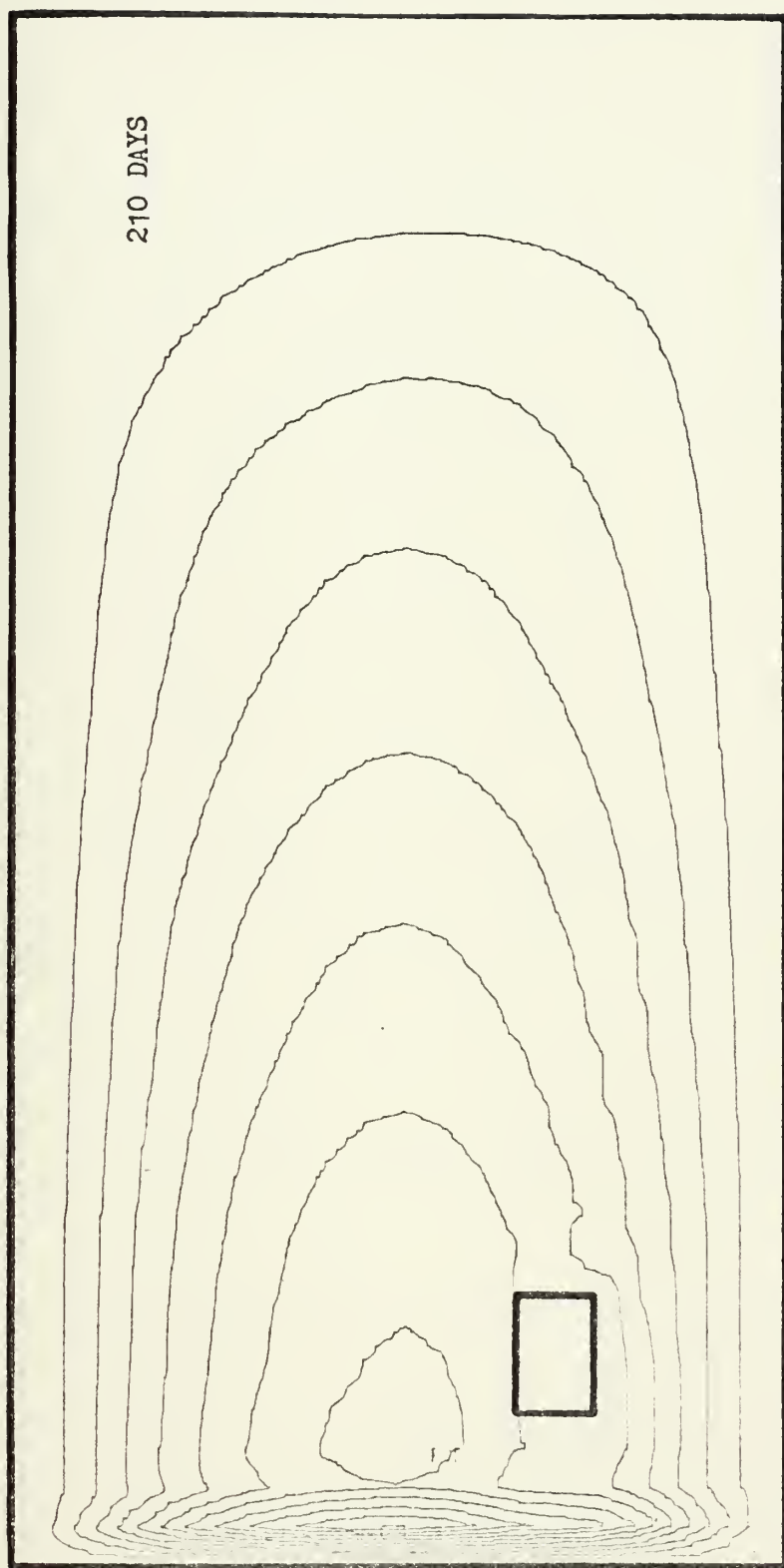


Figure 31: Same as Figure 10 except for Case 8b

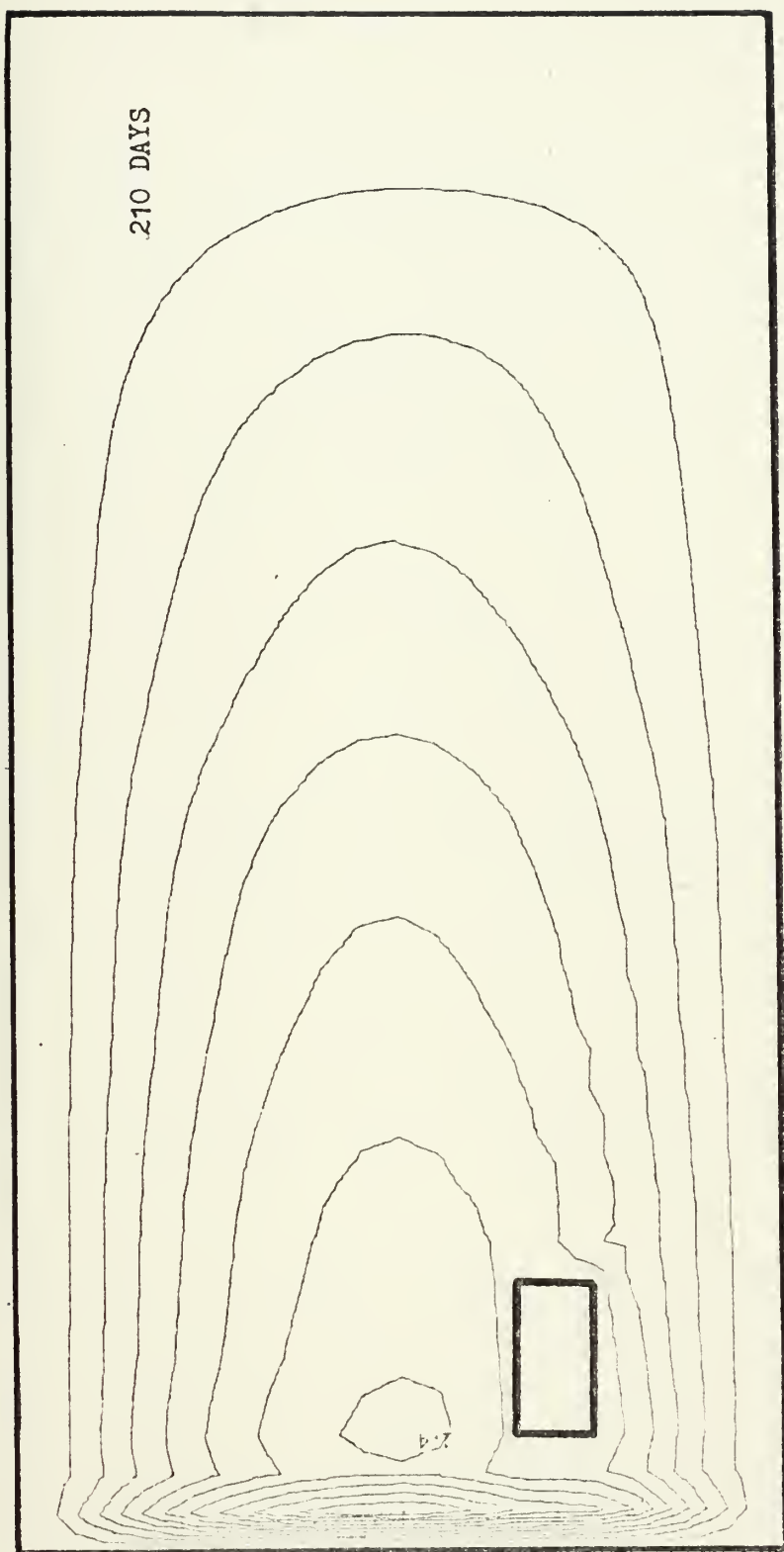


Figure 32: Same as Figure 10 except for Case 8c

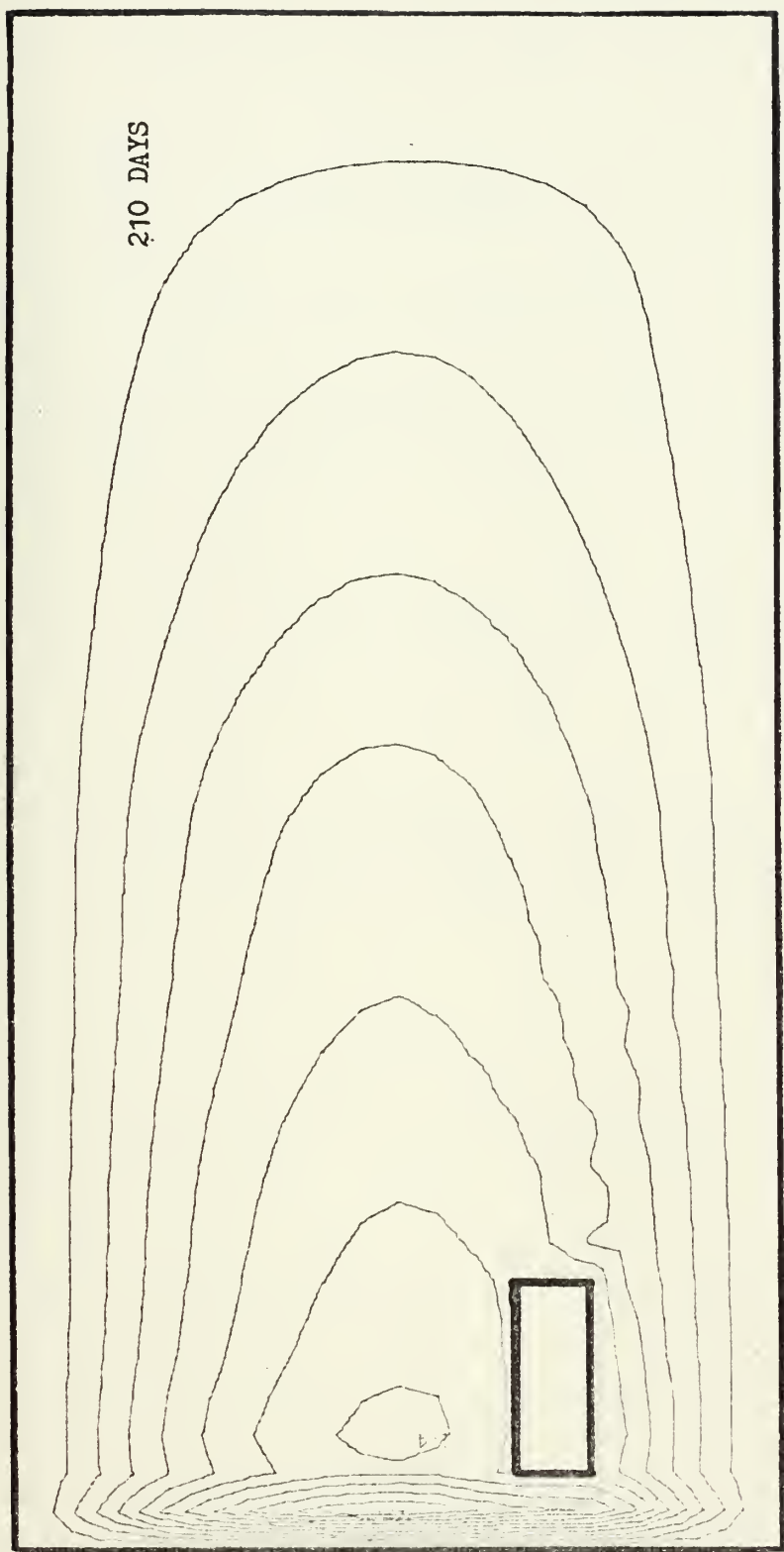


Figure 33: Same as Figure 10 except for Case 8d



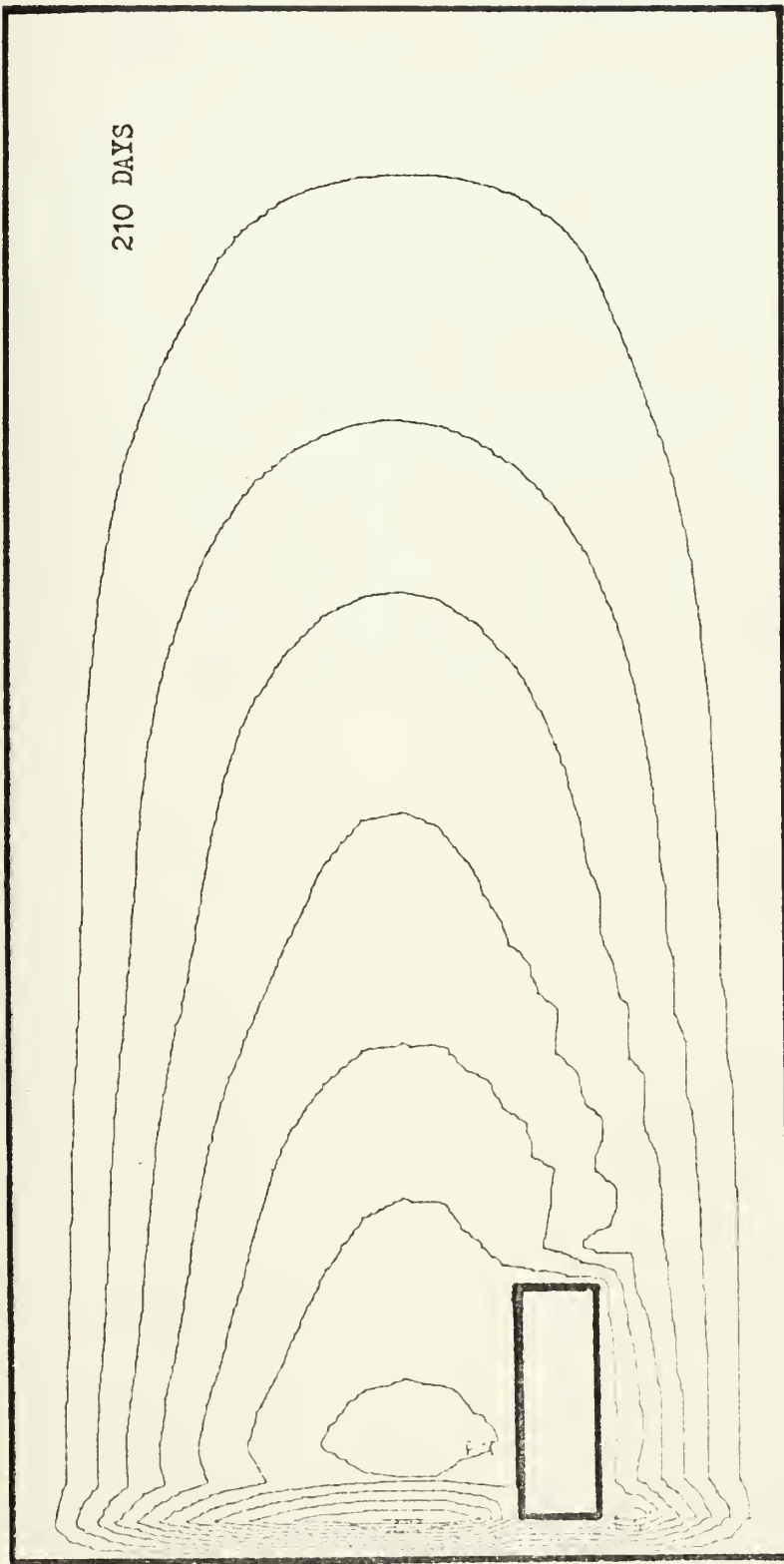


Figure 34: Same as Figure 10 except for Case 8e

V. CONCLUSIONS

This numerical model, depicting the wind-driven circulation in an ocean basin containing an island, was successful in portraying the boundary conditions and relaxation techniques to be evaluated. Furthermore, a firm numerical basis has been established for a future non-linear modification and still later comparative study with a free surface model. The study of the combined relaxation technique employed in this model has established a much needed data resource which displays the usefulness of the "Hole Relaxation" technique (Allen 1954) for the problem of the flow around an island.


```

                                APPENDIX A
// EXEC FORTCLGP,REGION.GO=160K
// FORT.SYSIN DD DSN=SSP3(CONTUR),DISP=SHR
// DD *
C   THE MAIN PROGRAM INITIATES THE SOLUTION OF THE
C   VORTICITY EQUATION BY ZEROING ALL DIMENSIONED
C   VARIABLES.THE SUBROUTINES,NAMELY CALF AND RELAX,THEN
C   TAKE CONTROL AND PERFORM THEIR RESPECTIVE FUNCTIONS.
C   AFTERWARDS,THE MAIN PROGRAM TAKES CONTROL AND PER-
C   FORMS THE TIME-STEPPING PHASE OF THE SOLUTION .
C
C   DVAR      MEANS   DIMENSIONED VARIABLES      *****
C
C   ***** DPSIDI IS THE VALUE OF DPSIDT ON THE PERIMETER
C   ***** OF THE ISLAND . THIS VALUE IS CONSTANT . *****
C
COMMON/ISLAND/IMIN,IMAX,JMIN,JMAX,DPSIDI
COMMON/DVAR/PSIM1,PSI,F1,U,V,DELSQU,DELSQV,DPSIDT,
1 RESID,PSTEMP
DIMENSION PSIM1(41,21),PSI(41,21),F1(41,21),U(42,22),
1 DELSQU(40,20),DELSQV(40,20),DPSIDT(41,21),RESID(41,21)
2 ,PSTEMP(41,21),V(42,22),DATA1(41,21)
5009 READ(5,5009) IMIN,IMAX,JMIN,JMAX
      FORMAT(4I4)
      REAL*8 TITLE1(12)
      REAL *4 CL(25)
      LOGICAL*1 LTG(3)/.TRUE.,.TRUE.,.FALSE./
      DATA CL/-2.4,-2.2,-2.0,-1.8,-1.6,-1.4,-1.2,-1.0,-0.8,
1 -0.6,-0.4,-0.2,0.0,0.2,0.4,0.6,0.8,1.0,1.2,1.4,1.6,
2 1.8,2.0,2.2,2.4/
C
C   START THE ZEROING PROCESS.
C
DPSIDI=0.0
DO 3000 J=1,21
DO 3000 I=1,41
PSIM1(I,J)=0.0
PSI(I,J)=0.0
F1(I,J)=0.0
RESID(I,J)=0.0
PSTEMP(I,J)=0.0
3000 DPSIDT(I,J)=0.0
DO 4000 J=1,20
DO 4000 I=1,40
DELSQV(I,J)=0.0
4000 DELSQU(I,J)=0.0
DO 5000 J=1,22
DO 5000 I=1,42
U(I,J)=0.0
5000 V(I,J)=0.0
C
C   LET'S GO TO THE MATSUNO SCHEME TO GET THIS PROJECT
C   GOING .
C
NPRINT=50
DELTAX=2.0 * 10.0**7
DELTAT= 5.0 *10.0**4
TIMEST=210.0*86400.0
TIME=0.0
WRITE(6,103) TIME
C
C   LEAPFROG TIME SCHEME *****
C
C   THE LEAPFROG SCHEME IS NEUTRAL IN CHARACTER BUT THE
C   PRESENCE AND UTILIZATION OF THREE TIME LEVELS IN THE
C   DESCRIPTION OF THE FIRST DERIVATIVE OF PSI WITH
C   RESPECT TO TIME ,PRODUCES A COMPUTATIONAL MODE IN
C   TIME.THIS MODE HAS TO BE AND IS REMOVED BY THE EULER-
C   BACKWARD SCHEME.THIS SCHEME USES TWO LEVELS IN TIME
C   IN ITS DESCRIPTION OF THE FIRST TIME DERIVATIVE OF

```



```

C      PSI.THEREFORE,THERE IS NO COMPUTATIONAL MODE IN TIME
C      AND A MORE ACCURATE SOLUTION FOR THE PSI FIELD AT
C      TIME LEVEL 'N+1' IS ATTAINED .

      DO 3100 K=1,1000
      IF(K.EQ.1) GO TO 2000
      L=MOD(K,NPRINT)
      IF (L.EQ.0) GO TO 2000
      CALL CALF
      CALL RELAX
      DO 6000 J=2,20
      DO 6000 I=2,40
      TEMP=PSI(I,J)
      PSI(I,J)= PSIM1(I,J)+2.0 * DELTAT * DPSIDT(I,J)
6000  PSIM1(I,J) = TEMP

C      PRINT THE PSI FIELD IN TABULAR FORM *****
C      GO TO 2800

C      AT THIS TIME , PSI IS KNOWN AT TWO CONSEQUITIVE TIME
C      LEVELS AND IS STORED IN PSI AND PSIM1 FIELDS
C      RESPECTIVELY.BY MEANS OF THE ' TEMP ' STATEMENT,THE
C      TWO TIME LEVELS ARE ADVANCED BY ONE INCREMENT OF TIME
C      ,I.E., DELTAT = 5.0*10.0**4 (SEC.) RESPECTIVELY .

C      THE EULER-BACKWARD OR MATSUNO TIME SCHEME ; NOTE: PSI
C      AT TIME LEVEL 'N' IS SAVED IN PSTEMP FIELD FOR
C      LATER USE IN SUBSEQUENT BACKWARD IMPLICIT STEPS..

C      2000 WRITE(6,103) TIME
C      2100 DO 2200 J=2,20
C      DO 2200 I=2,40
C      PSIM1(I,J)=PSI(I,J)
C      2200 PSTEMP(I,J)=PSI(I,J)

C      BY MEANS OF THE ABOVE LOOP(#2200),PSI AT TIME LEVEL N
C      IS PUT INTO THREE FIELDS,NAMELY PSI,PSTEMP AND PSIM1.
C      ALL FIELDS ARE AT THE SAME TIME LEVEL IN ORDER TO
C      PRESERVE LINEAR COMPUTATIONAL STABILITY IN THE
C      FRICTION TERM OF THE FORCING FUNCTION,F1.

C      COMMENCE THE FORWARD TIME STEP PHASE OF THE MATSUNO
C      SCHEME .

C      NOTE: ALL TERMS OF CALF AND RELAX ARE OUTPUTED AT TIME
C      LEVEL 'N' .

C      CALL CALF
C      SCALE=10.0**(-2)
C      DO 2910 J=2,20
C      DO 2910 I=2,40
2910  RESID(I,J)=F1(I,J)*SCALE
      WRITE(6,108) ((RESID(I,J),I=1,33),J=1,21)
108  FORMAT('0','RESID FIELD = F1 FIELD * SCALE',/,21(3F4
      1.2,//))
      CALL RELAX

C      DPSIDT IS NOW AT TIME LEVEL 'N' . *****

C      DO 2500 J=2,20
C      DO 2500 I=2,40
      PSI(I,J)= PSI(I,J) + DELTAT * DPSIDT(I,J)
2500  PSIM1(I,J)=PSI(I,J)

C      PRESENTLY, THE FIELDS PSI,PSIM1 AND PSTEMP HAVE
C      CONTAINED IN THEM,PSI VALUES AT TIME LEVELS 'N+1'

```



```

C      INTERMEDIATE, 'N+1' INTERMEDIATE AND 'N' RESPECTIVELY.
C
C      NOW AS A PART OF THE MATSUNO TIME SCHEME ; A SIMULATED
C      (IMPLICIT) BACKWARD TIME STEP IS EMPLOYED . THE
C      BACKWARD STEP IS USED AS A CALIBRATION STEP TO REFIN
C      THE PSI FIELD AT TIME LEVEL 'N+1' . NOW COMMENCE THE
C      BACKWARD TIME STEP PHASE OF THE MATSUNO SCHEME .
C      NOTE: ALL TERMS OF CALF CALCULATED AS A FUNCTION OF
C      PSI AT INTERMEDIATE TIME LEVEL 'N+1' .
C
C      CALL CALF
C      CALL RELAX
C
C      DPSIDT AT TIME LEVEL 'N+1' (INTERMEDIATE) OUTPUTED.  *
C      NOW OUTPUT PSI AT TIME LEVEL 'N+1'. *****
C
C      DO 2700 J=2,20
C      DO 2700 I=2,40
C      PSIMI(I,J)=PSTEMP(I,J)
2700 PSI(I,J)=PSTEMP(I,J) + DELTAT * DPSIDT(I,J)
2800 TIME= DELTAT*K
C      WRITE(6,103) TIME,K
C      SCALE= 10.0**(-8)
C      DO 2900 J=2,20
C      DO 2900 I=2,40
2900 RESID(I,J)= PSI(I,J) * SCALE
C      WRITE(6,104) ((RESID(I,J),I=1,33),J=1,21)
103 FORMAT(' ',T63,'TIME=',F10.1,I6,/)
104 FORMAT('0','RESID FIELD = PSI FIELD * SCALE',/,21(33F4
1.2,/))
C      LL=MOD(K,3)
C      TDAY=TIME/86400.0
C      WRITE(6,103) TDAY,LL
C
C      LOOP IS FOR THE CONVERSION OF DATA TO A FORM MORE
C      USEABLE IN THE COMPUTER SUBROUTINE , 'CONTUR' .
C
C      DO 2950 J=1,21
C      JS=22-J
C      DO 2950 I=1,41
2950 DATA1(I,J)=RESID(I,J)
C      IF((TDAY.GT.200.0).AND.(LL.EQ.0)) GO TO 9970
C      GO TO 9980
9970 READ(5,9999) (TITLE1(J),J=1,12)
9999 FORMAT(6A8)
C      CALL CONTUR(DATA1,41,21,41,CL,25,TITLE1,4,08,LTG)
9980 IF(TIME.GE.TIMEST) STOP
3100 CONTINUE
C      STOP
C      DEBUG
C      AT 3100
C      TRACE ON
C      DISPLAY K
C      END
C
C      SUBROUTINE CALF
C
C      THIS SUBROUTINE CALCULATES THE RIGHT HAND SIDE OF THE
C      VORTICITY EQUATION WHICH IS MULTIPLIED BY THE SQUARE
C      OF DELTAX. *****
C
C      DVAR      MEANS  DIMENSIONED VARIABLES *****
C
C      ** THE ENTIRE GRID IS DIVIDED INTO AREAS IN ORDER TO
C      ** PERMIT BETTER EASE FOR CALCULATIONS IN BOTH ISLAND*
C      ** RELATED REGIONS AND OCEANIC REGIONS . *****
C
C      COMMON/ISLAND/IMIN,IMAX,JMIN,JMAX,DPSIDI
C      COMMON/DVAR/PSIMI,PSI,F1,U,V,DELSQU,DELSQV,DPSIDT,RESI
C      1D,PSTEMP

```



```

DIMENSION PSIM1(41,21),PSI(41,21),F1(41,21),U(42,22),
1DELSQU(40,20),DELSQV(40,20),DPSIDT(41,21),RESID(41,21)
2, PSTEMP(41,21),V(42,22)

```

```

DEFINE INITIAL U(40,20) AND V(40,20) AS FUNCTIONS OF
PSIM1(41,21). REFERENCE SHOULD BE MADE TO SKETCHES OF
GRIDS IN THE JOURNAL NOTES: *****
U(I+1,J+1) AND V(I+1,J+1) TRANSFORM U,V(40,20)
INTERNAL GRID SYSTEM INTO EXTERNAL U,V (42,22) GRID
SYSTEM *****

```

```

DELTAX=2.0*10.0**7
A=10.0**8
DO 50 I=1,40
DO 50 J=1,20
AA= PSIM1(I+1,J+1) + PSIM1(I+1,J)
BB= PSIM1(I,J+1) + PSIM1(I,J)
CC= PSIM1(I+1,J+1) +PSIM1(I,J+1)
DD= PSIM1(I+1,J) + PSIM1(I,J)
EE = 2.0*DELTAX
V(I+1,J+1) = ((AA/EE) -(BB/EE))
50 U(I+1,J+1) = ((DD/EE) -(CC/EE))

```

```

NOTE: FOR ALL FRICTION FORCE TERMS ;
CALCULATION OF FRICTION TERM USING PSIM1
(FORWARD TIME SCHEME). *****

```

```

FRICTION TERMS ARE CALCULATED USING A FORWARD TIME
SCHEME. THIS IS DONE TO PRESERVE LINEAR COMPUTATIONAL
STABILITY. IF THE LEAPFROG SCHEME WAS UTILIZED, THE
FRICTION TERM WOULD BE UNSTABLE. *****

```

```

DEFINE EXTERNAL BOUNDARY VALUES OF U AND V *****

```

```

DO 60 I=2,41
U(I,1) = -U(I,2)
V(I,1) = -V(I,2)
U(I,22) = -U(I,21)
60 V(I,22) = -V(I,21)

```

```

NOTE THAT THE FOUR EXTERNAL CORNER VALUES OF U&V ARE
NOT DEFINED BJT A VALUE OF ZERO IS ASSUMED FOR EACH.
IF THEY ARE TO BE DEFINED THEN U(42,1)=J(41,2);U(1,1)=
U(2,2);U(1,22)=U(2,21); AND U(42,22)=U(41,21) *****

```

```

DO 70 J=2,21
U(1,J)=-U(2,J)
V(1,J)=-V(2,J)
U(42,J)=-U(41,J)
70 V(42,J)=-V(41,J)
***** AREAS ONE AND FOUR CALCULATIONS: *****
***** AREA ONE IS THE AREA WHICH DEPICTS THE *
***** OCEANIC REGION SOUTHWEST, SOUTH AND *****
***** SOUTHEAST OF THE ISLAND. AREA FOUR IS *
***** THE AREA WHICH DEPICTS THE OCEANIC *****
***** REGION NORTHWEST, NORTH AND NORTHEAST *****
***** OF THE ISLAND . *****

```

```

BETA TERM CALCULATION *****

```

```

BETA=1.94*10.0**(-13)
M=JMIN-1
IF(M.LT.2) GO TO 27
DO 25 J=2,M
DO 25 I=2,40
25 F1(I,J)=- (BETA)*(PSI(I+1,J)-PSI(I-1,J))*(DELTAX)/2.0
27 MM=JMAX +1
IF(MM.GT.20) GO TO 33
DO 30 J=MM,20

```


C
C
C
C
C

```
AAA= (DELSQV(I,J) + DELSQV(I,J-1)) /2.0
BBB= (DELSQV(I-1,J) + DELSQV(I-1,J-1)) /2.0
CCC= (DELSQU(I,J) + DELSQU(I-1,J)) /2.0
DDD= (DELSQU(I,J-1) + DELSQU(I-1,J-1)) /2.0
```

```
DELVX IS THE PARTIAL OF THE LAPLACIAN OF V WITH
RESPECT TO X. *****
DELUY IS THE PARTIAL OF THE LAPLACIAN OF U WITH
RESPECT TO Y . *****
```

```
DELVX= AAA - BBB
DELUY= CCC - DDD
95 F1(I,J)=F1(I,J)+((DELVX-DELUY)/(DELTAX))*A
97 MM=JMAX + 1
  IF(MM.GT.20) GO TO 98
  DO 99 J=MM,20
  DO 90 I=2,40
    AAA= (DELSQV(I,J) + DELSQV(I,J-1)) /2.0
    BBB= (DELSQV(I-1,J) + DELSQV(I-1,J-1)) /2.0
    CCC= (DELSQU(I,J) + DELSQU(I-1,J)) /2.0
    DDD= (DELSQU(I,J-1) + DELSQU(I-1,J-1)) /2.0
    DELVX= AAA - BBB
    DELUY= CCC - DDD
90 F1(I,J)=F1(I,J)+((DELVX-DELUY)/(DELTAX))*A
```

C
C
C
C
C
C
C

```
***** AREAS TWO AND THREE CALCULATIONS: *****
***** AREA TWO IS THE AREA WHICH DEPICTS THE*
***** OCEANIC REGION WEST OF THE ISLAND. *****
***** AREA THREE IS THE AREA WHICH DEPICTS *
***** THE OCEANIC REGION EAST OF THE ISLAND.*
```

```
BETA TERM CALCULATION *****
```

```
98 BETA=1.94*10.0**(-13)
  DELTAX=2.0*10.0**7
  NN=IMIN-1
  IF(NN.LT.2) GO TO 28
  DO 26 I=2,NN
  DO 26 J=JMIN,JMAX
26 F1(I,J)=-(BETA)*(PSI(I+1,J)-PSI(I-1,J))*(DELTAX)/2.0
28 MM=IMAX + 1
  IF(MM.GT.40) GO TO 34
  DO 31 I=MM,40
  DO 31 J=JMIN,JMAX
31 F1(I,J)=-(BETA)*(PSI(I+1,J)-PSI(I-1,J))*(DELTAX)/2.0
```

C
C
C

```
STRESS CURL TERM CALCULATION : *****
```

```
34 NN=IMIN - 1
  IF(NN.LT.2) GO TO 48
  DO 46 I=2,NN
  DO 46 J=JMIN,JMAX
  Y=PI*(J-1)*(1.0/B)*DELTAX
  STRESS=((F*PI)/(DEPTH*B))*SIN(Y)
46 F1(I,J)=F1(I,J)-(STRESS*DELTAX**2)
48 MM=IMAX + 1
  IF(MM.GT.40) GO TO 49
  DO 41 I=MM,40
  DO 41 J=JMIN,JMAX
  Y=PI*(J-1)*(1.0/B)*DELTAX
  STRESS=(( F*PI) / (DEPTH*B)) * SIN(Y)
41 F1(I,J)=F1(I,J)-(STRESS*DELTAX**2)
```

C
C
C

```
DEFINE EXTERNAL BOUNDARY VALUES OF U AND V . *****
```

```
49 MN=JMIN + 1
  DO 71 J=MN,JMAX
  U(IMIN+1,J) =-U(IMIN,J)
  V(IMIN+1,J) =-V(IMIN,J)
  U(IMAX,J) =-U(IMAX+1,J)
71 V(IMAX,J)=-V(IMAX+1,J)
  MX=JMAX-1
```



```

DO 801 J=JMIN,MX
NN=IMIN-1
DO 601 I=1,NN
DELSQU(I,J) =(U(I+1,J+2)+U(I+1,J)+U(I+2,J+1)+U(I,J+1)-
1 (4.0*U(I+1,J+1)))
601 DELSQV(I,J)=(V(I+1,J+2)+V(I+1,J)+V(I+2,J+1)+V(I,J+1)-
1 (4.0*V(I+1,J+1)))
DO 801 I=IMAX,40
DELSQU(I,J) =(U(I+1,J+2)+U(I+1,J)+U(I+2,J+1)+U(I,J+1)-
1 (4.0*U(I+1,J+1)))
801 DELSQV(I,J)=(V(I+1,J+2)+V(I+1,J)+V(I+2,J+1)+V(I,J+1)-
1 (4.0*V(I+1,J+1)))

```

CURL OF THE FRICTION FORCE TERM . *****

```

NN=IMIN-1
IF(NN.LT.2) GO TO 92
DO 96 I=2,NN
DO 96 J=JMIN,JMAX
AAA= (DELSQV(I,J) + DELSQV(I,J-1)) /2.0
BBB= (DELSQV(I-1,J) + DELSQV(I-1,J-1)) /2.0
CCC= (DELSQU(I,J) + DELSQU(I-1,J)) /2.0
DDD= (DELSQU(I,J-1) + DELSQU(I-1,J-1)) /2.0
DELVX= AAA - BBB
DELUY= CCC - DDD
96 F1(I,J)=F1(I,J)+((DELVX-DELUY)/(DELTAX))*A
92 NM=IMAX + 1
IF(NM.GT.40) GO TO 93
DO 91 I=NM,40
DO 91 J=JMIN,JMAX
AAA= (DELSQV(I,J) + DELSQV(I,J-1)) /2.0
BBB= (DELSQV(I-1,J) + DELSQV(I-1,J-1)) /2.0
CCC= (DELSQU(I,J) + DELSQU(I-1,J)) /2.0
DDD= (DELSQU(I,J-1) + DELSQU(I-1,J-1)) /2.0
DELVX= AAA - BBB
DELUY= CCC - DDD
91 F1(I,J)=F1(I,J)+((DELVX-DELUY)/(DELTAX))*A

```

```

***** AREA FIVE CALCULATIONS: *****
***** AREA FIVE IS THE AREA WHICH DEPICTS *****
***** ONLY THE PERIMETER OF THE ISLAND . *****
** BETA TERMS FOR AREA FIVE'S NORTH AND SOUTH PERIME- **
** TERS ARE ZERO . *****
** WHEN J =JMIN OR JMAX AND CALCULATIONS ARE PER- **
** FORMED AT THE ISLAND CORNERS FOR THE BETA TERM, **
** THE ACTUAL FINITE DIFFERENCE FORM IS PSI(I+1) **
** -PSI(I-1) DEVIDED BY 2.0,BUT BECAUSE PSI(I+1)= **
** PSI(I)=CONSTANT FOR THE SW/NW CORNERS AND PSI(I) **
** =PSI(I-1)=CONSTANT FOR THE SE/NE CORNERS,THE ****
** PRESENT FORM OF FINITE DIFFERENCE CAN BE USED **
** VALIDLY FOR SIMPLICITY . ****
** COMMENCE BETA TERM CALCULATIONS FOR AREA FIVE'S **
** EASTERN AND WESTERN PERIMETERS. *****

```

BETA TERM CALCULATION *****

```

93 BETA=1.94*10.0**(-13)
DELTAX = 2.0*10.0**7
FACT = 1.0
DO 32 J=JMIN,JMAX
IF((J.EQ.JMIN).OR.(J.EQ.JMAX)) FACT = 0.5
I=IMIN
F1(I,J)= -(BETA)*(PSI(I,J)-PSI(I-1,J))*(DELTAX)*FACT
I=IMAX
32 F1(I,J)=- (BETA)*(PSI(I+1,J)-PSI(I,J))*(DELTAX)*FACT

```

```

** COMMENCE CALCULATION OF WIND STRESS CURL TERM ON **
** THE NORTHERN AND SOUTHERN PERIMETERS . *****

```

```

N=IMIN+1
F=1.0
PI=3.1415926

```



```

DEPTH=2.0*10.0**5
B=4.0*10.0**8
II=IMAX-IMIN
IF(II.LE.1) GO TO 11
NX=IMAX-1
DO 42 I=N,NX
J=JMIN
Y=PI*(J-1)*(1.0/B)*DELTAX
STRESS=((F*PI)/(DEPTH*B))*SIN(Y)
F1(I,J)=-(STRESS*DELTAX**2)
J=JMAX
Y=PI*(J-1)*(1.0/B)*DELTAX
STRESS=((F*PI)/(DEPTH*B))*SIN(Y)
42 F1(I,J)=-(STRESS*DELTAX**2)

** COMMENCE CALCULATION OF WIND STRESS CURL TERM ON **
** THE EASTERN AND THE WESTERN PERIMETERS . *****

11 DO 43 J=JMIN,JMAX
Y=PI*(J-1)*(1.0/B)*DELTAX
STRESS=((F*PI)/(DEPTH*B))*SIN(Y)
I=IMIN
F1(I,J)=F1(I,J)-(STRESS*DELTAX**2)
I=IMAX
43 F1(I,J)=F1(I,J)-(STRESS*DELTAX**2)

****AREA FIVE FRICTION FORCE TERM CALCULATION ****
****NOTE: ALL CALCULATIONS DO NOT INCLUDE CORNER GRID*
****POINTS . THESE CALCULATIONS WILL BE COMPLETED LAST
****FOLLOWING CALCULATIONS ARE FOR NORTHERN AND SOUTH-
****ERN PERIMETERS ONLY . *****
****TEST FOR ZERO NODAL POINT ISLAND . *****

II=IMAX - IMIN
IF(II.LE.1) GO TO 200

****LOOP FOR N/S PERIMETER LESS CORNERS : *****

N=IMIN+1
NX=IMAX-1
DO 343 I=N,NX
IF(I.EQ.IMIN+1) GO TO 10
IF(I.EQ.IMAX-1) GO TO 20

****HERE THE NORMAL CONDITIONS ALONG THE N/S PERIMETER
****BETWEEN I=IMIN+2 AND I=IMAX-2 ARE GENERALLY STATED

J=JMIN
DELVX=0.0
DELUY = (4*(U(I,J)+U(I+1,J)))-U(I-1,J) -U(I,J-1)-U(I+1,
1,J-1)-U(I+2,J)
F1(I,J)=F1(I,J)+((DELVX-DELUY)/(DELTAX))*A
J=JMAX
DELVX=0.0
DELUY=(-4*(U(I,J+1)+U(I+1,J+1))+U(I-1,J+1)+U(I+2,J+1)
1+U(I,J+2)+U(I+1,J+2)))
F1(I,J)=F1(I,J)+((DELVX-DELUY)/(DELTAX))*A
GO TO 343
10 J=JMIN
DELVX = (-V(I-1,J+1)-V(I-1,J))/2.0
DELUY = (U(I-1,J+1)-U(I-1,J))/2.0 + (4*(U(I,J)+U(I+1,
1J))-U(I+2,J)-U(I+1,J-1)-U(I,J-1))
F1(I,J)=F1(I,J)+((DELVX-DELUY)/(DELTAX))*A
J=JMAX
DELVX = (-V(I-1,J)-V(I-1,J+1))/2.0
DELUY = (U(I-1,J+1)-U(I-1,J))/2.0 + (-4*(U(I,J+1)+U(I+1,
1,J+1))+U(I+2,J+1)+U(I+1,J+2)+U(I,J+2))
F1(I,J)=F1(I,J)+((DELVX-DELUY)/(DELTAX))*A
GO TO 343
20 J=JMIN
DELVX=(V(I+2,J)+V(I+2,J+1))/2.0
DELUY = (U(I+2,J+1)-U(I+2,J))/2.0 + (4*(U(I,J)+U(I+1,J

```



```

      DELVX=((4*(V(I,J)+V(I,J+1)))-(V(I,J+2)+V(I-1,J+1)+V(I-
11,J)+V(I,J-1)))/2.0
      DELUY=((4*(U(I,J+1)+U(I+1,J+1)))+U(I-1,J+1)+U(I,J+2)+
1U(I+1,J+2)+U(I+2,J+1))/2.0
      F1(I,J)=F1(I,J)+((DELVX-DELUY)/(DELTAX))*A

```

```

      ****CASE THREE *** THE NORTHEAST CORNER OF ISLAND. ***

```

```

      I=IMAX
      J=JMAX
      DELVX=((4*(V(I+1,J+1)+V(I+1,J)))+V(I+1,J+2)+V(I+2,J+1)
1)+V(I+2,J)+V(I+1,J-1))/2.0
      DELUY=((4*(U(I,J+1)+U(I+1,J+1)))+U(I-1,J+1)+U(I,J+2)+
1U(I+1,J+2)+U(I+2,J+1))/2.0
      F1(I,J)=F1(I,J)+((DELVX-DELUY)/(DELTAX))*A

```

```

      ****CASE FOUR **** THE SOUTHEAST CORNER OF ISLAND. ***

```

```

      I=IMAX
      J=JMIN
      DELVX=((4*(V(I+1,J)+V(I+1,J+1)))+V(I+1,J+2)+V(I+2,J+1)
1)+V(I+2,J)+V(I+1,J-1))/2.0
      DELUY=((4*(U(I,J)+U(I+1,J)))-(U(I-1,J)+U(I,J-1)+U(I+1,
1J-1)+U(I+2,J)))/2.0
      F1(I,J)=F1(I,J)+((DELVX-DELUY)/(DELTAX))*A

```

```

      *****AREA SIX CALCULATIONS: *****
      *****AREA SIX IS THE AREA WHICH DEPICTS *****
      *****ONLY THE INTERIOR OF THE ISLAND. *****
      ** TEST IS ESTABLISHED TO DETERMINE THE POSSIBILITY **
      ** OF A ZERO NODAL POINT ISLAND . *****

```

```

      II=IMAX-IMIN
      JJ=JMAX-JMIN
      IF((II.LE.1).OR.(JJ.LE.1)) GO TO 19
      NX=IMAX-1
      N=IMIN+1
      DO 850 I=N,NX
      MN=JMIN+1
      MX=JMAX-1
      DO 850 J=MN,MX
850 F1(I,J)=0.0
19 RETURN
END

```

```

      SUBROUTINE RELAX

```

```

      THIS SUBROUTINE PERFORMS THE RELAXATION PHASE OF THIS
      THESIS PROJECT .

```

```

      DVAR      MEANS      DIMENSIONED VARIABLES      *****

```

```

      COMMON/ISLAND/IMIN,IMAX,JMIN,JMAX,DPSIDI
      COMMON/DVAR/PSIM1,PSI,F1,U,V,DELSQU,DELSQV,DPSIDT,
1RESID,PSTEMP
      DIMENSION PSIM1(41,21),PSI(41,21),F1(41,21),U(42,22),
1DELSQU(40,20),DELSQV(40,20),DPSIDT(41,21),RESID(41,21)
2,PSTEMP(41,21),V(42,22)

```

```

      START THE RELAXATION

```

```

      SET CONSTANTS: EPSS AND ALPHA

```

```

      DELTAX= 2.0*10.0**(7)
      B=4.0*10.0**(8)
      ALPHA=0.75
      WRITE(6,105) ALPHA
      CF1=20.
      EPSS= CF1*1.E-04
      WRITE(6,106) EPSS

```


USE THE LAST KNOWN VALUE OF DPSIDT AS THE FIRST GUESS.

SET A SYSTEM OF ITERATIVE COUNTING.

```

306      KCOUNT=0
      ICOUNT=0

```

START THE COMPUTATION OF THE RESIDUAL.

NOTE: $DPSIDT = \frac{\partial \Psi}{\partial t}$ THE PARTIAL OF Ψ WRT TIME, HAVING
UNITS OF $(CM.^{**2}) * (SEC.^{**(-2)})$. IT IS NOT THE
PARTIAL OF Ψ WRT TIME MULTIPLIED BY DELTAX SQUARED.

NOTE: THE RESIDUAL IS THE LAPLACIAN OF DPSIDT
MULTIPLIED BY THE SQUARE OF DELTAX, AND SUBTRACTING
THE FORCING FUNCTION, F1 .

```

DO 444 JAREA=1,4
IF((JMIN.EQ.2).AND.(JAREA.EQ.1)) GO TO 444
IF((JMAX.EQ.20).AND.(JAREA.EQ.4)) GO TO 444
IF((IMIN.EQ.2).AND.(JAREA.EQ.2)) GO TO 444
IF((IMAX.EQ.40).AND.(JAREA.EQ.3)) GO TO 444
IF((JAREA.EQ.1).OR.(JAREA.EQ.2).OR.(JAREA.EQ.4))
1 ILEFT=2
IF((JAREA.EQ.1).OR.(JAREA.EQ.3).OR.(JAREA.EQ.4))
1 IRIGHT=40
IF((JAREA.EQ.1)) JBOTM=2
L=JMIN-1
IF((JAREA.EQ.1)) JTOP=L
IF((JAREA.EQ.2).OR.(JAREA.EQ.3)) JBOTM=JMIN
IF((JAREA.EQ.2).OR.(JAREA.EQ.3)) JTOP=JMAX
K=IMIN-1
IF((JAREA.EQ.2)) IRIGHT=K
KK=IMAX+1
IF((JAREA.EQ.3)) ILEFT=KK
LL=JMAX+1
IF((JAREA.EQ.4)) JBOTM=LL
IF((JAREA.EQ.4)) JTOP=20
DO 400 J=JBOTM,JTOP
DO 400 I=ILEFT,IRIGHT
RESID(I,J)=(DPSIDT(I+1,J)+DPSIDT(I-1,J)+DPSIDT(I,J+1)
1+DPSIDT(I,J-1)-4*DPSIDT(I,J))-F1(I,J)

```

CHECK FOR CONVERGENCE AND IF NECESSARY INITIALIZE
VALUE OF CONSTANT C .

THE REAL TEST FOR CONVERGENCE IS THE COMPARISON OF CF1
AND RESID, THEREFORE 'LE.EPSS ' MEANS 'MUCH LESS THAN
CF1 ' .

```

      IF (ABS (RESID (I, J)) .LE. EPSS) GO TO 400
      C = ((1.0 + ALPHA) / 4.0) * (RESID (I, J))
      ICOUNT = ICOUNT + 1
      DPSIDT (I, J) = DPSIDT (I, J) + C
400  CONTINUE
444  CONTINUE

```

AREA FIVE CALCULATION

```

DO 445 J=JMIN,JMAX
DO 445 I=IMIN,IMAX
445 RESID(I,J)=(DPSIDT(I+1,J)+DPSIDT(I-1,J)+DPSIDT(I,J+1)+
1DPSIDT(I,J-1)-4*DPSIDT(I,J)) -F1(I,J)
RESB=0.0
IMAXM1=IMAX-1
JMAXM1=JMAX-1
RESIDI=0.0

```



```

DO 480 J=JMIN,JMAXM1
DO 480 I=IMIN,IMAXM1
RESB= 0.25*(RESID(I,J)+RESID(I+1,J) +RESID(I,J+1) +
1 RESID(I+1,J+1))
480 RESIDI=RESIDI + RESB
WRITE(6,107)KCOUNT,RESIDI,RESID(IMIN,JMIN),RESID(10,20
1)

CHECK FOR CONVERGENCE AND IF NECESSARY INITIALIZE
VALUE OF CONSTANT C1 .

IICOUT=0
TERM =(IMAX-IMIN + JMAX-JMIN)
EPSI = EPSS
IF(ABS(RESIDI).LE.EPSI) GO TO 83
ALPHAI=0.4
CI= ((1.0+ALPHAI)/TERM)*(RESIDI)
ICOUNT= ICOUNT + 1
IICOUT=10
DPSIDI = DPSIDI + CI
DO 490 J=JMIN,JMAX
DO 490 I=IMIN,IMAX
490 DPSIDT(I,J)= DPSIDI
83 IF(ICOUNT.EQ.0) GO TO 500
KCOUNT = KCOUNT + 1
IF(KCOUNT.LT.400) GO TO 306
WRITE(6,224)KCOUNT,ICOUNT,TKE,IICOUT
WRITE(6,104)
STOP

PRINT OUT NEW DPSIDT ARRAY

COMPUTATION THE TOTAL KINETIC ENERGY FOLLOWS: *****
THIS IS PLACED IN THE PROGRAM TO HELP INDICATE A **
STEADY-STATE CONDITION. ****

500 DO 50 I=1,40
DO 50 J=1,20
AA= PSI (I+1,J+1) + PSI (I+1,J)
BB= PSI (I,J+1) + PSI (I,J)
CC= PSI (I+1,J+1) +PSI (I,J+1)
DD= PSI (I+1,J) + PSI (I,J)
EE = 2.0*DELTAX
V(I,J) = ((AA/EE) -(BB/EE))
50 U(I,J) = ((DD/EE) -(CC/EE))
TKE=0.0
DO 100 I=1,40
DO 100 J=1,20
E= 0.5 * (U(I,J)**2 + V(I,J)**2)
100 TKE=TKE + E
WRITE(6,224)KCOUNT,ICOUNT,TKE,IICOUT
C WRITE(6,102)
DO 600 J=2,20
DO 600 I=2,40
SCALE=10.0**(-3)
600 RESID(I,J)=DPSIDT(I,J) * SCALE
C WRITE(6,101) ((RESID(I,J),I=1,33),J=1,21)
101 FORMAT('0',///,21(33F4.2,///))
102 FORMAT('0',T63,'RESID FIELD=DPSIDT FIELD * SCALE ',///
1)
104 FORMAT(' ',T43,'COMPUTATION TERMINATED DUE TO ',
1'EXCESSIVE' SWEEPS,--KCOUNT = 400 OR MORE ',//)
105 FORMAT('0',T63,'ALPHA=',F4.2,//)
106 FORMAT('0',T63,'EPSS=',F8.6,//)
107 FORMAT(' ',I4,3F10.5)
224 FORMAT('0','KCOUNT = ',I4,'ICOUNT = ',I4,'TKE= ',E10.
14,'IICOUT= ',I4,//)
RETURN
END
//GO.FT06F001 DD SYSOUT=A,SPACE=(CYL,(10,2))

```



```

//GO.SYSIN DD *
      DATA CASE STUDY TWO-B USED.
      5   9   9  13
J.V.SULLIVAN JR. STREAMFUNCTION FIELD  PLOT 1
ISLAND-OCEAN MODEL(IMIN= 5IMAX= 9JMIN= 9JMAX=13)
J.V.SULLIVAN JR. STREAMFUNCTION FIELD  PLOT 2
ISLAND-OCEAN MODEL(IMIN= 5IMAX= 9JMIN= 9JMAX=13)
J.V.SULLIVAN JR. STREAMFUNCTION FIELD  PLOT 3
ISLAND-OCEAN MODEL(IMIN= 5IMAX= 9JMIN= 9JMAX=13)
J.V.SULLIVAN JR. STREAMFUNCTION FIELD  PLOT 4
ISLAND-OCEAN MODEL(IMIN= 5IMAX= 9JMIN= 9JMAX=13)
J.V.SULLIVAN JR. STREAMFUNCTION FIELD  PLOT 5
ISLAND-OCEAN MODEL(IMIN= 5IMAX= 9JMIN= 9JMAX=13)
J.V.SULLIVAN JR. STREAMFUNCTION FIELD  PLOT 6
ISLAND-OCEAN MODEL(IMIN= 5IMAX= 9JMIN= 9JMAX=13)

```


LIST OF REFERENCES

1. Allen, D. N. DeG., 1954: Relaxation Methods. McGraw-Hill Book Co., Inc.
2. Bryan, K., 1969: "Climate and the Ocean Circulation, Part III: The Ocean Model." Monthly Weather Review, 97, p. 806-826.
3. _____, 1969: "A Numerical Method for the Study of the Circulation of the World Ocean." Journal of Computational Physics, 4, p. 347-368.
4. _____, and Manabe, 1969: "Climate Calculations with a Combined Ocean-Atmospheric Model." Journal of Atmospheric Sciences, 26, p. 786-789.
5. Gates, W. L., 1967: "A Numerical Study of Transient Rossby Waves in a Wind-Driven Homogeneous Ocean." Journal of Atmospheric Sciences, 25, p. 3-23.
6. Kamenkovich, V. M., 1962: Trudy Instituta Okeanologii. Akad. Nauk. SSSR, 56, p. 241.
7. _____, and others, 1969: "On the Calculation of the Complete Circulation in the World Ocean (Stationary Problem)." Atmospheric Oceanic Physics, 5, p. 1160-1171, translated by J. D. L. McIntosh.
8. Munk, W. H., 1950: "On the Wind-Driven Ocean Circulation." Journal of Meteorology, 7, p. 79-93.
9. Stommel, H., 1948: "The Westward Intensification of Wind-Driven Ocean Currents." Transactions, American Geophysical Union, 29, p. 202-206.
10. Sverdrup, H. U., 1947: "Wind-Driven Currents in a Baroclinic Ocean; with Applications to the Equatorial Currents of the Ocean Pacific." Proceedings of National Academy of Sciences, 33, p. 318-326.
11. Takano, K., 1969: "Barotropic World Ocean Model." Journal of Oceanographic Society of Japan, 25, p. 48-50.

INITIAL DISTRIBUTION LIST

	No. Copies
1. Defense Documentation Center Cameron Station Alexandria, Virginia 22314	2
2. Library, Code 0212 Naval Postgraduate School Monterey, California 93940	1
3. Dr. R. L. Haney, Code 51Hy Department of Meteorology Naval Postgraduate School Monterey, California 93940	10
4. Lieutenant James V. Sullivan, Jr., USN Class 40 U.S.N. Destroyer School Newport, Rhode Island 02840	5
5. Naval Weather Service Command Washington Navy Yard Washington, D. C. 20390	1
6. Commanding Officer United States Fleet Weather Central COMNAVMARIANAS, Box 12 FPO San Francisco, California 96630	1
7. Commanding Officer Fleet Weather Central Box 31 FPO New York, New York 09540	1
8. Director, Naval Research Laboratory Attn: Tech. Services Info. Officer Washington, D. C. 20390	1
9. Office of Naval Research Department of the Navy Washington, D. C. 20360	1
10. Commanding Officer Fleet Weather Central Box 110 FPO San Francisco, California 96610	1
11. Department of Meteorology, Code 51 Naval Postgraduate School Monterey, California 93940	1

- | | | |
|-----|--|---|
| 12. | Department of Oceanography, Code 58
Naval Postgraduate School
Monterey, California 93940 | 1 |
| 13. | Prof. George J. Haltiner
Chairman, Department of Meteorology, Code 51Ha
Naval Postgraduate School
Monterey, California 93940 | 1 |
| 14. | Dr. R. L. Elsberry, Code 51Es
Department of Meteorology
Naval Postgraduate School
Monterey, California 93940 | 1 |
| 15. | Dr. R. T. Williams, Code 51Wu
Department of Meteorology
Naval Postgraduate School
Monterey, California 93940 | 1 |
| 16. | Prof. Dale F. Leipper
Chairman, Department of Oceanography
Naval Postgraduate School
Monterey, California 93940 | 1 |
| 17. | Dr. J. A. Galt, Code 58G1
Department of Oceanography
Naval Postgraduate School
Monterey, California 93940 | 1 |
| 18. | Commanding Officer
Fleet Numerical Weather Central
Naval Postgraduate School
Monterey, California 93940 | 1 |
| 19. | Commander Celia Barteau
Fleet Numerical Weather Central
Naval Postgraduate School
Monterey, California 93940 | 1 |
| 20. | Dr. Jack Kaitala
Fleet Numerical Weather Central
Naval Postgraduate School
Monterey, California 93940 | 1 |
| 21. | Lieutenant Commander W. Roger Lambertson
Fleet Numerical Weather Central
Naval Postgraduate School
Monterey, California 93940 | 1 |
| 22. | Commanding Officer
Environmental Prediction Research Facility
Naval Postgraduate School
Monterey, California 93940 | 1 |

23. Lieutenant Byron Maxwell, USN 1
Environmental Prediction Research Facility
Naval Postgraduate School
Monterey, California 93940
24. Mrs. Olivera Haney 1
Environmental Prediction Research Facility
Naval Postgraduate School
Monterey, California 93940
25. Dr. W. L. Gates 1
The Rand Corporation
1700 Main Street
Santa Monica, California 90406
26. Dr. Richard Alexander 1
The Rand Corporation
1700 Main Street
Santa Monica, California 90406
27. Prof. Y. Mintz 1
Department of Meteorology
U.C.L.A.
Los Angeles, California 90024
28. Prof. A. Arakawa 1
Department of Meteorology
U.C.L.A.
Los Angeles, California 90024
29. Dr. Joseph Huang 1
NORPAX Project-T-28
Scripps Institution of Oceanography
P. O. Box 109
La Jolla, California 92037
30. Dr. F. Winninghoff 1
Department of Meteorology
U.C.L.A.
Los Angeles, California 90024
31. Dr. Tim Barnett 1
NORPAX Project-T-28
Scripps Institution of Oceanography
P. O. Box 109
La Jolla, California 92037
32. Dr. Kenzo Takano 1
Rikagaku Kenkyusho
Yamato-Machi
Saitama Pref. JAPAN

DOCUMENT CONTROL DATA - R & D

(Security classification of title, body of abstract and indexing annotation must be entered when the overall report is classified)

1. ORIGINATING ACTIVITY (Corporate author)		2a. REPORT SECURITY CLASSIFICATION	
Naval Postgraduate School Monterey, California 93940		Unclassified	
2b. GROUP			
3. REPORT TITLE			
A Numerical Model Depicting a Wind-Driven Circulation in an Ocean Basin Containing an Island			
4. DESCRIPTIVE NOTES (Type of report and inclusive dates)			
Master's Thesis; September 1972			
5. AUTHOR(S) (First name, middle initial, last name)			
James V. Sullivan, Jr.			
6. REPORT DATE		7a. TOTAL NO. OF PAGES	7b. NO. OF REFS
September 1972		90	11
8a. CONTRACT OR GRANT NO.		9a. ORIGINATOR'S REPORT NUMBER(S)	
b. PROJECT NO.			
c.		9b. OTHER REPORT NO(S) (Any other numbers that may be assigned this report)	
d.			
10. DISTRIBUTION STATEMENT			
Approved for public release; distribution unlimited.			
11. SUPPLEMENTARY NOTES		12. SPONSORING MILITARY ACTIVITY	
		Naval Postgraduate School Monterey, California 93940	
13. ABSTRACT			
<p>A numerical model was developed depicting the wind-driven circulation in an ocean basin containing an island. This linear, barotropic, filtered model was utilized to test and evaluate the "Hole Relaxation" technique (Allen 1954) in preparation for future comparative studies with a free surface model and later incorporation in a multi-level world-ocean model with islands. Eight different data cases were studied to evaluate the model's ability to properly treat a variety of island sizes and locations. It was found that as the relative size of the island was increased at a specific location in the western half of the basin, the volume transport per unit depth between the mainland and the island, as well as the total kinetic energy at the end of a 210 day integration decreased; if the island size were decreased, the parameters' magnitudes were noted to be larger.</p>			

KEY WORDS

LINK A

LINK B

LINK C

ROLE

WT

ROLE

WT

ROLE

WT

Numerical model

Wind-driven circulation

Ocean basin

Island

Hole relaxation

20 JUN 75

22660

Thesis

S8593

c.1

Sullivan

A numerical model depicting a wind-driven circulation in an ocean basin containing an island.

138012

0 JUN 75

22660

Thesis

S8593

c.1

Sullivan

A numerical model depicting a wind-driven circulation in an ocean basin containing an island.

138012

thesS8593

A numerical model depicting a wind-drive



3 2768 002 02187 5

DUDLEY KNOX LIBRARY